Supporting Information for

On- and Off-Cycle Catalyst Cooperativity in Anion-Binding Catalysis

David D. Ford[†], Dan Lehnherr[†], C. Rose Kennedy, Eric N. Jacobsen*

Department of Chemistry and Chemical Biology, Harvard University, 12 Oxford Street, Cambridge, Massachusetts 02138, United States

jacobsen@chemistry.harvard.edu

Table of Contents for the Supporting Information

1. Procedures, Materials and Instrumentation

1.1 General experimental procedures

All reactions were performed in standard, oven- or flame-dried glassware fitted with rubber septa under an inert atmosphere of nitrogen unless otherwise described. Stainless steel syringes or cannulae were used to transfer air- and moisture-sensitive liquids. Reported concentrations refer to solution volumes at room temperature. Evaporation and concentration *in vacuo* was performed using house vacuum (~ 40 mm Hg). Column chromatography (using a Biotage® Isolera Four™) was done using reusable cartridges filled with ZEOprep® 60 (40–63 micron) silica gel from American Scientific. Thin layer chromatography (TLC) was used for reaction monitoring and product detection using pre-coated glass plates covered with 0.20 mm silica gel with fluorescent indicator; visualization by UV light (λ_{ex} = 254 nm) or $KMnO_4$ stain.

1.2 Materials

Reagents were purchased in reagent grade from commercial suppliers and used without further purification, unless otherwise described. Anhydrous solvents (toluene, *tert*-butylmethylether, CH_2Cl_2, MeOH) were prepared by passing the solvent through an activated alumina column. Triethylamine, *N*,*N*-diisopropylethylamine, and pyridine were distilled from CaH_2 at atmospheric pressure. Toluene-d_8 used for NMR experiments other than structure elucidation (e.g. NOESY and TOCSY experiments, serial dilution experiments) was distilled from CaH_2 and degassed by four freeze-pump-thaw cycles in which solvent was frozen in liquid nitrogen and the headspace was evacuated (~ 0.5 Torr). The solvent was then allowed to thaw while the flask isolated from the vacuum manifold. Synthetic procedures making use of H_2O refer to distilled water; brine refers to saturated aq. NaCl.

1.3 Instrumentation

Proton nuclear magnetic resonance (^{1}H NMR) spectra and proton-decoupled carbon nuclear magnetic resonance (^{13}C {^{1}H} NMR) spectra were recorded at 25 °C (unless stated otherwise) on Varian-Mercury-400 (400 MHz) or Varian Unity/Inova 500 (500 MHz) spectrometers at the Harvard University nuclear magnetic resonance facility. Chemical shifts for protons are reported in parts per million downfield from tetramethylsilane and are referenced to residual protium in the NMR solvent according to values reported in the literature.[1] Chemical shifts for carbon are reported in parts per million downfield from tetramethylsilane and are referenced to the carbon resonances of the solvent. The solvent peak was referenced to 7.26 ppm for ^{1}H and 77.0 ppm for ^{13}C for $CDCl_3$, to 3.31 ppm for ^{1}H and 49.15 ppm for ^{13}C for CD_3OD, to 5.32 ppm for ^{1}H and 54.0 ppm for ^{13}C for CD_2Cl_2, and to 2.09 ppm for ^{1}H and 20.4 ppm for ^{13}C for toluene-d_8. Data are represented as follows: chemical shift, integration, multiplicity (br = broad, s = singlet, d = doublet, t = triplet, q = quartet, qn = quintet, sp = septet, m = multiplet), coupling constants in Hertz (Hz). In the case of compounds containing one or more fluorine atom(s), it should be noted that ^{13}C NMR experiments were obtained without ^{19}F decoupling.

Optical rotations were measured using a 1 mL cell with a 5 cm path length on a Jasco P-2000 digital polarimeter.

Infrared spectra were recorded using a Bruker Tensor 27 FT-IR spectrometer. Data are represented as follows: frequency of absorption (cm^{-1}), intensity of absorption (s = strong, m = medium, w = weak, br = broad). In-situ IR kinetic experiments were carried out using a Mettler Toledo ReactIR™ iC 10 ATR FTIR spectrometer and a 9 mm AgX probe with a SiComp (silicon-based) window.

Low-resolution mass spectrometry was measured using an Agilent 6120 Quadrupole LC/MS, samples were injected in 0.1% formic acid in methanol and bypassed the LC column en route to the MS detector. High-resolution mass spectrometry was measured using a Bruker micrOTOF-QII™ ESI-Qq-TOF mass spectrometer calibrated using an aqueous sodium formate solution (prepared via adding 1 mL of 1 M aq. NaOH in 100 mL of 1% aq. formic acid). Additional high-resolution mass spectrometry was measured at the Small Molecule Mass Spectrometry Facility at Harvard University within the Faculty of Arts and Sciences using an Agilent 6220 Electrospray Time-of-Flight LC/MS.

---

(1) Gottlieb, H. E.; Kotlyar, V.; Nudelman, A. *J. Org. Chem.* **1997**, *62*, 7512–7515.

Chiral gas chromatography (GC) analysis was performed on a Hewlett-Packard 5890 gas chromatograph using an Alltech Cyclodex β (20 m x 0.25 mm) column, chiral high performance liquid chromatography (HPLC) analysis was performed using an Agilent 1200 quaternary HPLC system with a commercially available *S,S*-Whelk-01 chiral column.

X-ray crystallographic data was collected at the Harvard X-ray Laboratory. The structural refinement details for the X-ray crystallographic data is described in the individual CIFs. X-ray crystallographic data for (*ent*-**1a**)$_2$•hexane (CCDC 1478173), (*ent*-**1a**)$_2$•Me_4NCl (CCDC 1478172), (**1a**)•(*ent*-**1a**) (CCDC 1478175), (*ent*-**1b**)$_2$•Me_4NCl (CCDC 1478224), and **1c** (CCDC 1478176) have been deposited at the Cambridge Crystallographic Data Centre (CCDC), 12 Union Road, Cambridge CB21EZ, UK; fax: (+44)122-333-6033. These data can be obtained free of charge from The Cambridge Crystallographic Data Centre via the Internet at www.ccdc.cam.ac.uk/data_request/cif using the CCDC numbers given above.

1.4 Software

All curve fitting presented in this paper was carried out using KaleidaGraph 4.1.3[2] or the MatPlotLib[3] package in iPython Notebooks.[4] NMR spectra were processed with ACD/NMR Processor.[5] Computations were performed with Gaussian 09.[6] X-ray crystallographic and computed structures were rendered with CYLview.[7]

1.5 Abbreviations

aq = aqueous, atm = atmosphere, Boc = *tert*-butyl carbamate, *n*-BuLi = *n*-butyllithium, *s*-BuLi = *sec*-butyllithium, CSP = chiral stationary phase, DIPEA = diisopropylethylamine, DMAP = 4-dimethylaminopyridine, DMPU = 1,3-dimethyl-3,4,5,6-tetrahydro-2(1*H*)-pyrimidinone, EDC•HCl = 1-3(dimethylamino)propyl)-3-ethyl-carbodiimide hydrochloride, ee = enantiomeric excess, ESI = electrospray ionization, Et_2O = diethyl ether, Et_3N = triethylamine, EtOAc = ethyl acetate, EXSY = exchange spectroscopy, GC = gas chromatography, HBTU = *O*-benzotriazol-1-yl-*N*,*N*,*N*',*N*'-tetramethyluronium hexafluorophosphate, HPLC = high pressure liquid chromatography, HR = high-resolution, LC = liquid chromatography, LDA = lithium diisopropylamide, LR = low-resolution, MeOH = methanol, MS = mass spectrometry, NA = not applicable, NaOMe = sodium methoxide, ND = not determined, NOESY = nuclear Overhauser effect spectroscopy, PTFE = polytetrafluoroethylene, rt = room temperature, TBME = *tert*-butylmethyl ether, THF = tetrahydrofuran, TMAC = tetramethylammonium chloride, TLC = thin-layer chromatography, TOCSY = total correlation spectroscopy, TOF = time-of-flight, XRD = X-ray diffraction.

---

(2) KaleidaGraph Version 4.1.3 for Mac OS X, Synergy Software, Reading PA, 2011 (http://www.synergy.com).

(3) Hunter, J. D. *Comput. Sci. Eng.* **2007**, *9*, 90–95.

(4) Pérez, F.; Granger, B. E. *Comput. Sci. Eng.* **2007**, *9*, 21–29.

(5) ACD/NMR Processor Academic Edition, version 12.01. Advanced Chemistry Development, Inc.: Toronto, On, Canada, 2010.

(6) Gaussian 09, Revision A.02, M. J. Frisch, G. W. Trucks, H. B. Schlegel, G. E. Scuseria, M. A. Robb, J. R. Cheeseman, G. Scalmani, V. Barone, B. Mennucci, G. A. Petersson, H. Nakatsuji, M. Caricato, X. Li, H. P. Hratchian, A. F. Izmaylov, J. Bloino, G. Zheng, J. L. Sonnenberg, M. Hada, M. Ehara, K. Toyota, R. Fukuda, J. Hasegawa, M. Ishida, T. Nakajima, Y. Honda, O. Kitao, H. Nakai, T. Vreven, J. A. Montgomery, Jr., J. E. Peralta, F. Ogliaro, M. Bearpark, J. J. Heyd, E. Brothers, K. N. Kudin, V. N. Staroverov, R. Kobayashi, J. Normand, K. Raghavachari, A. Rendell, J. C. Burant, S. S. Iyengar, J. Tomasi, M. Cossi, N. Rega, J. M. Millam, M. Klene, J. E. Knox, J. B. Cross, V. Bakken, C. Adamo, J. Jaramillo, R. Gomperts, R. E. Stratmann, O. Yazyev, A. J. Austin, R. Cammi, C. Pomelli, J. W. Ochterski, R. L. Martin, K. Morokuma, V. G. Zakrzewski, G. A. Voth, P. Salvador, J. J. Dannenberg, S. Dapprich, A. D. Daniels, O. Farkas, J. B. Foresman, J. V. Ortiz, J. Cioslowski, and D. J. Fox, Gaussian, Inc., Wallingford CT, 2009.

(7) CYLview, Version 1.0b, C. Y. Legault, Université de Sherbrooke, Sherbrooke QC, 2009 (http://www.cylview.org/).

2. Synthetic Procedures and Characterization Data

2.1 Catalyst Synthesis

Scheme S1. General Procedure for Synthesis of Catalysts **1a** and **1b**

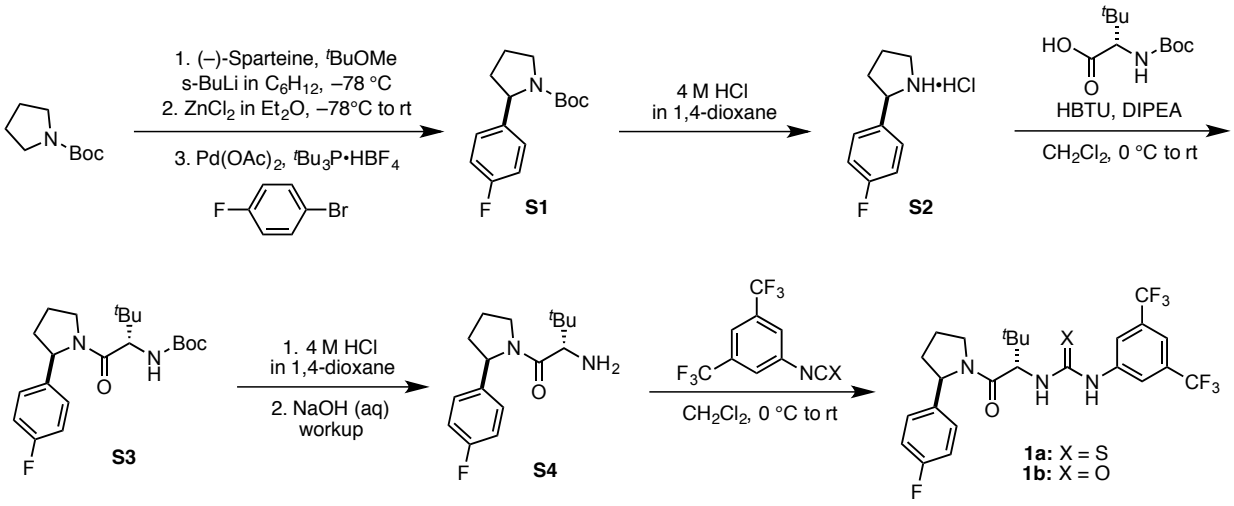

1-(3,5-bis(trifluoromethyl)phenyl)-3-((*S*)-1-((*R*)-2-(4-fluorophenyl)pyrrolidin-1-yl)-3,3-dimethyl-1-oxobutan-2-yl)thiourea (1a) was synthesized from **S4** following the published procedure, as shown in Scheme S1. Spectral data were in agreement with the published values.[8] $[\alpha]_D^{23}$ = +14.2° (c = 1.0, $CHCl_3$).

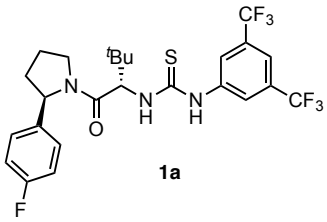

1-(3,5-bis(trifluoromethyl)phenyl)-3-((*R*)-1-((*S*)-2-(4-fluorophenyl)pyrrolidin-1-yl)-3,3-dimethyl-1-oxobutan-2-yl)thiourea (*ent*-1a) was synthesized from *ent*-**S4** in analogy to the literature procedure shown for **1a** in Scheme S1.[8] White solid. ^{1}H NMR (500 MHz, C_6D_6; under these conditions, *ent*-**1a** is a mixture of two rotamers in a 1:1.3 ratio, major rotamer denoted with *, minor denoted with §) δ 8.99 (br. s, 1H§), 7.99 (br. s, 1H*), 7.94 (s, 2H§), 7.78 (s, 2H*), 7.58 (d, *J* = 10.3 Hz, 1H§), 7.51 (br. s, 1 H§), 7.47 (br. s, 1 H*), 7.39 (d, *J* = 9.3 Hz, 1H*), 6.95–7.01 (m, 2H§, coincident with solvent ^{13}C satellite), 6.69–6.78 (m, 2H*, 2H§), 6.53 (t, *J* = 8.6 Hz, 2H*), 5.88 (d, *J* = 7.3 Hz, 1H§), 5.67 (d, *J* = 10.3 Hz, 1H§), 5.62 (d, *J* = 9.3 Hz, 1H*), 4.82 (d, *J* = 7.3 Hz, 1H*), 3.99–4.07 (m, 1 H*), 3.19–3.31 (m, 1H*, 2H§), 1.63–1.73 (m, 1H§), 1.47–1.58 (m, 1H*), 1.30–1.47 (m, 3H§), 1.14–1.29 (m, 3 H*), 1.08 (s, 9H*), 0.83 (s, 9H§). $[\alpha]_D^{23}$ = −15.2° (c = 1.0, $CHCl_3$). ESI HRMS *m/z* calculated for $C_{25}H_{27}F_7N_3OS$ ([M + H]$^+$) 550.1758, found 550.1773.

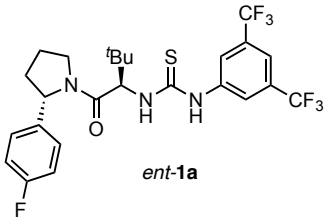

Crystals suitable for X-ray crystallographic analysis were obtained from a solution of *ent*-**1a** in CH_2Cl_2 which had been layered with hexanes and allowed to slowly evaporate at rt. X-ray data for (*ent*-**1a**)$_2$•*n*-hexane (CCDC 1478173): $C_{56}H_{66}F_{14}N_6O_2S_2$, M_r = 1185.27; crystal dimensions (mm) 0.36 × 0.24 × 0.18; triclinic space group *P*1; *a* = 11.5955(2) Å, *b* = 11.8094(2) Å, *c* = 13.3744(2) Å; α =112.922(1) °, β = 92.390(1) °, γ = 117.085(1) °; *V* = 1447.26(4) Å^3; *Z* = 1; ρ_{calcd} = 1.360 g cm^{-3}; μ = 1.63 mm^{-1}; λ = 1.54178 Å; *T* = –173 °C; 9239 measured, 9239 independent, and 8978 observed [$I \geq 2\sigma(I)$] reflections, R_{int} = 0.059; $R[F^2 \geq 2\sigma(F^2)]$ = 0.052, $wR(F_o^2)$ = 0.129 for 773 parameters, 123 restraints, and 9239 unique reflections; $\Delta\rho_{max}$ = 0.68 e Å^{-3}, $\Delta\rho_{min}$ = –0.35 e Å^{-3}; flack parameter = 0.08(2). See Section 4.1 for discussion.

[8] Reisman, S. E.; Doyle, A. G.; Jacobsen, E. N. *J. Am. Chem. Soc.* **2008**, *130*, 7198–7199.

Crystals suitable for X-ray crystallographic analysis were obtained from a solution of *ent*-**1a** and tetramethylammonium chloride (TMAC) in MeOH/$CHCl_3$ which had been layered with hexanes and allowed to slowly evaporate at rt. X-ray data for (*ent*-**1a**)$_2$•TMAC (CCDC 1478172): $C_{54}H_{64}ClF_{14}N_7O_2S_2$, M_r = 1208.69; crystal dimensions (mm) 0.22 × 0.16 × 0.10; monoclinic space group $P2_1$; a = 10.1941 (8) Å, b = 26.676 (2), Å, c = 12.0718 (9) Å; β = 113.107 (1) °; V = 3019.4 (4) Å^3; Z = 2; ρ_{calcd} = 1.329 g cm^{-3}; μ = 0.22 mm^{-1}; λ = 1.54178 Å; T = –173 °C; 40884 measured, 15584 independent, and 15584 observed [$I \geq 2\sigma(I)$] reflections, R_{int} = 0.035; $R[F^2 \geq 2\sigma(F^2)]$ = 0.040, $wR(F_o^2)$ = 0.088 for 760 parameters, 44 restraints, and 15584 unique reflections; $\Delta\rho_{max}$ = 0.38 e Å^{-3}, $\Delta\rho_{min}$ = –0.33 e Å^{-3}; flack parameter = 0.00(3). See Section 4.2 for discussion.

Crystals suitable for X-ray crystallographic analysis were obtained from a solution of approximately 1:1 ratio of **1a** and *ent*-**1a** in CH_2Cl_2 which had been layered with hexanes and allowed to slowly evaporate at rt. X-ray data for [(**1a**•*ent*-**1a**)(**1a**•*ent*-**1a**)] (CCDC 1478175): $C_{100}H_{104}F_{28}N_{12}O_4S_4$, M_r = 2198.21; crystal dimensions (mm) 0.24 × 0.18 × 0.14; triclinic space group $P1$; a = 113.1841 (3) Å, b =20.3186 (4), Å, c = 20.8594 (4) Å; α =104.092 (1) °, β = 101.305 (1) °, γ = 100.497 (1) °; V = 5156.93 (18) Å^3; Z = 2; ρ_{calcd} = 1.416 g cm^{-3}; μ = 1.79 mm^{-1}; λ = 1.54178 Å; T = –173 °C; 133726 measured, 16852 independent, and 13541 observed [$I \geq 2\sigma(I)$] reflections, R_{int} = 0.044; $R[F^2 \geq 2\sigma(F^2)]$ = 0.079, $wR(F_o^2)$ = 0.206 for 1413 parameters, 403 restraints, and 16852 unique reflections; $\Delta\rho_{max}$ = 0.87 e Å^{-3}, $\Delta\rho_{min}$ = –0.84 e Å^{-3}.

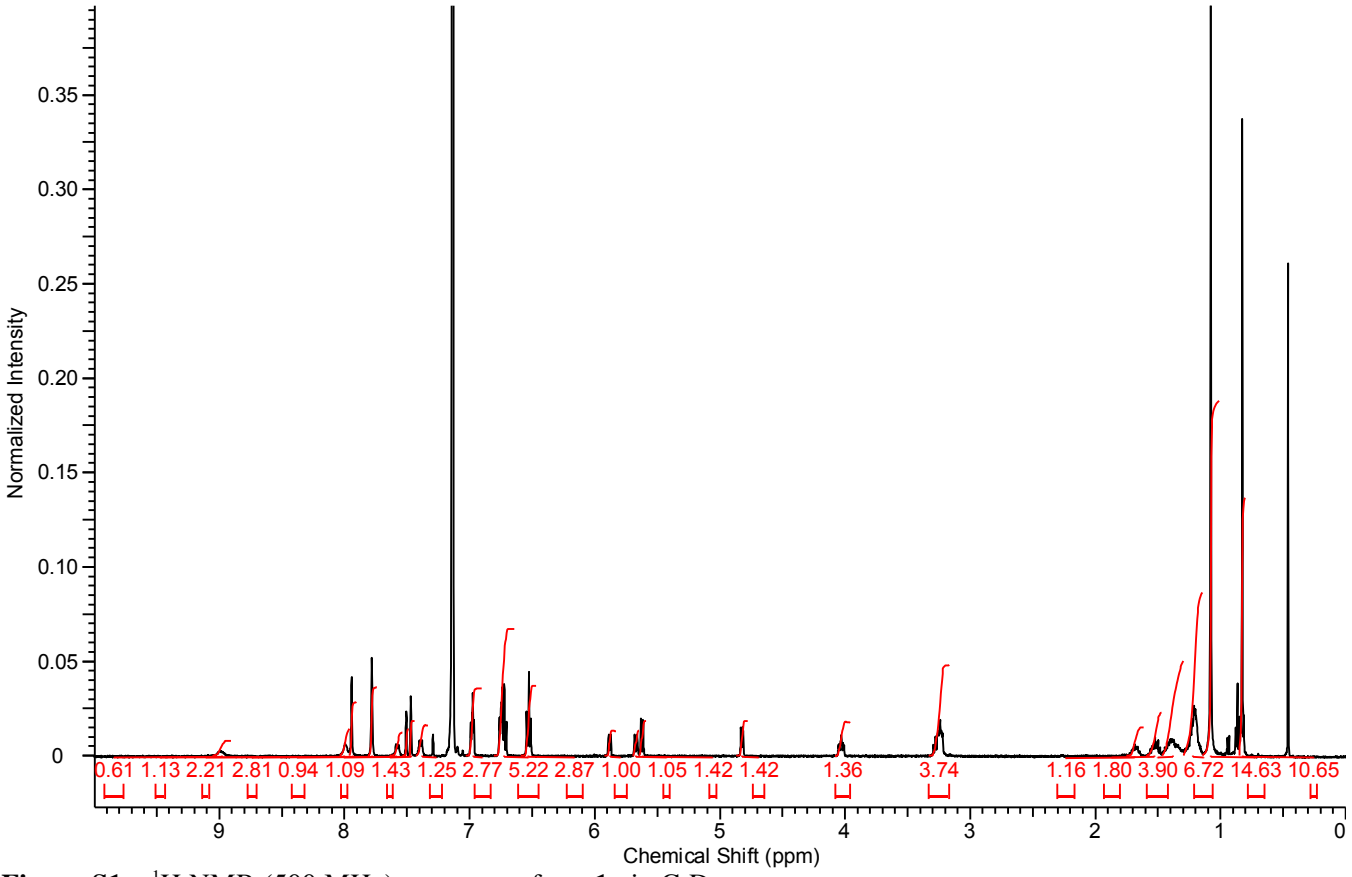

Figure S1a. ^{1}H NMR (500 MHz) spectrum of *ent*-**1a** in C_6D_6.

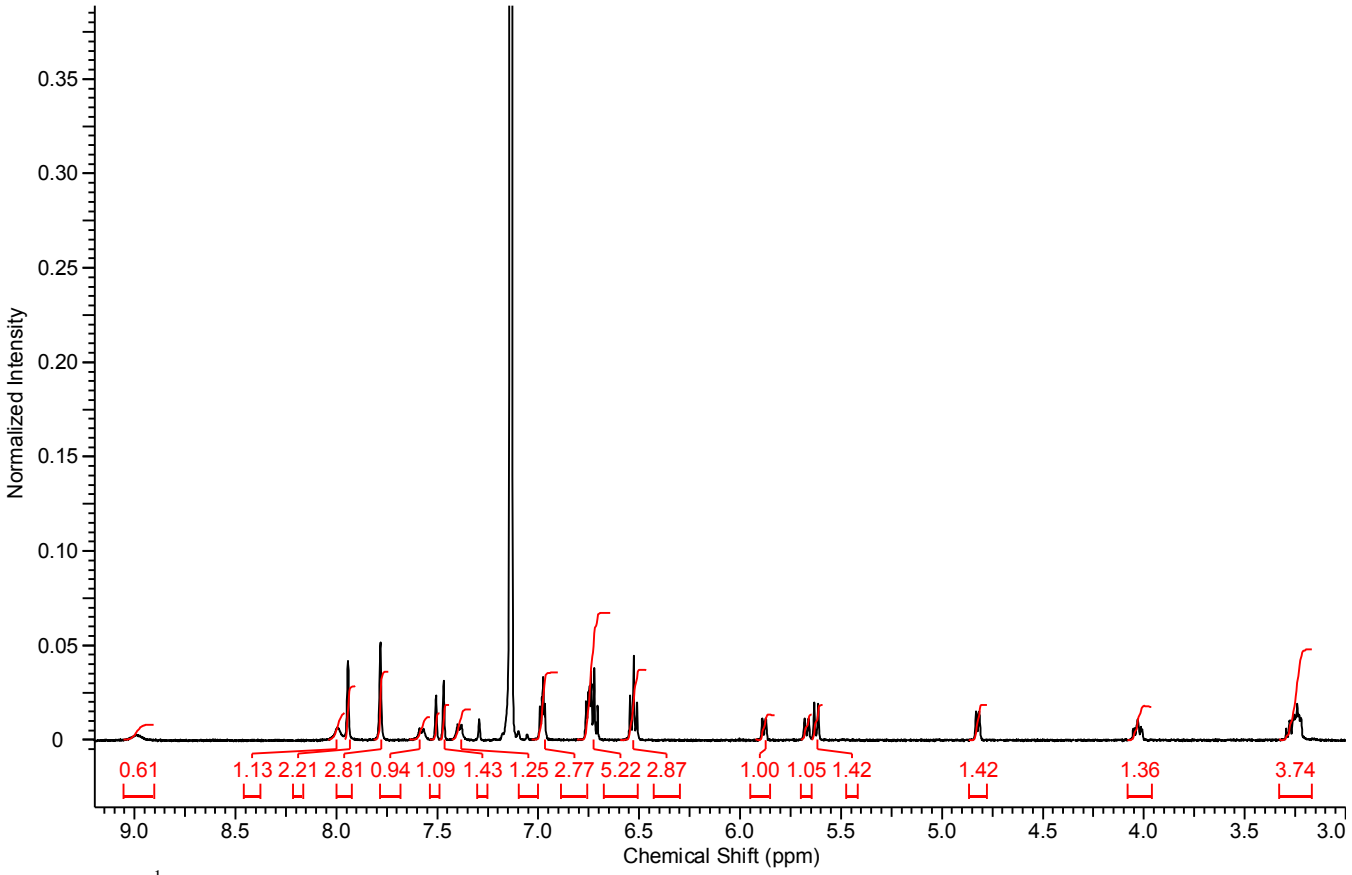

Figure S1b. ^{1}H NMR (500 MHz) spectrum of *ent*-**1a** in C_6D_6 (detail).

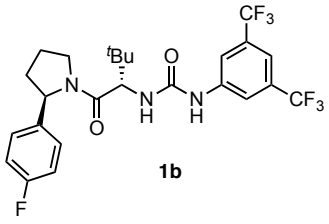

1b

1-(3,5-bis(trifluoromethyl)phenyl)-3-((*S*)-1-((*R*)-2-(4-fluorophenyl)pyrrolidin-1-yl)-3,3-dimethyl-1-oxobutan-2-yl)urea (1b) was synthesized from **S3** in analogy to the literature procedure shown for **1a** in Scheme S1.[8] To *tert*-butyl ((*S*)-1-((*R*)-2-(4-fluorophenyl)pyrrolidin-1-yl)-3,3-dimethyl-1-oxobutan-2-yl)carbamate (**S3**, 0.470 g, 1.24 mmol), was added hydrogen chloride (4 M solution in 1,4-dioxane; 5 mL, 16 equiv). This mixture was maintained at room temperature for 1 h, and the reaction mixture was diluted with CH_2Cl_2 (30 mL) before careful addition of 1 M aq. NaOH (30 mL). The mixture was stirred rapidly, and NaOH pellets were slowly added until the pH of the aqueous layer measured to be > 12 using pH paper. The organic layer was separated, and dried over Na_2SO_4 before concentrating under reduced pressure. The residue was dissolved in 6 mL CH_2Cl_2, and 3,5-bis(trifluoromethyl)phenyl isocyanate (236 µL, 1.36 mmol, 1.1 equiv) was added while stirring. This mixture was maintained for 12 h at rt before removing the solvent *in vacuo*. The crude residue was purified by column chromatography (silica gel, gradient 10% to 30% EtOAc in hexanes) to afford **1b** (0.510 g, 77% yield over 2 steps) as a white powder. ^{1}H NMR (500 MHz, $CDCl_3$; under these conditions, **1b** is a mixture of two rotamers in a 1:1.3 ratio, major rotamer denoted with *, minor denoted with §) δ 8.44 (br. s. 1H§), 8.29–8.29 (m, 1H*), 8.29 (s, 2H*), 7.91 (s, 2 H§), 7.86 (s, 2 H*), 7.51 (s, 1 H*, 1 H§), 7.34 (dd, *J* = 8.7, 5.0 Hz, 2H§), 7.10 (t, *J* = 8.5 Hz, 2H§), 6.74–6.80 (m, 2 H*), 6.66–6.73 (m, 2H*), 5.95 (app. d, *J* = 10.1 Hz, 1H*, 1H§), 5.30 (d, *J* = 6.4 Hz, 1 H§), 5.08 (d, *J* = 7.3 Hz, 1H*), 4.84 (d, *J* = 9.6 Hz, 1H*), 4.52 (d, *J* = 10.1 Hz, 1H§), 4.09–4.19 (m, 1H*), 3.83 (d, *J* = 7.3 Hz, 1H*), 3.59–3.73 (m, 2H§), 2.34–2.44 (m, 1H§), 2.23–2.33 (m, 1H*), 2.10–2.21 (m, 1H§), 1.83–2.03 (m, 3H*, 2H§), 1.12 (s, 9H*), 0.69 (s, 9H§). ^{13}C NMR (126 MHz, $CDCl_3$): δ 173.3, 171.9, 162.3 (d, *J* = 246 Hz), 161.4 (d, *J* = 245 Hz), 155.0, 154.4, 141.3, 141.2, 139.2 (d, *J* = 4 Hz), 136.3 (d, *J* = 3 Hz), 132.0 (q, *J* = 33 Hz), 132.0 (q, *J* = 33 Hz), 128.4 (d, *J* = 8 Hz), 126.4 (d, *J* = 8 Hz), 123.4 (q, *J* = 273 Hz), 123.3 (q, *J* = 273 Hz), 118.5 (br s), 118.3 (br s), 115.8 (d, *J* = 22 Hz), 115.2–115.5 (m), 115.0–115.2 (m), 114.7 (d, *J* = 21 Hz), 61.9, 60.1, 57.9, 56.6, 49.0, 47.5, 35.5, 35.4, 35.0, 34.0, 26.6, 26.5, 23.0, 21.6. IR (ATR, neat): 2361 (w), 2342 (w), 1706 (m), 1646 (m), 1613 (m), 1570 (m), 1510 (m), 1442 (m), 1387 (m), 1276 (s), 1223 (m), 1175 (s), 1128 (s), 1062 (m), 949 (m), 880 (m) cm^{-1}. $[\alpha]_D^{23}$ = +81.6° (c = 1.0, $CHCl_3$). ESI MS *m/z* calculated for $C_{25}H_{27}F_7N_3NaO_2$ ($[M + Na]^+$) 556.2, found 556.2.

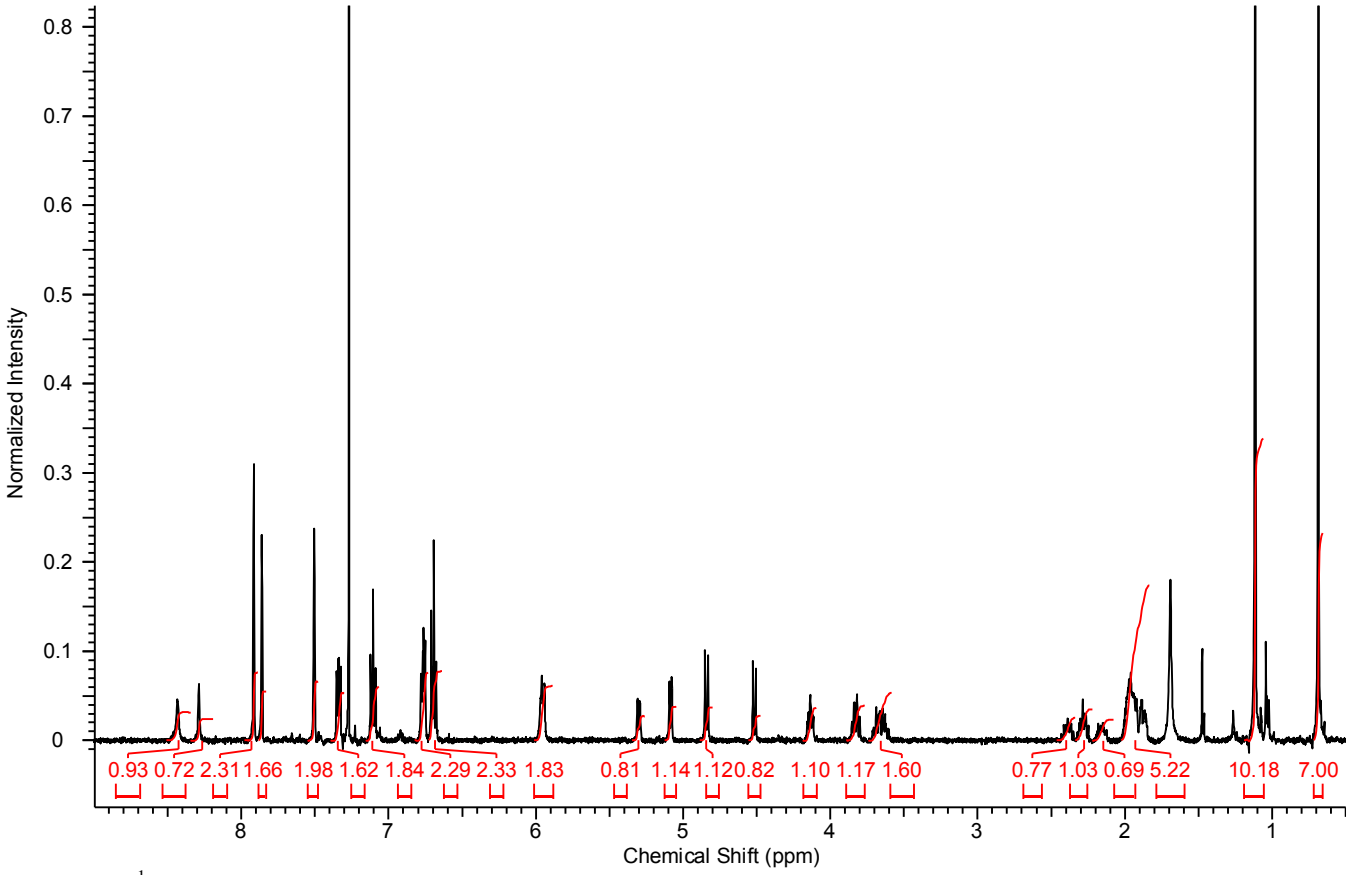

Figure S2. ^{1}H NMR (500 MHz) spectrum of **1b** in $CDCl_3$.

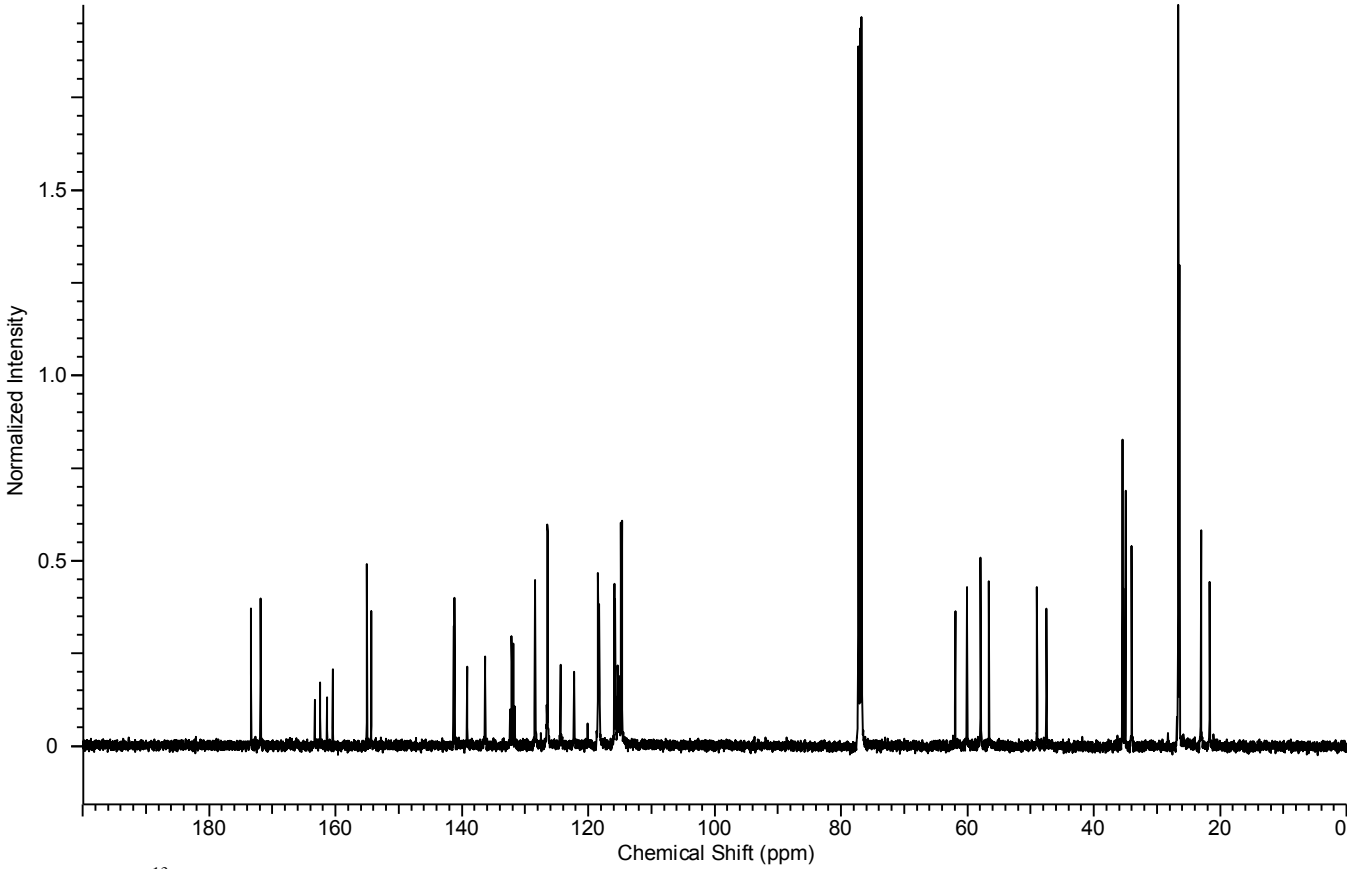

Figure S3a. ^{13}C NMR (126 MHz) spectrum of **1b** in $CDCl_3$.

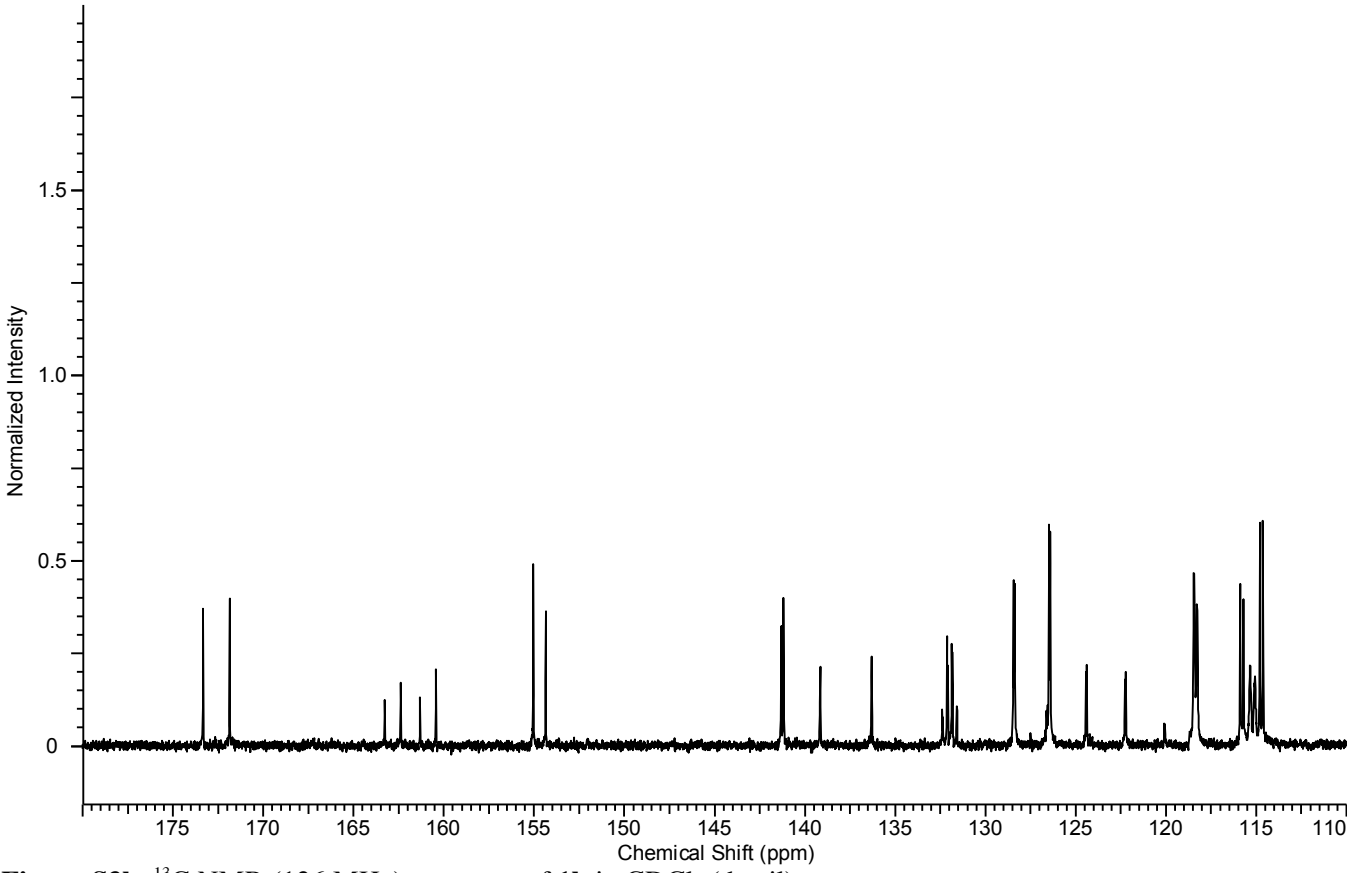

Figure S3b. ^{13}C NMR (126 MHz) spectrum of **1b** in $CDCl_3$ (detail).

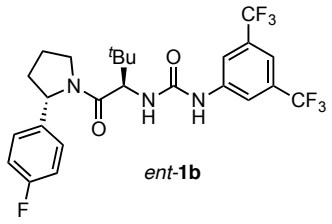

ent-**1b**

1-(3,5-bis(trifluoromethyl)phenyl)-3-((*R*)-1-((*S*)-2-(4-fluorophenyl)pyrrolidin-1-yl)-3,3-dimethyl-1-oxobutan-2-yl)urea (*ent*-1b) was synthesized from *ent*-**S3** in analogy to the procedure described for **1b** (above), which was adapted from the literature procedure shown for **1a** in Scheme S1.[8] White solid. ^{1}H NMR (500 MHz, $CDCl_3$; under these conditions, *ent*-**1b** is a mixture of two rotamers in a 1:1.3 ratio, major rotamer denoted with *, minor denoted with §): δ 8.55 (br s, 1H*), 8.33 (br s, 1H§), 7.92 (s, 2H*), 7.86 (s, 2H§), 7.51 (br. s., 1H*, 1H§), 7.38–7.31 (m, 2H§), 7.11 (t, J = 8.5 Hz, 2H§), 6.79–6.71 (m, 2H*), 6.71–6.65 (m, 2H*), 5.97 (m, 1H*, 1H§), 5.30 (d, J = 6.9 Hz, 1H§), 5.08 (d, J = 7.3 Hz, 1H*), 4.86 (d, J = 9.6 Hz, 1H*), 4.52 (d, J = 10.1 Hz, 1H§), 4.10–4.19 (m, 1 H*), 3.83 (m, 1H*), 3.73–3.58 (m, 2H§), 2.39 (m, 1H§), 2.28 (m, 1H*), 2.15 (m, 1H§), 2.04 (m, 3H*, 2H§), 1.13 (s, 9H*), 0.69 (s, 9H§). $[\alpha]_D^{23}$ = −87.2º (c = 1.0, $CHCl_3$). ESI HRMS *m/z* calculated for $C_{25}H_{27}F_7N_3NaO_2$ ($[M + H]^+$) 534.1986, found 534.1998.

Crystals suitable for X-ray crystallographic analysis were obtained from a solution of *ent*-**1b** and TMAC in MeOH/$CHCl_3$ which had been layered with hexanes and allowed to slowly evaporate at rt. X-ray data for (*ent*-**1b**)$_2$• (TMAC) (CCDC 1478224): $C_{54}H_{64}ClF_{14}N_7O_4$, M_r = 1176.57; crystal dimensions (mm) 0.18 × 0.08 × 0.02; monoclinic space group $C2$; a = 21.9073(11) Å, b = 10.2539(5), Å, c = 15.4936(8) Å; β = 119.671(3) °; V = 3024.1(3) Å^3; Z = 2; ρ_{calcd} = 1.292 g cm^{-3}; μ = 1.36 mm^{-1}; λ = 1.54178 Å; T = –93 °C; 30851 measured, 4931 independent, and 4321 observed [$I \geq 2\sigma(I)$] reflections, R_{int} = 0.068; $R[F^2 \geq 2\sigma(F^2)]$ = 0.078, $wR(F_o^2)$ = 0.202 for 410 parameters, 119 restraints, and 4931 unique reflections; $\Delta\rho_{max}$ = 0.33 e Å^{-3}, $\Delta\rho_{min}$ = –0.31 e Å^{-3}; flack parameter = 0.03(4). See Section 4.1 for discussion.

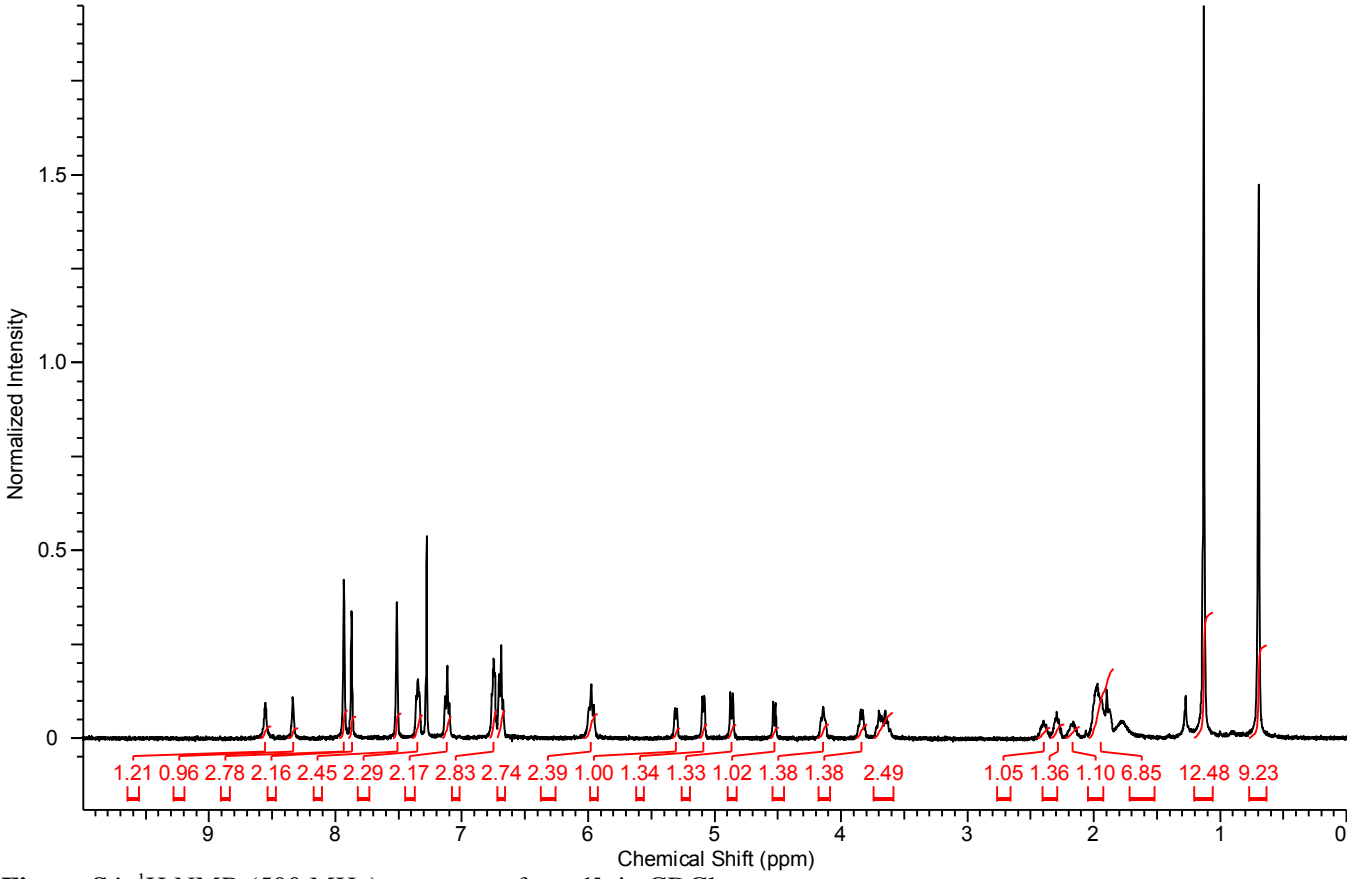

Figure S4. ^{1}H NMR (500 MHz) spectrum of *ent*-**1b** in $CDCl_3$.

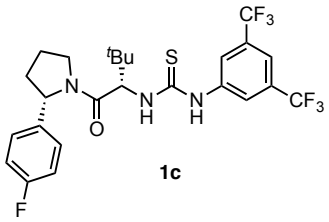

1c

1-(3,5-bis(trifluoromethyl)phenyl)-3-((*S*)-1-((*S*)-2-(4-fluorophenyl)pyrrolidin-1-yl)-3,3-dimethyl-1-oxobutan-2-yl)thiourea (1c) was synthesized from *ent*-**S2** and (*S*)-2-((*tert*-butoxycarbonyl)amino)-3,3-dimethylbutanoic acid in analogy to the literature procedure shown for **1a** in Scheme S1.[8] White solid. $[\alpha]_D^{24}$ = –154 ° (c = 1.0, $CHCl_3$). IR (ATR, film cast from $CHCl_3$): 3311 (w), 3106 (w), 2967 (w), 2881 (w), 1606 (w), 1532 (m), 1510 (m), 1473 (w), 1458 (w), 1441 (w), 1382 (w), 1322 (w), 1275 (s), 1221 (m), 1176 (s), 1127 (s), 1108 (m), 1036 (w), 1015 (w), 1001 (w), 963 (m), 940 (w), 908 (m), 879 (w), 832 (m), 781 (w), 731 (s), 698 (m), 680 (m), 650 (w), 635 (w), 622 (w) cm^{-1}. ^{1}H NMR (500 MHz, $CDCl_3$): δ 9.05 (s, 1H), 7.91 (s, 2H), 7.86 (d, *J* = 8.7 Hz, 1H), 1H, 7.57 (s, 1H), 7.12 (dd, *J* = 8.5, 5.3 Hz, 2H), 6.94 (t, *J* = 8.5 Hz, 2H), 5.33. (d, *J* = 9.2 Hz, 1H), 4.90 (t, *J* = 7.1 Hz, 1H), 4.51–4.40 (m, 1H), 3.84–3.75 (m, 1H), 2.30–1.82 (m, 4H), 0.97 (s, 9H). ^{13}C NMR (125 MHz, $CDCl_3$): δ 181.7, 172.5, 161.7 (d, *J* = 246 Hz), 140.1, 138.1 (d, *J* = 2.8 Hz), 131.6 (q, *J* = 33.3 Hz), 127.9 (d, *J* = 8.2 Hz), 123.5, 123.0 (d, *J* = 273 Hz), 118.1, 115.1 (d, *J* = 22.0 Hz), 63.7, 62.1, 49.7, 35.7, 34.0, 27.2, 24.9. ESI HRMS *m/z* calculated for $C_{25}H_{26}F_7N_3OSNa$ ([M + Na]$^+$) 572.1577, found 572.1581.

Crystals suitable for X-ray crystallographic analysis were obtained from a solution of **1c** in CH_2Cl_2 which had been layered with hexanes and allowed to slowly evaporate at rt. X-ray data for **1c** (CCDC 1478176): $C_{75}H_{78}F_{21}N_9O_3S_3$, M_r = 1648.64; crystal dimensions (mm) 0.20 × 0.18 × 0.12; monoclinic space group *C*2; *a* = 22.6193(6) Å, *b* = 12.2384(3), Å, *c* = 29.5286(7) Å; β = 92.679(2) °; *V* = 8165.3(4) Å^3; *Z* = 4; ρ_{calcd} = 1.341 g cm^{-3}; μ = 0.19 mm^{-1}; λ = 1.54178 Å; *T* = –173 °C; 9479 measured, 9479 independent, and 8658 observed [$I \geq 2\sigma(I)$] reflections, R_{int} = 0.051; $R[F^2 \geq 2\sigma(F^2)]$ = 0.035, $wR(F_o^2)$ = 0.089 for 1083 parameters, 128 restraints, and 9479 unique reflections; $\Delta\rho_{max}$ = 0.44 e Å^{-3}, $\Delta\rho_{min}$ = –0.31 e Å^{-3}; flack parameter = 0.07(2). See Section 4.1 for discussion.

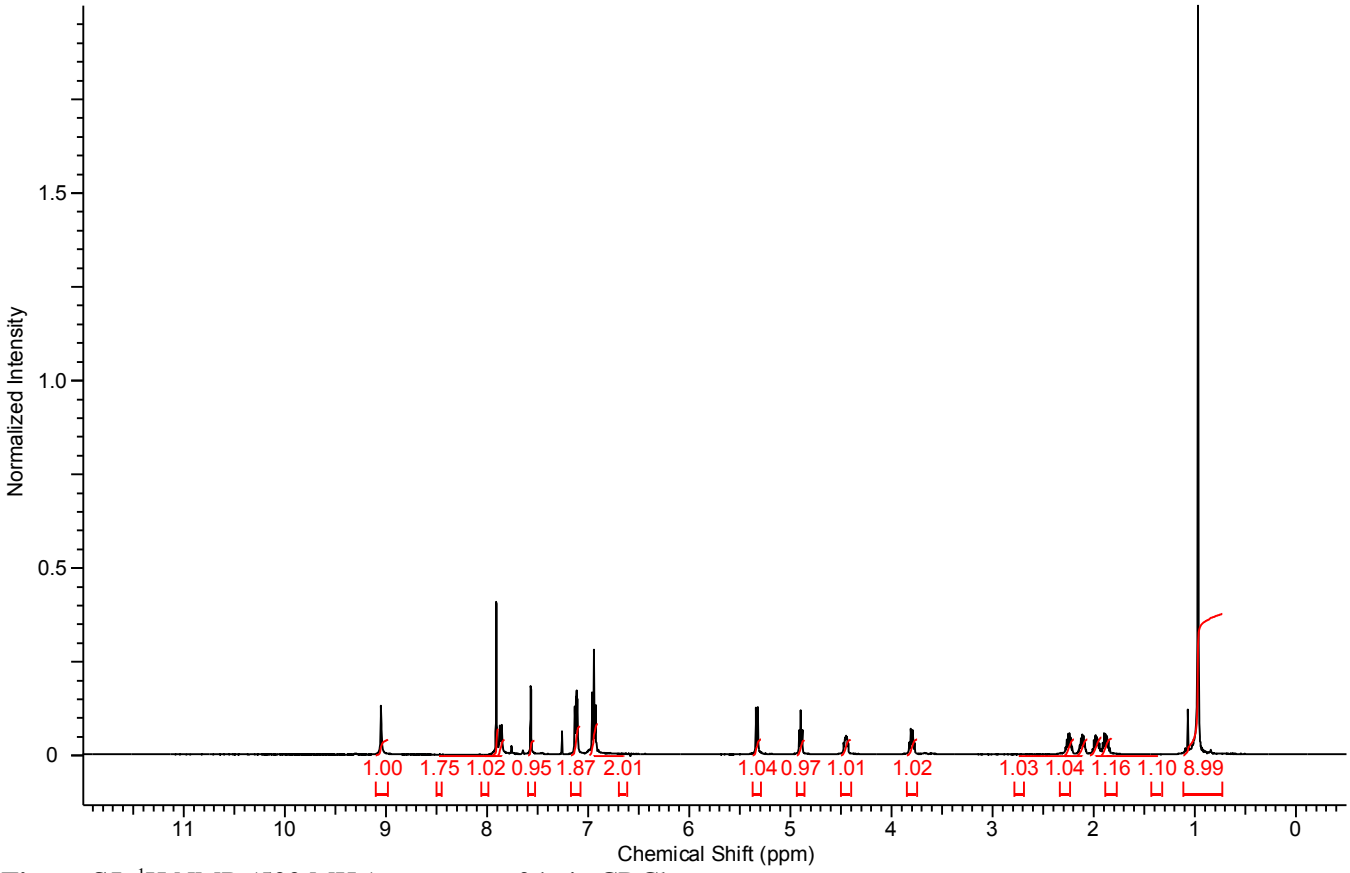

Figure S5. ^{1}H NMR (500 MHz) spectrum of **1c** in $CDCl_3$.

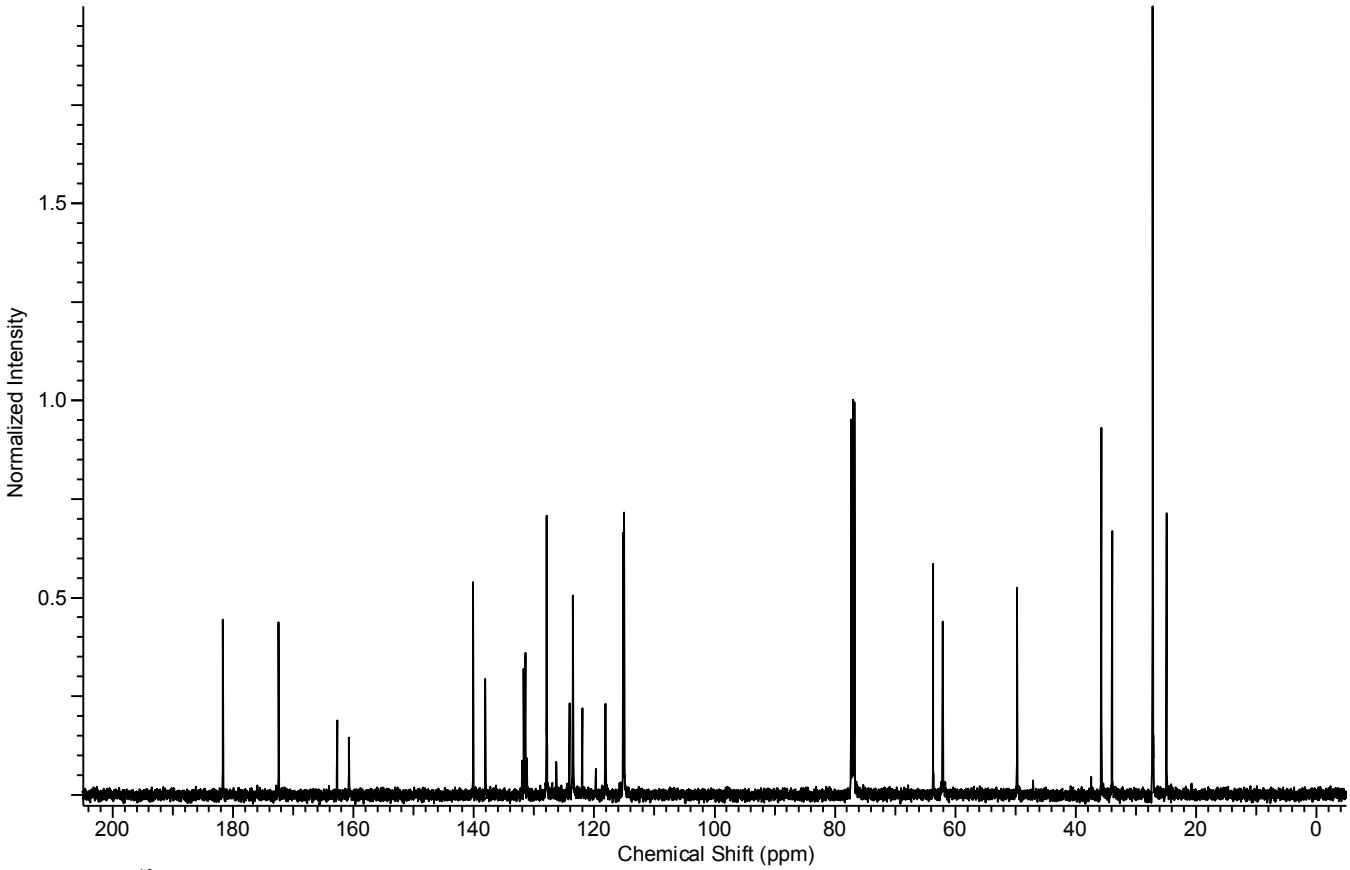

Figure S6. ^{13}C NMR (125 MHz) spectrum of **1c** in $CDCl_3$.

1-(3,5-bis(trifluoromethyl)phenyl)-3-((*S*)-1-((*S*)-2-(4-fluorophenyl)pyrrolidin-1-yl)-3,3-dimethyl-1-oxobutan-2-yl)urea (1d) was synthesized from *ent*-**S2** and (*S*)-2-((*tert*-butoxycarbonyl)amino)-3,3-dimethylbutanoic acid in analogy to the procedure described for **1b** (above), which was adapted from the literature procedure shown for **1a** in Scheme S1.[8] White solid. $[\alpha]_D^{24}$ = –161 ° (c = 1.0, $CHCl_3$). IR (ATR, film cast from $CHCl_3$): 3356 (w), 3115 (w), 2974 (w), 2884 (w), 1703 (w), 1609 (m), 1562 (w), 1511 (w), 1475 (w), 1440 (w), 1387 (m), 1325 (w), 1277 (s), 1224 (w), 1177 (m), 1126 (s), 1065 (w), 1033 (w), 1015 (w), 1000 (w), 949 (w), 909 (w), 878 (w), 848 (w), 831 (w), 733 (m), 702 (w), 682 (w), 650 (w), 620 cm^{-1}. ^1H NMR (500 MHz, $CDCl_3$, under these conditions, **1d** is a mixture of two rotamers in a 1:3.1 ratio, major rotamer denoted with *, minor denoted with §): δ 8.52 (s, 1H§), 7.94 (s, 1H*), 7.58 (s, 2H§), 7.53 (s, 2H*), 7.42 (s, 1H§), 7.28 (s, 1H*), 7.17 (dd, *J* = 8.5, 5.3 Hz, 2H*), 7.09 (dd, *J* = 8.7, 5.0 Hz, 2H§), 7.00–6.87 (m, 2H* + 2H§), 6.60 (d, *J* = 9.1 Hz, 1H*), 6.31 (d, *J* = 8.7 Hz, 1H§), 5.35 (d, *J* = 7.3 Hz, 1H§), 5.08 (t, *J* = 6.9 Hz, 1H*), 4.64 (d, *J* = 9.2 Hz, 1H*), 4.50 (d, *J* = 8.7 Hz, 1H§), 4.28–4.12 (m 1H*), 3.88–3.80 (m 1H* + 1H§), 3.74–3.62 (m, 1H§), 2.52–1.80 (m, 4H*, 4H§), 1.06§ (s, 9H), 0.96* (s, 9H). ^{13}C NMR (125 MHz, $CDCl_3$, under these conditions, **1d** is a mixture of two rotamers in a 1:3.1 ratio, major rotamer denoted with *, minor denoted with §): δ 173.4*, 172.5§, 162.2§ (d, *J* = 242 Hz), 161.8* (d, *J* = 245 Hz), 155.4*, 154.0§, 140.9§, 140.5*, * 138.1 (d, *J* = 2.8 Hz), 137.4§ (d, *J* = 2.8 Hz), 131.9§ (q, *J* = 33.5 Hz), 131.5* (q, *J* = 33.3 Hz), 127.9* (d, *J* = 8.2 Hz), 126.9§ (d, *J* = 8.2 Hz), 123.2§ (q, *J* = 273 Hz), 123.1* (q, *J* = 273 Hz), 119.1, 118.1*, 115.7§ (d, *J* = 22.0 Hz), 115.1* (d, *J* = 21.1 Hz), 62.2§, 61.8*, 59.2*, 58.3§, 49.5*, 47.3§, 36.4§, 35.7§, 35.1*, 33.8*, 27.0*, 26.7§, 24.7*, 21.1§. ESI HRMS *m/z* calculated for $C_{25}H_{26}F_7N_3O_2Na$ ([M + Na]$^+$) 556.1805, found 556.1814.

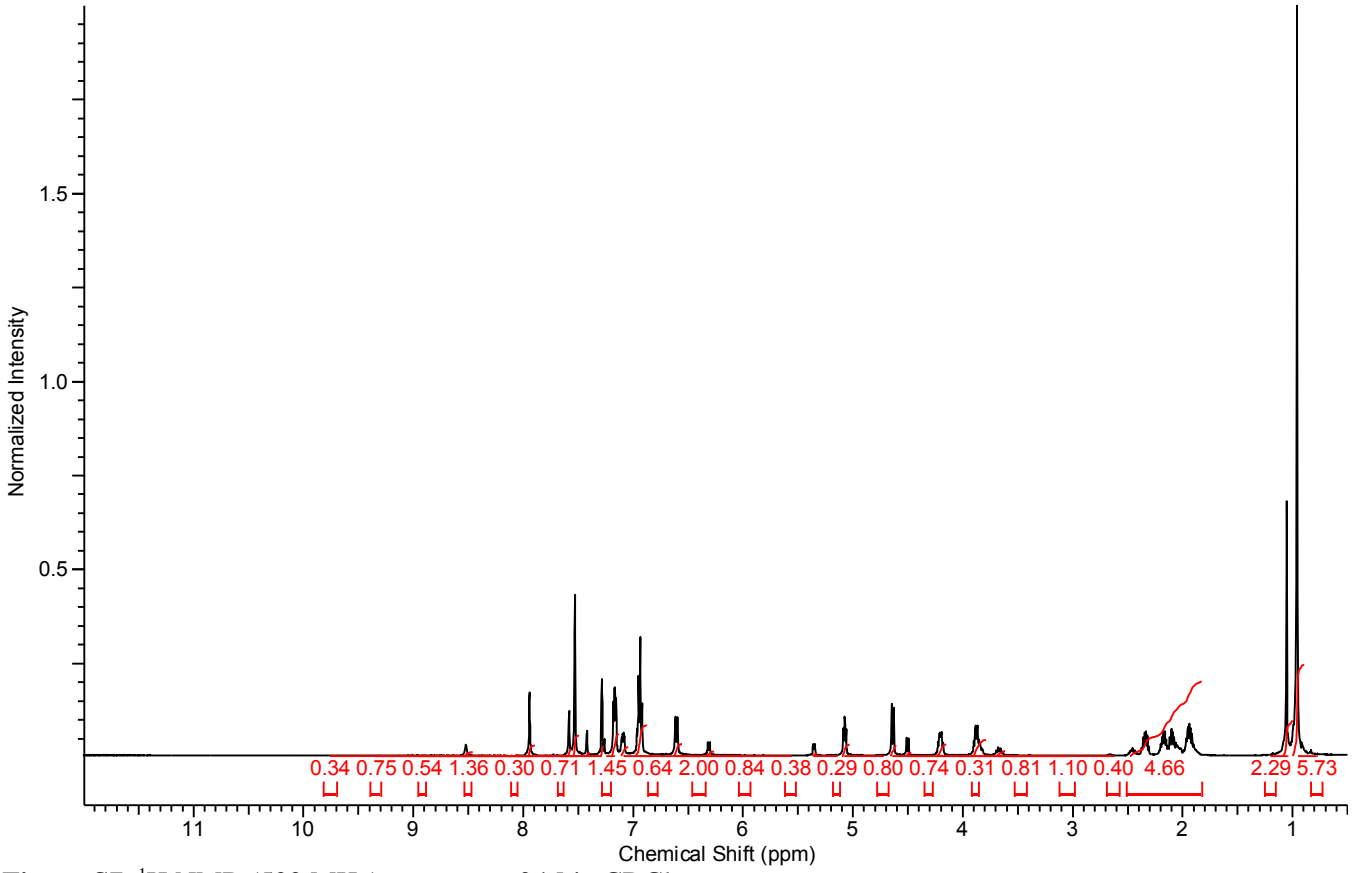

Figure S7. ^1H NMR (500 MHz) spectrum of **1d** in $CDCl_3$.

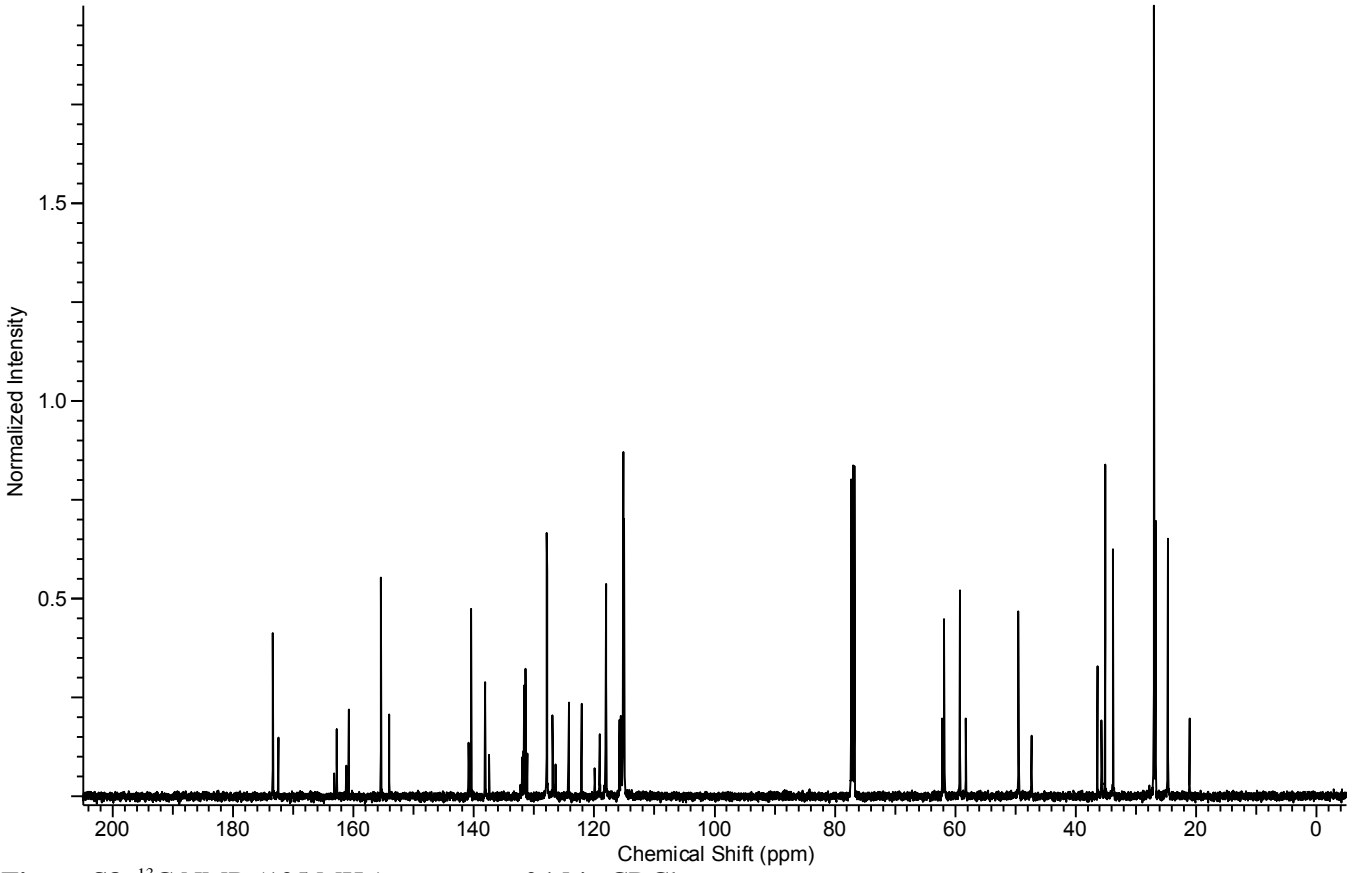

Figure S8. ^{13}C NMR (125 MHz) spectrum of **1d** in $CDCl_3$.

2.2 α-Chloroisochroman Synthesis

Scheme S2. Procedure for Synthesis of α-Chloroisochroman **(2)**

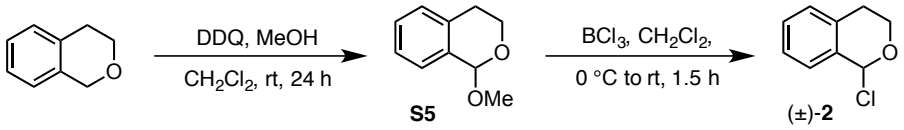

α-Chloroisochroman (2) was synthesized from isochroman following a published procedure shown in Scheme S2.[8] Spectral data were in agreement with the previously reported values.

2.3 Silyl Ketene Acetal Synthesis

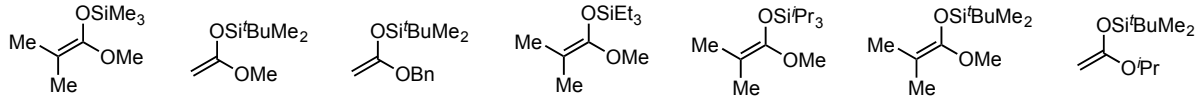

Silyl ketene acetals (**3a–g)** were synthesized according to the procedure described previously for **3b**[9] or purchased from commercial sources (**3a**). Deuterated silyl ketene acetal **3c**-d_2 was prepared via the modified sequence shown in Scheme S3.

Scheme S3. Synthesis of deuterated silyl ketene acetal **3c**-d_2.

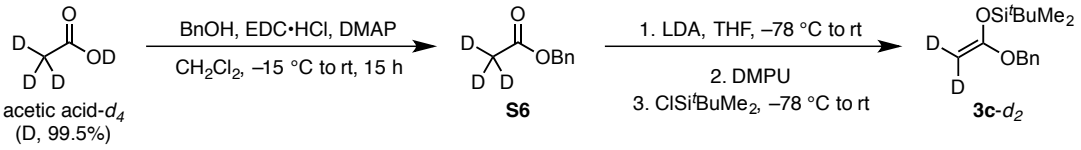

benzyl acetate-d_3 (S6): To a solution of EDC•HCl (9.57 g, 49.9 mmol) in dichloromethane (30 mL) at –15 °C was added acetic acid-d_4 (2.91 mL, 3.05 g, 47.5 mmol; 99.5% deuterium, commercially available from Cambridge Isotope Labs), benzyl alcohol (5.91 mL, 6.17 g, 57.1 mmol), and DMAP (5.81 g, 47.5 mmol). The mixture was stirred at –15 °C for 20 min, then cooling bath was removed and the mixture was allowed to warm to rt and stir for 14 h before being diluted with CH_2Cl_2 and poured into 5% aq. $NaHCO_3$. The combined organic phase was washed with H_2O, dried over anhyd. Na_2SO_4, filtered, and the solvent was removed *in vacuo*. Column chromatography (silica gel, gradient 20% to 40% CH_2Cl_2 in hexanes) afforded **S10** (6.04 g, 83%) as a clear colorless liquid. R_f = 0.40 (30% CH_2Cl_2 in hexanes). IR (ATR, neat): 3067 (w), 3035 (w), 2954 (w), 2894 (w), 1733 (s), 1587 (w), 1499 (w), 1456 (w), 1376 (w), 1241 (s), 1074 (m), 1030 (w), 973 (w), 915 (w), 821 (w), 786 (w), 744 (m), 697 (m) cm^{-1}. ^1H NMR (500 MHz, $CDCl_3$): δ 7.42–7.26 (m, 5H), 5.17 (s, 2H). ^{13}C NMR (125 MHz, $CDCl_3$): δ 170.7, 135.9, 128.4, 128.1, 128.1, 66.1, 20.2 (sp, $J_{C–D}$ = 20.1 Hz). ESI HRMS *m/z* calculated for $C_9H_7D_3O_2$ ($[M + Na]^+$) 176.0761, found 176.0760.

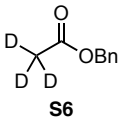

(9) Wenzel, A. G.; Jacobsen, E. N. *J. Am. Chem. Soc.* **2002**, *124*, 12964–12965.

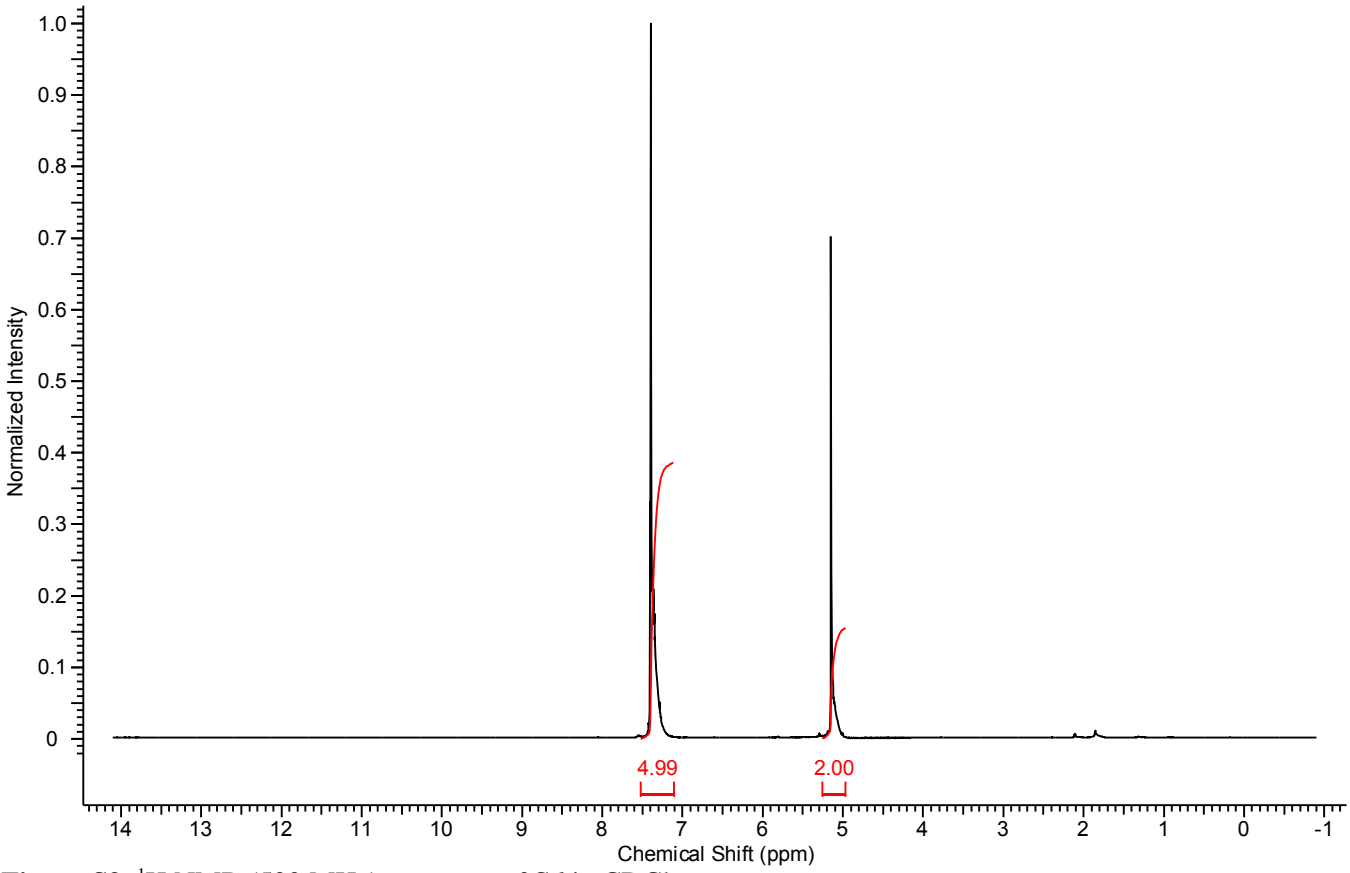

Figure S9. ^{1}H NMR (500 MHz) spectrum of **S6** in $CDCl_3$.

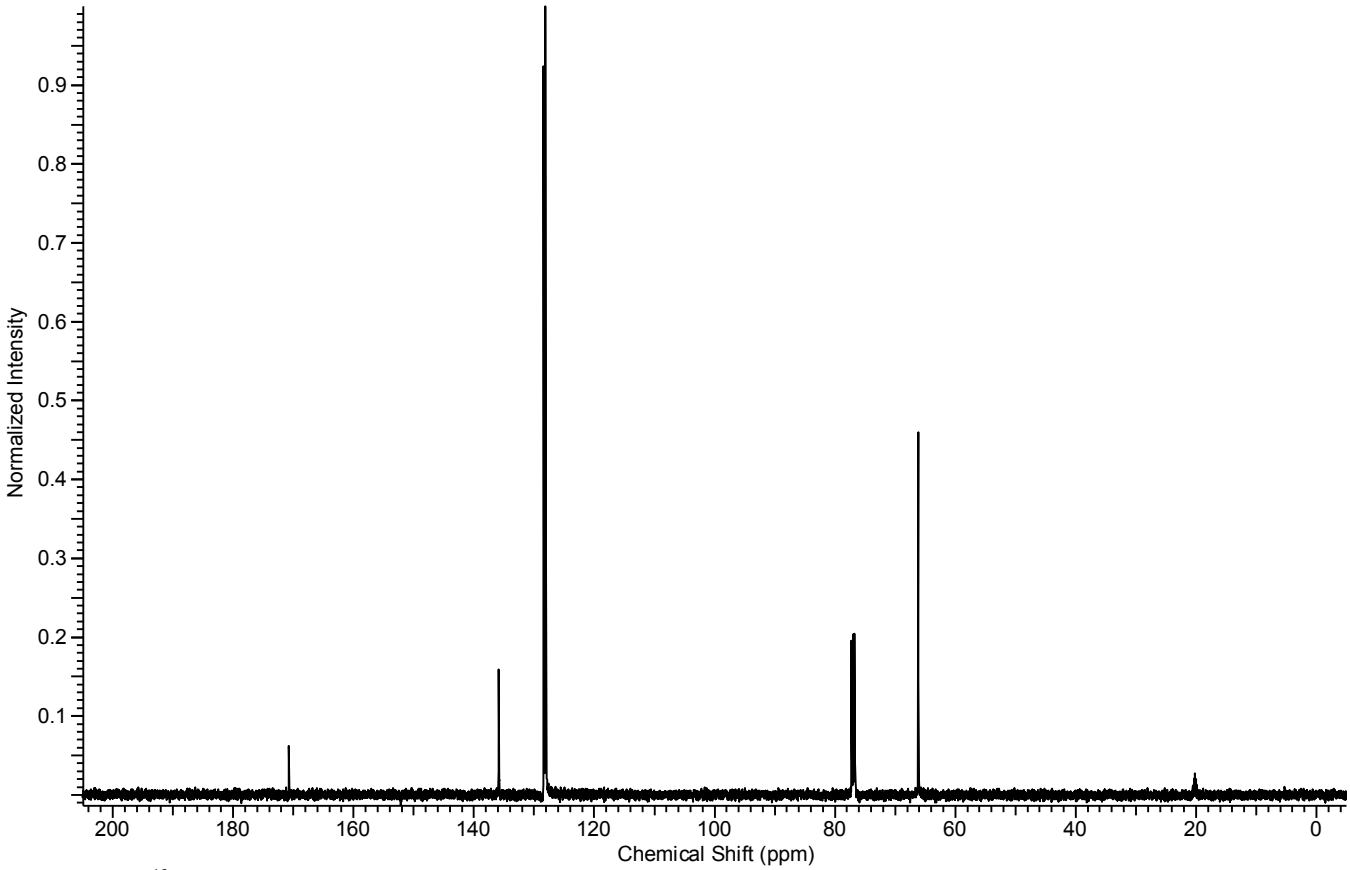

Figure S10. ^{13}C NMR (125 MHz) spectrum of **S6** in $CDCl_3$.

((1-(benzyloxy)vinyl)oxy)(*tert*-butyl)dimethylsilane (3c) was synthesized from benzyl acetate in analogy to the procedure described below for **3c**-d_2. Clear colorless liquid. IR (ATR, $CDCl_3$): 3068 (w), 3034 (w), 2956 (w), 2931 (w), 2886 (w), 2859 (w), 1746 (w), 1650 (m), 1588 (w), 1498 (w), 1472 (w), 1382 (w), 1363 (w), 1271 (s), 1159 (w), 1071 (w), 1013 (m), 945 (w), 908 (w), 879 (w), 831 (m), 812 (m), 785 (m), 735 (m), 696 (m) cm^{-1}. ^1H NMR (500 MHz, $CDCl_3$): δ 7.41–7.28 (m, 5H), 4.79 (s, 2H), 3.36 (d, J = 2.8 Hz, 1H), 3.24 (d, J = 2.8 Hz, 1H), 0.96 (s, 9H), 0.20 (s, 6H). ^{13}C NMR (125 MHz, $CDCl_3$): δ 161.1, 136.5, 128.4, 127.8, 127.4, 69.8, 61.7, 25.6, 18.1, –4.6. micrOTOF-Q ESI HRMS m/z calculated for $C_{15}H_{24}NaO_2Si$ ($[M + Na]^+$) 287.1438, found 287.1438.

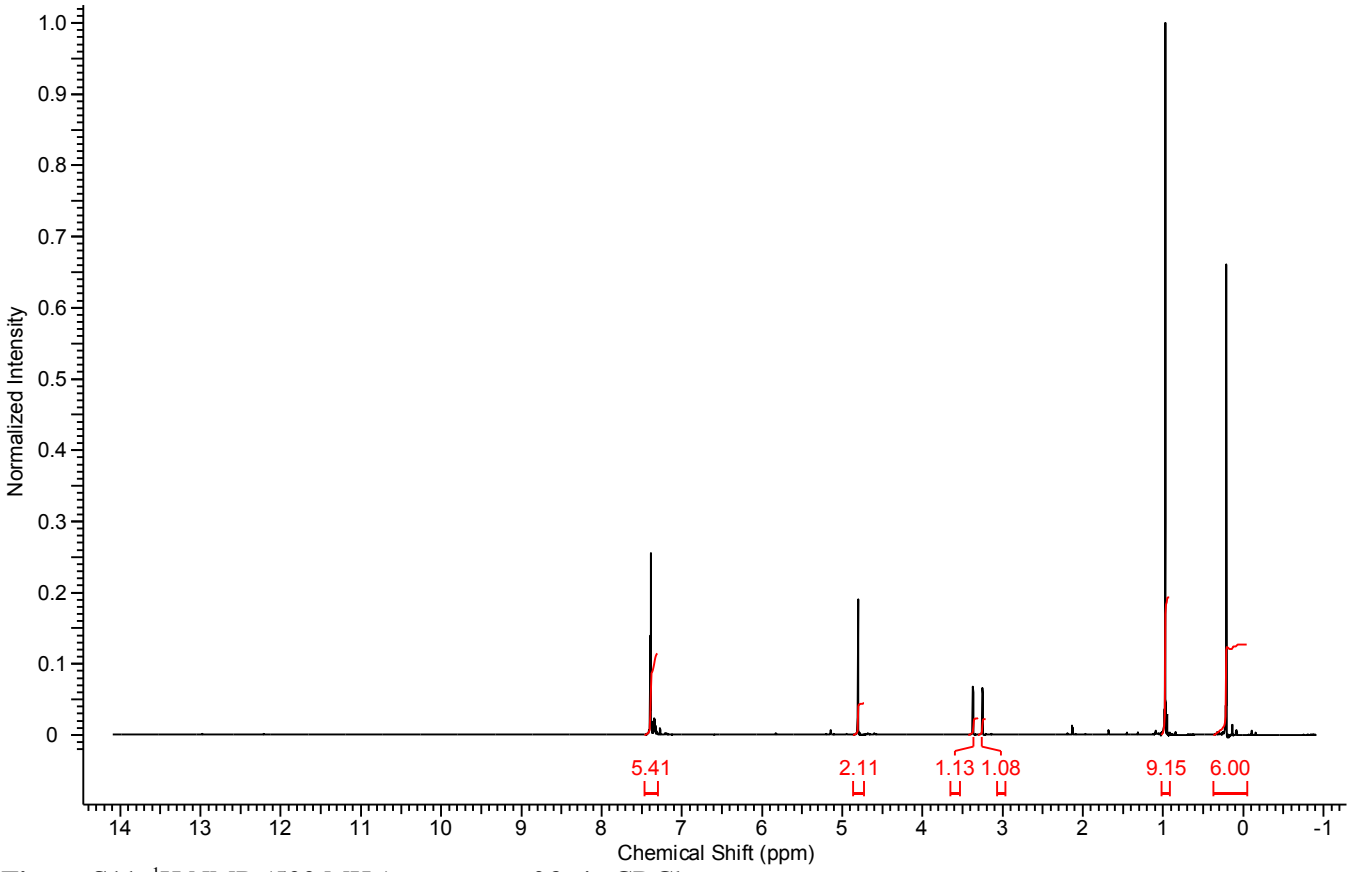

Figure S11. ^1H NMR (500 MHz) spectrum of **3c** in $CDCl_3$.

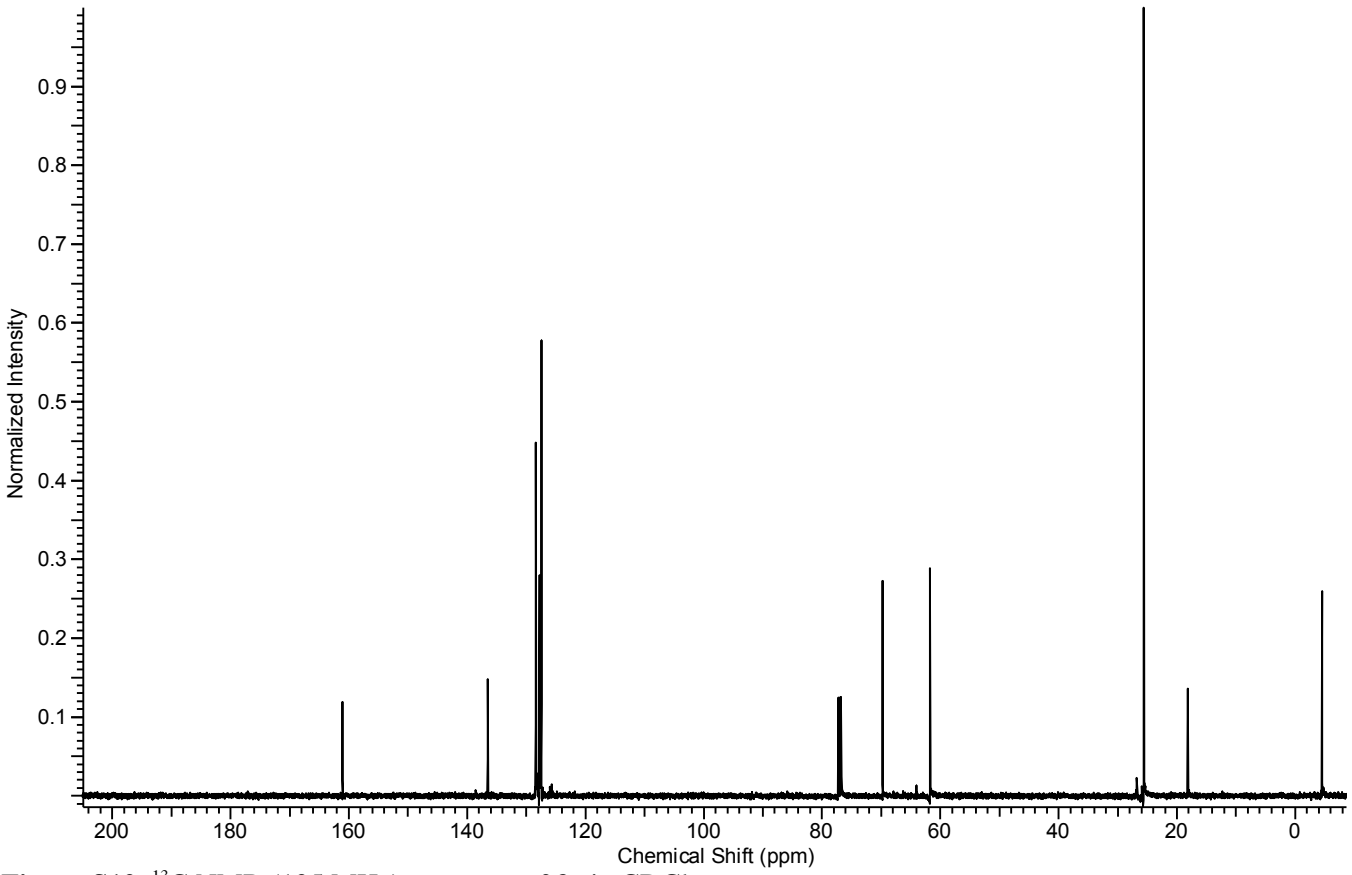

Figure S12. ^{13}C NMR (125 MHz) spectrum of **3c** in $CDCl_3$.

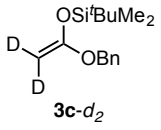

3c-d_2

((1-(benzyloxy)vinyl-2,2-d_2)oxy)(*tert*-butyl)dimethylsilane (3c-d_2): To a solution of *N*,*N*-diisopropylamine (5.58 mL, 3.96 g, 39.2 mmol) in THF (75 mL) at –15 °C was added *n*-BuLi (2.5 M in THF, 14.4 mL, 36 mmol). The reaction was stirred at –15 °C for 5 min, then cooled to –78 °C and a solution of **S10** (5.00 g, 32.6 mmol) in THF (10 mL) was added dropwise. The reaction mixture was stirred for 30 min at –78 °C, then 1,3-dimethyl-3,4,5,6-tetrahydro-2(1*H*)-pyrimidinone (DMPU; 5.90 mL, 6.28 g, 49.0 mmol) was added dropwise, followed by a solution of *tert*-butyldimethylsilylchloride (4.67 g, 31.0 mmol) in THF (8 mL) via cannula transfer. The mixture was stirred at –78 °C for 30 min then the cooling bath was removed and the mixture was allowed to warm to rt slowly over a 1 h period. The solvent was removed *in vacuo* and the resulting residue was taken up in pentane and washed successively with H_2O, saturated aq. $CuSO_4$, saturated aq. $NaHCO_3$, and twice with H_2O. The organic layer was then dried over anhyd. Na_2SO_4, filtered, and the solvent was removed *in vacuo*. The crude silyl ketene acetal was further purified via vacuum distillation (ca. 4 mmHg) to afford **3d**-d_2 (6.11 g, 74% yield) as a colorless liquid. IR (ATR, $CDCl_3$): 3034 (w), 2957 (w), 2931 (w), 2886 (w), 2859 (w), 1673 (w), 1615 (m), 1499 (w), 1472 (w), 1463 (w), 1384 (w), 1363 (w), 1251 (s), 1109 (w), 1029 (w), 1006 (w), 932 (m), 871, 840 (m), 824, 808, 784 (m), 735, 695 (m), 645 (w) cm^{-1}. ^{1}H NMR (500 MHz, $CDCl_3$): δ 7.45–7.33 (m, 5H), 4.83 (s, 2H), 1.00 (s, 9H), 0.24 (s, 6H). ^{13}C NMR (125 MHz, $CDCl_3$): δ 161.0, 136.5, 128.4, 127.8, 127.4, 69.7, 61.3 (qn, $J_{C–D}$ = 24.5 Hz), 25.6, 18.1, –4.6. micrOTOF-Q ESI HRMS *m*/*z* calculated for $C_{15}H_{22}D_2NaO_2Si$ ($[M + NH_4]^+$) 284.2009, found 284.2011.

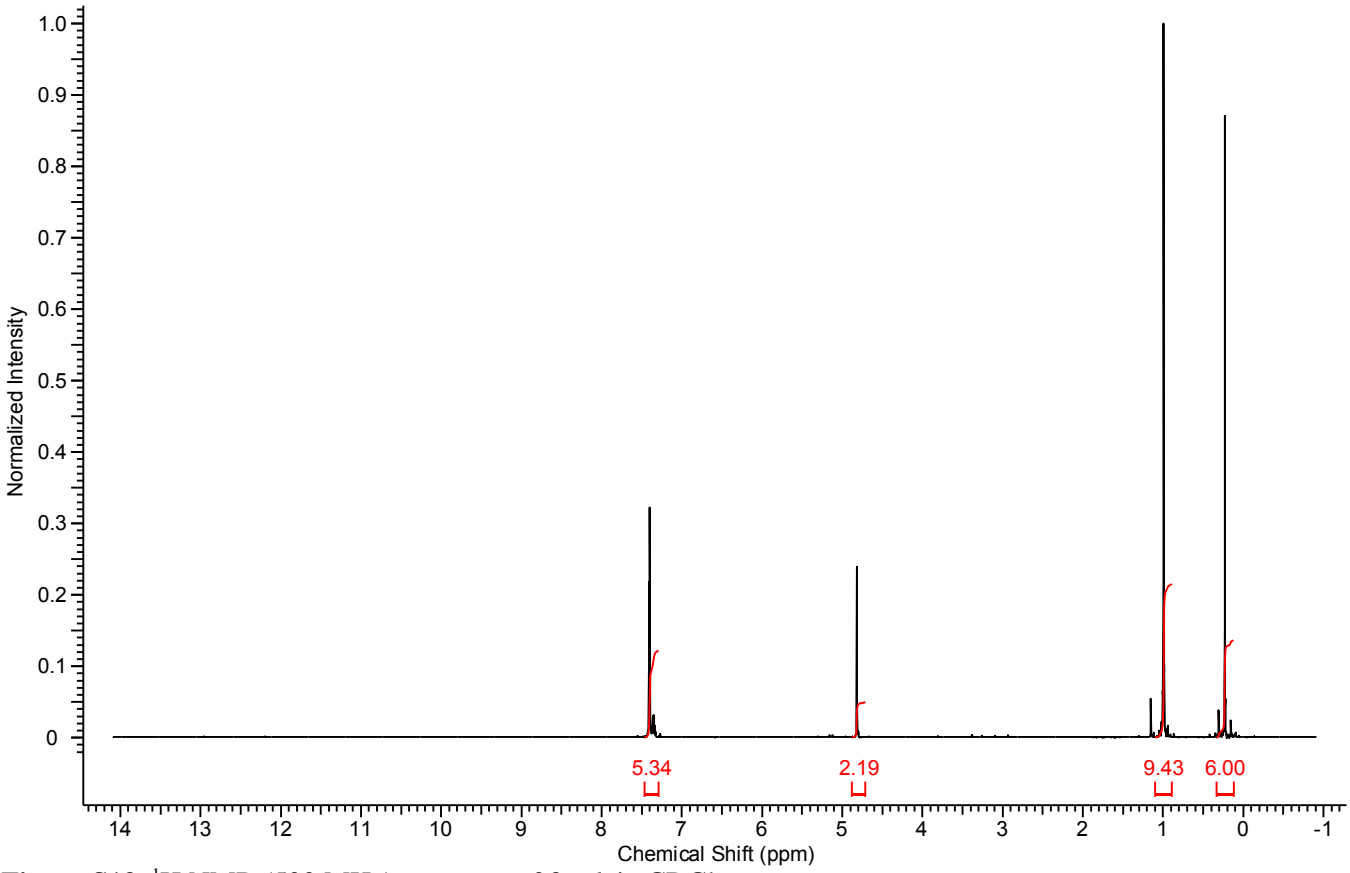

Figure S13. ^{1}H NMR (500 MHz) spectrum of **3c**-d_2 in $CDCl_3$.

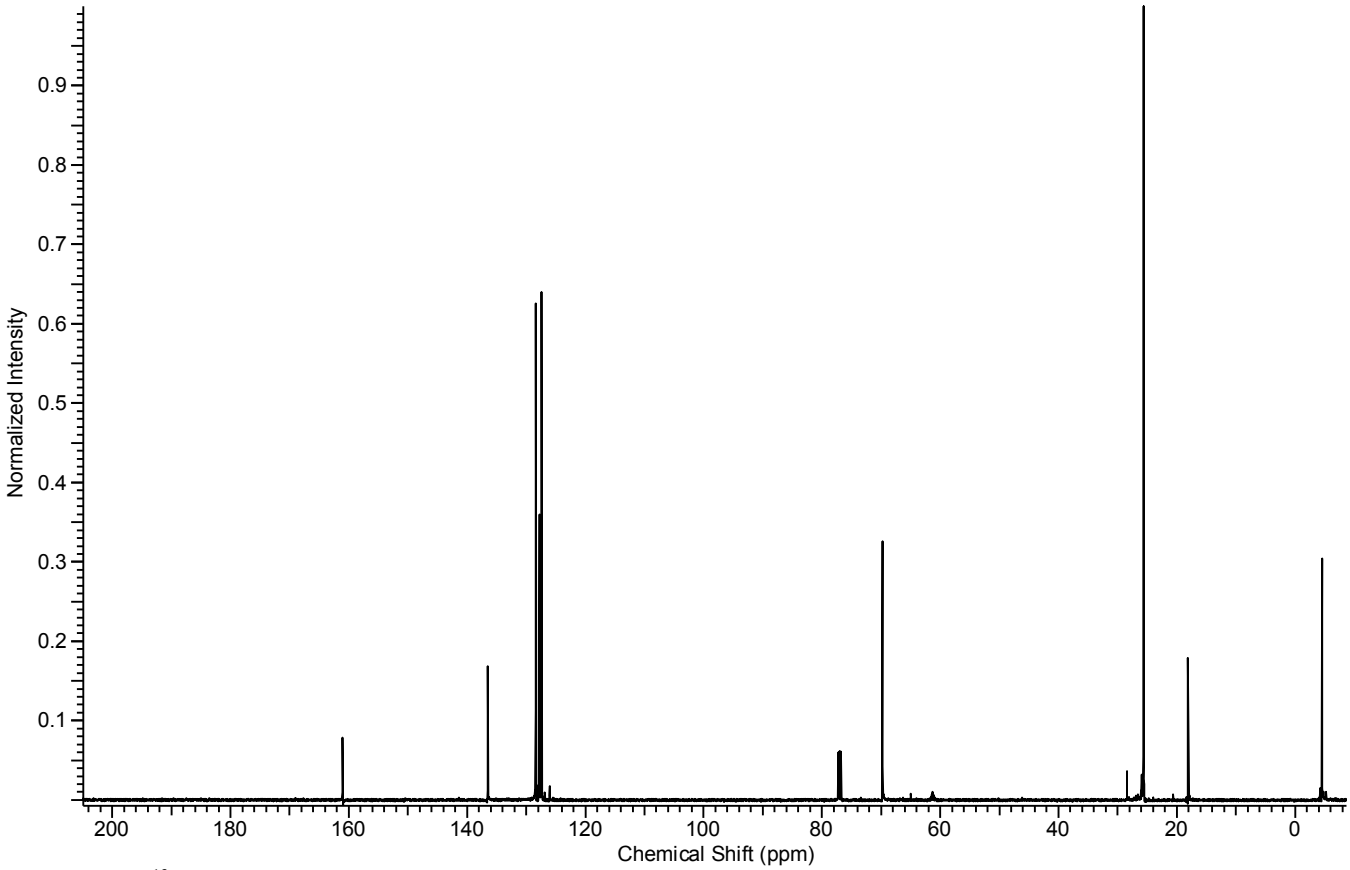

Figure S14. ^{13}C NMR (125 MHz) spectrum of **3c**-d_2 in $CDCl_3$.

3. Alkylation Reaction Kinetic Experiments

3.1 Derivation of Rate Law

Scheme S4. Proposed mechanism for enantioselective H-bond donor-catalyzed α-chloroisochroman alkylation.

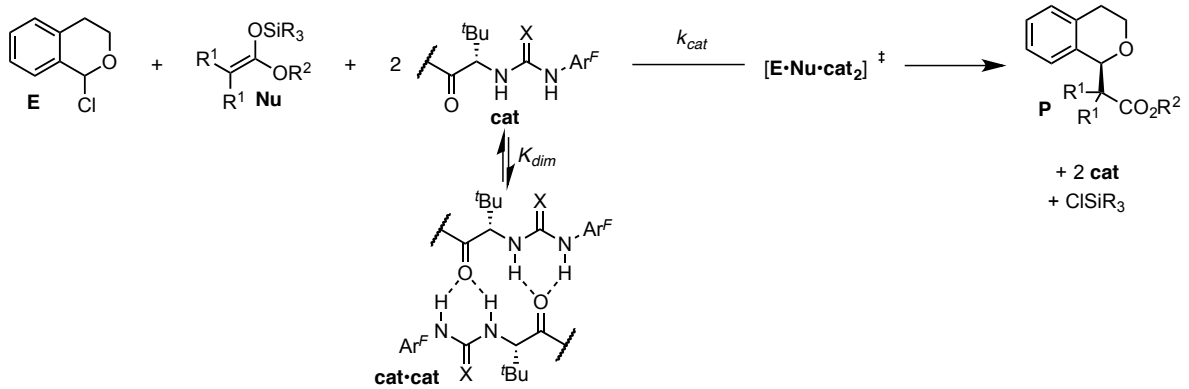

For the mechanism shown in Scheme S4, in which C–C bond formation between one molecule of electrophile (**E**) and one molecule of nucleophile (**Nu**) mediated by two molecules of catalyst (**cat**) is the rate-limiting step,[10] the differential rate law is defined as:

$$\frac{d[\mathbf{P}]}{dt} = rate = k_{cat}[\mathbf{cat}]^2\,[\mathbf{E}]^1\,[\mathbf{Nu}]^1 \tag{S1}$$

However, this rate law is expressed in terms of the concentration of free catalyst monomer, [**cat**]. In order to express the rate law in terms of known quantities, [**cat**] must be expressed as a function of the total catalyst concentration, $[\mathbf{cat}]_T$. This can be obtained through analysis of the catalyst self-dimerization equilibrium, where the equilibrium constant (K_{dim}) is defined as:

$$K_{dim} = \frac{[\mathbf{cat{\bullet}cat}]}{[\mathbf{cat}]^2} \tag{S2}$$

Equation S2 can be rewritten as:

$$[\mathbf{cat \bullet cat}] = K_{dim}[\mathbf{cat}]^2 \tag{S3}$$

From the conservation of mass:

$$[\mathbf{cat}]_T = 2[\mathbf{cat \bullet cat}] + [\mathbf{cat}] \tag{S4}$$

Substituting Equation S3 into Equation S4 affords:

$$[\mathbf{cat}]_T = 2K_{dim}[\mathbf{cat}]^2 + [\mathbf{cat}] \tag{S5}$$

Equation S5 can be rewritten in quadratic form as:

$$2K_{dim}[\mathbf{cat}]^2 + [\mathbf{cat}] - [\mathbf{cat}]_T = 0 \tag{S6}$$

The roots of a quadratic equation in the form:

$$ax^2 + bx + c = 0 \tag{S7}$$

(10) Intermediate catalyst–substrate complexes are likely formed rapidly and reversibly en route to the rate-determining alkylation transition state. Because the concentrations of these fleeting intermediates are negligible, they have no kinetically meaningful impact on the overall rate law for the reaction.

can be obtained from the equation:

$$x = \frac{-b \pm \sqrt{b^2 - 4ac}}{2a} \tag{S8}$$

Thus, the roots of Equation S6, as obtained from Equation S8, are:

$$[\mathbf{cat}] = \frac{-1 \pm \sqrt{(1^2 + -4(2K_{dim})(-[\mathbf{cat}]_T)}}{2(2K_{dim})} \tag{S9}$$

which may be simplified to afford:

$$[\mathbf{cat}] = \frac{-1 \pm \sqrt{(1 + 8K_{dim}[\mathbf{cat}]_T)}}{4K_{dim}} \tag{S10}$$

Since $[\mathbf{cat}] \geq 0$ and $\sqrt{(1 + 8K_{\mathrm{dim}}[\mathbf{cat}]_T)} > 0$, the only real root is:

$$[\mathbf{cat}] = \frac{-1 + \sqrt{(1 + 8K_{dim}[\mathbf{cat}]_T)}}{4K_{dim}} \tag{S11}$$

The numerator of Equation S11 can be rationalized as shown here:

$$[\mathbf{cat}] = \frac{(-1 + \sqrt{(1 + 8K_{dim}[\mathbf{cat}]_T)}\ )}{4K_{dim}} \bullet \frac{(1 + \sqrt{(1 + 8K_{dim}[\mathbf{cat}]_T)}\ )}{(1 + \sqrt{(1 + 8K_{dim}[\mathbf{cat}]_T)}\ )} \tag{S12}$$

to provide an equation that describes catalyst monomer concentration only in terms of $[\mathbf{cat}]_T$.:

$$[\mathbf{cat}] = \frac{2[\mathbf{cat}]_T}{1 + \sqrt{(1 + 8K_{\mathrm{dim}}[\mathbf{cat}]_T)}} \tag{S13}$$

Substituting equation S13 into the proposed rate law for product formation (Equation S1) affords:

$$\frac{d[\mathbf{P}]}{dt} = k_{cat}\left[\frac{2[\mathbf{cat}]_T}{1 + \sqrt{(1 + 8K_{\mathrm{dim}}[\mathbf{cat}]_T)}}\right]^2 [\mathbf{E}]^1\,[\mathbf{Nu}]^1 \tag{S14}$$

$$\frac{d[\mathbf{P}]}{dt} = k_{cat}\frac{4[\mathbf{cat}]_T^2[\mathbf{E}]\,[\mathbf{Nu}]}{(1 + \sqrt{(1 + 8K_{\mathrm{dim}}[\mathbf{cat}]_T)}\ )^2} \tag{S15}$$

An abbreviated version of Equation S15, in which known substrate concentrations were included in an "observed" rate constant, was used for curve fitting:

$$\mathrm{rate}_{[\mathrm{E}],[\mathrm{Nu}]} = k_{cat,obs}\frac{4\,([\mathbf{cat}]_T)^2}{(1 + \sqrt{(1 + 8K_{\mathrm{dim}}[\mathbf{cat}]_T)}\ )^2} \tag{S16}$$

When $8K_{\mathrm{dim}}\,[\mathrm{cat}]_T >> 1$ (resting state dimer), Equation S16 can be simplified to describe a simple first-order dependence on $[\mathbf{cat}]_T$:

$$\mathrm{rate}_{[\mathrm{E}],[\mathrm{Nu}]} = k_{cat,obs}\frac{[\mathbf{cat}]_T}{2K_{\mathrm{dim}}} \tag{S17}$$

Likewise, when $8K_{\mathrm{dim}}\,[\mathrm{cat}]_T << 1$ (resting state monomer), Equation S16 can be simplified to describe a simple second-order dependence on $[\mathrm{cat}]_T$:

$$\mathrm{rate}_{[\mathrm{E}],[\mathrm{Nu}]} = k_{cat,obs}[\mathrm{cat}]_T^2 \tag{S18}$$

3.2 General Kinetic Procedures

General Information: In situ IR kinetic experiments were carried out using a Mettler Toledo ReactIR™ iC 10 ATR FTIR spectrometer and a 9 mm probe with a SiComp (silicon-based) window. The custom-made reaction vessel shown in Figure S15 was used in all experiments to facilitate maintenance of air- and moisture-free conditions at low temperature. 1-chloroisochroman (**2**), which was prepared as described in Section 2.2, was distilled to purity and stored in an inert atmosphere glovebox at –30 ºC prior to use. Catalysts and silyl ketene acetals were synthesized as described in Sections 2.1 and 2.3. Small but non-negligible differences in rate were observed when using different batches of the same reagents, particularly different batches of silyl ketene acetal. To eliminate this source of error, all of the kinetics experiments on each plot were performed using a single batch of reagents.

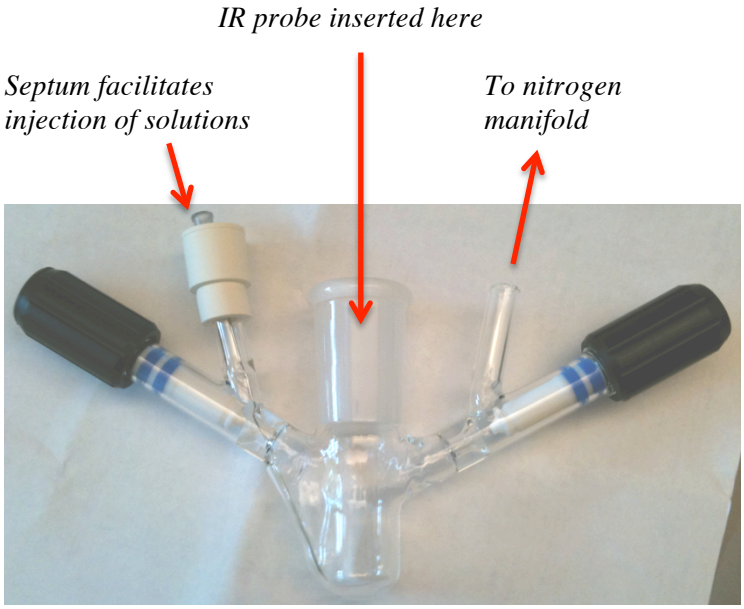

Figure S15. Photograph of custom-made reaction vessel used for alkylation kinetics monitored by ReactIR.

Sample Procedure: *10 mol% catalyst* **1a**, *silyl ketene acetal* **3b**
An oven-dried flask (see Figure S15) equipped with a stir bar was attached to a ReactIR probe that had been warmed with a heat gun and the system was purged with N_2. After the purge outlet was closed, the system was kept under a positive pressure of N_2 for the remainder of the experiment. The flask was allowed to cool to rt, charged with TBME (1.65 mL), then cooled to –78 °C (using a dry ice/acetone cooling bath.) After the temperature had stabilized (~ 15–20 min) a background spectrum was acquired (600–3400 cm^{-1}). All spectra were measured with a two-point correction baseline. To the reaction vessel was added a solution of silyl ketene acetal **3b** (165 µL, 0.300 mmol, 0.182 M in TBME; prepared by diluting 342 mg to 1.00 mL total volume in TBME), followed by 1-chloroisochroman **2** (135 µL, 0.200 mmol, 1.48 M in TBME; prepared by dissolving 250 mg to 1.00 mL total volume in TBME). The reaction was initiated by adding catalyst as a stock solution in THF (50 µL, 0.020 mmol, 0.40 M in THF, prepared by dissolving 220 mg of **1a** to 1.00 mL total volume in THF). Volumes of injections (dispensed using precision glass syringes) were maintained constant for all experiments, unless stated otherwise, and the amounts of reagents was altered by changing the concentration of the stock solutions used. Changing the volume of the THF catalyst solution had observable effects on the rate data. Reactions were quenched by the addition of NaOMe (0.15 mL, 0.5 M NaOMe in MeOH). The reaction mixture was diluted with 1 mL of 50% Et_2O in hexanes, filtered through a pipette filled with ¾ inch of silica gel using ca. 15 mL of 50% Et_2O in hexanes. The solvent was removed by rotary evaporation under reduced pressure to give the crude residue, which was purified by silica gel chromatography (6% Et_2O in hexanes).

The reaction was monitored by following the consumption of the silyl ketene acetal **3** and the formation of product **4** at appropriate wavelengths (see Table S1). Spectra (with resolution of 1 cm^{-1}) were collected every 15 seconds for the first hour, then every 30 seconds for the next two hours, and every minute for the remainder of the

experiment. A two-point baseline correction was used for monitoring the peak intensities (e.g., 1800 cm^{-1} and 1550 cm^{-1} for silyl ketene acetals **3b** and **3c**).

Data Manipulation:
The data were treated using the methods for reaction progress kinetic analysis described previously by Blackmond.[11] The temperature- and solvent-dependent absorption response factor (R_o) was determined for each silyl ketene acetal (**3**) and alkylation product (**4**) at –78°C in the reaction solvent (TBME) to mirror the reaction conditions employed in the kinetics experiments. The absorption intensity (A) was plotted as a function of [**3**] or [**4**], and the linear region of the plot was fitted with a linear least-squares fit corresponding to the equation, where **c** is compound **3** or **4**:

$$A = R_o\,[\mathbf{c}] \tag{S19}$$

The raw absorption intensity data obtained from each kinetics experiment was converted to concentration vs. time data at the relevant wavelengths (see Table S1) for compounds **3** and **4**. The data were fit to the following 7th order polynomial using an unweighted least-squares fit:

$$[\mathbf{3}] = f(t) = a_0 + a_1t^1 + a_2t^2 + a_3t^3 + a_4t^4 + a_5t^5 + a_6t^6 + a_7t^7 \tag{S20}$$

The rate of consumption of **3** (–d[**3**]/dt) was obtained from the derivative of $f(t)$, namely d$f(t)$/dt:

$$\frac{d[\mathbf{3}]}{dt} = \frac{df(t)}{dt} = a_1 + 2a_2t^1 + 3a_3t^2 + 4a_4t^3 + 5a_5t^4 + 6a_6t^5 + 7a_7t^6 \tag{S21}$$

The rates extracted from $df(t)/dt$ are valid only over the range of concentrations of **3** for which experimental data was collected. An analogous analysis using the concentration **4** at a function of time allows for determination of the rate of formation of **4** (d[**4**]/dt).

Scheme S5. A representative kinetic procedure

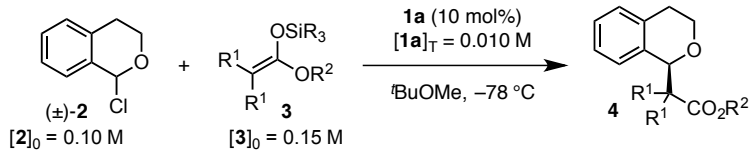

Table S1. Wavelength of diagnostic IR peaks monitored for reactions kinetics, relative rates and product ee.[a]

3:	R^1	R^2	R^3	Silyl ketene acetal C=C stretch (cm^{-1})	Product C=O stretch (cm^{-1})	–d[**3**]/dt at 30% conversion ($\times 10^{-5}$ $M^{-1}\bullet s^{-1}$)	Product ee (%)
3a	Me	OMe	$SiMe_3$	1715	1745	0.48	92
3b	H	OMe	Si(*t*-Bu)Me_2	1659	1745	10.5	85
3c	H	OBn	Si(*t*-Bu)Me_2	1656	1740	7.0	86
3c-d_2	D	OBn	Si(*t*-Bu)Me_2	1622	1740	ND	86
3d	Me	OMe	$SiEt_3$	1712	1745	0.97	93
3e	Me	OMe	Si(*i*-Pr)$_3$	1710	1745	0.36	95
3f	Me	OMe	Si(*t*-Bu)Me_2	1712	1745	0.43	94
3g	H	O(*i*-Pr)	Si(*t*-Bu)Me_2	1659	1749	8.9	84

[a] See Scheme S5 for definition of structures of **3a–f** and **4a–f**.

(11) Blackmond, D. G. *Angew. Chem. Int. Ed.* **2005**, *44*, 4302–4320.

3.3 "Same-Excess" Experiments

The "same-excess" experiments were performed with silyl ketene acetal **3b** and catalyst **1a** (Scheme S6). The reactions were initiated by adding neat **3b** last to a solution of **2** and **1a** in TBME at –78 °C. Rate was determined from the appearance of ester product **4b**. The concentration [**2**] was inferred from the known initial concentration, $[\mathbf{2}]_0$, and the measured amount of **4b** formed, assuming quantitative conversion to product. The data are presented in Table S2 and visualized in Figure S16. The excellent overlay of the rate vs. concentration plots from all three experiments indicates that no catalyst deactivation, either by product inhibition or by decomposition, occurs under the reaction conditions.[11]

Scheme S6. The "same-excess" experiments represented in Figure S16 and Table S2.

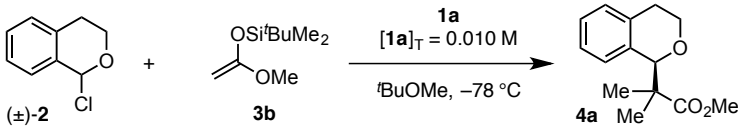

Experiment	$[\mathbf{2}]_0$	$[\mathbf{3b}]_0$	*excess* = $[\mathbf{2}]_0 - [\mathbf{3b}]_0$
1	0.100 M	0.150 M	0.050 M
2	0.075 M	0.125 M	0.050 M
3	0.050 M	0.100 M	0.050 M

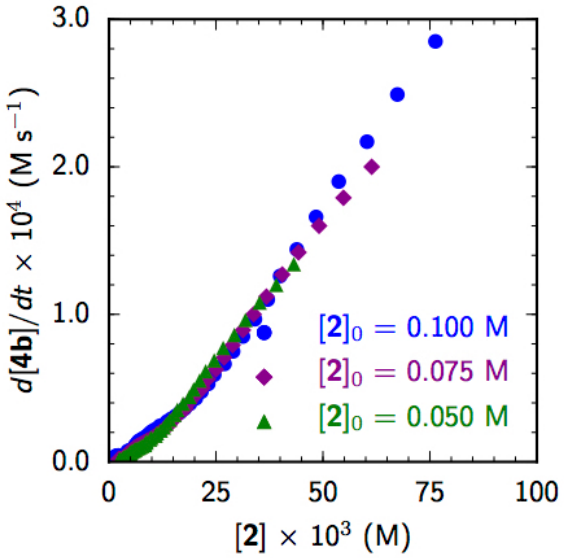

Figure S16. Plot illustrating the rate data for the "same-excess" experiment.

Table S2. Data used to generate Figure S16. The units of the rate $d[\mathbf{4b}]/dt$ are "$\times 10^{-4}$ M•s^{-1}".

$[\mathbf{2}]_0$ = 0.10 M		$[\mathbf{2}]_0$ = 0.075 M		$[\mathbf{2}]_0$ = 0.050 M	
[**2**] (M)	$d[\mathbf{4b}]/dt$	[**2**] (M)	$d[\mathbf{4b}]/dt$	[**2**] (M)	$d[\mathbf{4b}]/dt$
0.0763	2.85	0.0614	2.00	0.0432	1.34
0.0674	2.49	0.0548	1.79	0.0391	1.2
0.0603	2.17	0.0491	1.60	0.0352	1.08
0.0537	1.90	0.0443	1.42	0.0319	0.962
0.0484	1.66	0.0405	1.27	0.0293	0.86
0.0439	1.44	0.0368	1.12	0.0267	0.772
0.04	1.26	0.0338	1.00	0.0246	0.688
0.0371	1.10	0.0313	0.893	0.0226	0.614
0.0341	0.967	0.0289	0.791	0.0212	0.551
0.0313	0.85	0.0269	0.707	0.0198	0.491
0.029	0.749	0.025	0.627	0.0188	0.441
0.027	0.664	0.0231	0.561	0.0173	0.394
0.0246	0.591	0.0219	0.501	0.016	0.353
0.0232	0.529	0.0201	0.447	0.0153	0.319
0.0216	0.476	0.0188	0.403	0.0142	0.286
0.0203	0.431	0.0179	0.362	0.0134	0.258
0.0189	0.394	0.0165	0.328	0.0128	0.234
0.0177	0.362	0.0155	0.297	0.0121	0.213
0.0166	0.335	0.0146	0.271	0.0112	0.195
0.0156	0.312	0.014	0.248	0.0109	0.178
0.0145	0.291	0.0131	0.229	0.0099	0.164
0.0136	0.274	0.0125	0.211	0.0096	0.152
0.0131	0.258	0.0117	0.197	0.00876	0.14
0.0119	0.244	0.0112	0.184	0.00872	0.131
0.0115	0.23	0.0107	0.173	0.00834	0.122
0.0107	0.218	0.0101	0.163	0.0084	0.115
0.01	0.206	0.00964	0.154	0.00775	0.108
0.0096	0.195	0.00909	0.146	0.00735	0.102
0.00922	0.184	0.00869	0.139	0.00702	0.0967
0.00882	0.174	0.00825	0.133	0.00664	0.0917
0.00819	0.163	0.00796	0.127	0.00608	0.0871
0.00766	0.153	0.00754	0.121	0.00619	0.0829
0.00702	0.143	0.00718	0.115	0.00589	0.0787
0.00672	0.133	0.00676	0.11	0.00571	0.0748

$[\mathbf{2}]_0$ = 0.10 M		$[\mathbf{2}]_0$ = 0.075 M		$[\mathbf{2}]_0$ = 0.050 M	
[**2**] (M)	$d[\mathbf{4b}]/dt$	[**2**] (M)	$d[\mathbf{4b}]/dt$	[**2**] (M)	$d[\mathbf{4b}]/dt$
0.00658	0.123	0.00663	0.105	0.00531	0.0711
0.00616	0.114	0.0062	0.0999	0.0052	0.0675
0.0063	0.104	0.00602	0.0948	0.00503	0.0641
0.00597	0.0959	0.00575	0.0898	0.00485	0.0606
0.0055	0.0877	0.00563	0.0849	0.00499	0.0572
0.00498	0.0801	0.00543	0.0798	0.00488	0.054
0.00436	0.0732	0.00504	0.0751	0.00459	0.0507
0.00469	0.0667	0.00504	0.0702	0.00493	0.0477
0.00449	0.0612	0.00475	0.0653	0.00426	0.0445
0.00429	0.0563	0.00469	0.0608	0.00451	0.0416
0.00416	0.0521	0.00432	0.0561	0.00421	0.0388
0.00388	0.0486	0.00445	0.0519	0.00385	0.0359
0.00365	0.0459	0.00425	0.0477	0.00356	0.0334
0.00367	0.0438	0.00432	0.0435	0.00381	0.0308
0.00334	0.0423	0.00379	0.0399	0.00372	0.0284
0.00317	0.0413	0.004	0.0363	0.00326	0.0262
0.00319	0.0409	0.00376	0.0331	0.00363	0.0243
0.00299	0.0409	0.00376	0.0301	0.00386	0.0224
0.00256	0.0412	0.00345	0.0273	0.00334	0.0207
0.0022	0.0416	0.00339	0.025	0.00317	0.0192
0.0027	0.0422	0.00331	0.023	0.00344	0.0179
0.00221	0.0427	0.00304	0.0212	0.0031	0.0168
0.00217	0.043	0.00301	0.0198	0.0031	0.0158
0.00223	0.0431	0.00299	0.0187	0.00313	0.0151
0.00185	0.0428	0.00285	0.0179	0.00273	0.0145
0.00222	0.042	0.0029	0.0174	0.00317	0.0141
0.00194	0.0407	0.0027	0.0171	0.0026	0.0138
0.00254	0.0387	0.00259	0.0171	0.00311	0.0136
0.00139	0.036	0.00251	0.0173	0.00251	0.0136
0.00182	0.0327	0.00243	0.0177	0.00274	0.0136
0.00192	0.0286	0.00259	0.0182	0.00244	0.0137
0.0015	0.0238	0.00246	0.0189	0.00257	0.0139
0.00149	0.0189	0.00229	0.0196	0.00234	0.0141
0.00153	0.0134	0.00239	0.0203	0.00249	0.0142

3.4 "Different-Excess" Experiments

3.4.1 Order in α-Chloroisochroman

The "different-excess" experiments to determine the kinetic order in **2**, were performed with silyl ketene acetal **3b** and catalyst **1a** (Scheme S7). The reactions were initiated by adding neat **3b** last to a solution of **2** and **1a** in TBME at –78 °C. Rate was determined from the disappearance of silyl ketene acetal **3b** and corroborated with the appearance of ester product **4b**. The concentration [**2**] was inferred from the known initial concentration, $[\mathbf{2}]_0$, and the measured amount of **4b** formed, assuming quantitative conversion to product. The data are presented in Table S3 and visualized in Figure S17. The linear dependence of the rate on [**2**] at 13% ([**3b**] = 0.13 M), 40% ([**3b**] = 0.09 M), and 60% ([**3b**] = 0.06 M) conversion of the silyl ketene acetal is indicative of a 1st-order rate dependence on [**2**].[11]

Scheme S7. "Different-excess" experiments to determine the kinetic order in **2**.

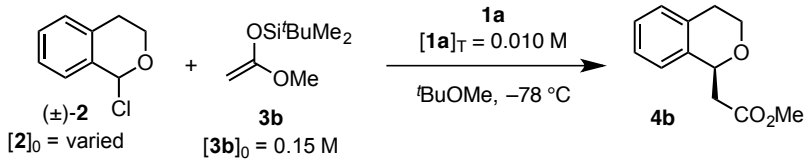

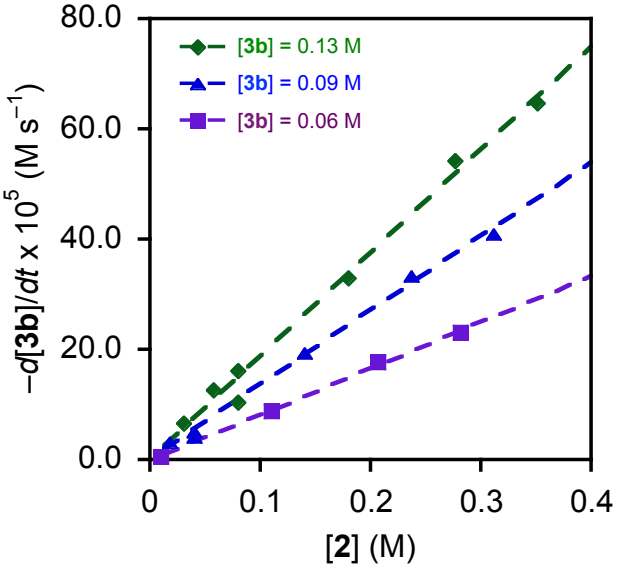

Figure S17. Rate as a function of [**2**]. The data were fit to a simple linear model, showing that the reaction obeys strict first-order kinetics with respect to **2**.

Table S3. Rate as a function of initial concentration of **2** over the full course of the reaction.[a]

	$-d[\mathbf{3b}]/dt$ ($\times 10^{-5}$ M•s^{-1})										
$[\mathbf{2}]_0$ (M)	[**4b**] = 0.01 M	[**4b**] = 0.02 M	[**4b**] = 0.03 M	[**4b**] = 0.04 M	[**4b**] = 0.05 M	[**4b**] = 0.06 M	[**4b**] = 0.07 M	[**4b**] = 0.08 M	[**4b**] = 0.09 M	[**4b**] = 0.10 M	[**4b**] = 0.11 M
0.0500	9.10	6.55	4.02	1.73	NA	NA	NA	NA	NA	NA	NA
0.0780	15.0	12.7	10.4	8.02	5.58	3.08	0.903	NA	NA	NA	NA
0.100	20.4	16.1	12.4	9.54	7.19	4.98	3.09	NA	NA	NA	NA
0.100	11.8	10.4	8.88	7.37	5.82	4.25	2.65	1.19	0.551	NA	NA
0.200	36.3	33.0	29.6	26.2	22.8	19.3	15.8	12.3	8.90	5.72	3.24
0.297	59.7	54.4	49.2	43.9	38.6	33.3	28.1	22.8	17.8	12.9	8.47
0.371	70.5	64.7	58.8	53.0	47.0	41.1	35.2	29.2	23.3	17.5	12.0

[a] All reactions run with $[\mathbf{3b}]_0 = 0.150$ M and $[\mathbf{1a}]_T = 0.010$ M, in TBME at –78 °C.

3.4.2 Order in Silyl Ketene Acetal

The "different-excess" experiments to determine the kinetic order in **3**, were performed with silyl ketene acetal **3b** and catalyst **1a** (Scheme S8). The reactions were initiated by adding neat **3b** last to a solution of **2** and **1a** in TBME at –78 °C. Rate was determined from the appearance of ester product **4b**. The concentration [**2**] was inferred from the known initial concentration, $[\mathbf{2}]_0$, and the measured amount of **4b** formed, assuming quantitative conversion to product. The concentration [**3**] was measured directly. The data are presented in Table S4 and visualized in Figure S18. At low concentrations of silyl ketene acetal, the dependence of the rate on [**3b**] at 20% ([**2**] = 0.08 M), 40% ([**2**] = 0.06 M), and 60% ([**2**] = 0.04 M) conversion of the α-chloroisochroman is roughly linear, indicative of a 1st-order rate dependence on [**3b**].[11] However, at high concentrations [**3b**], a deleterious effect on rate is observed upon increasing [**3b**]. Given the fact that the reaction mixture is frozen solid at [**3b**] = 0.8 M, it seems likely that this deviation is due to a medium effect. Regardless of the exact interpretation of the shape of the curve, it is clear that there is a positive dependence of rate on [**3b**] at the low concentrations most representative of synthetic conditions, indicating that **3b** is present in the turnover-limiting transition state.

Scheme S8. "Different-excess" experiments to determine the kinetic order in silyl ketene acetal **3b**.

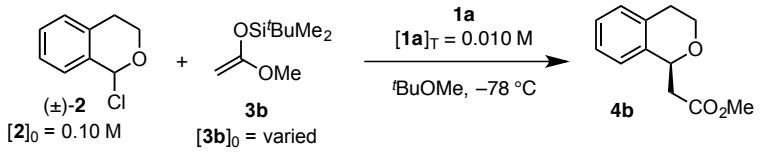

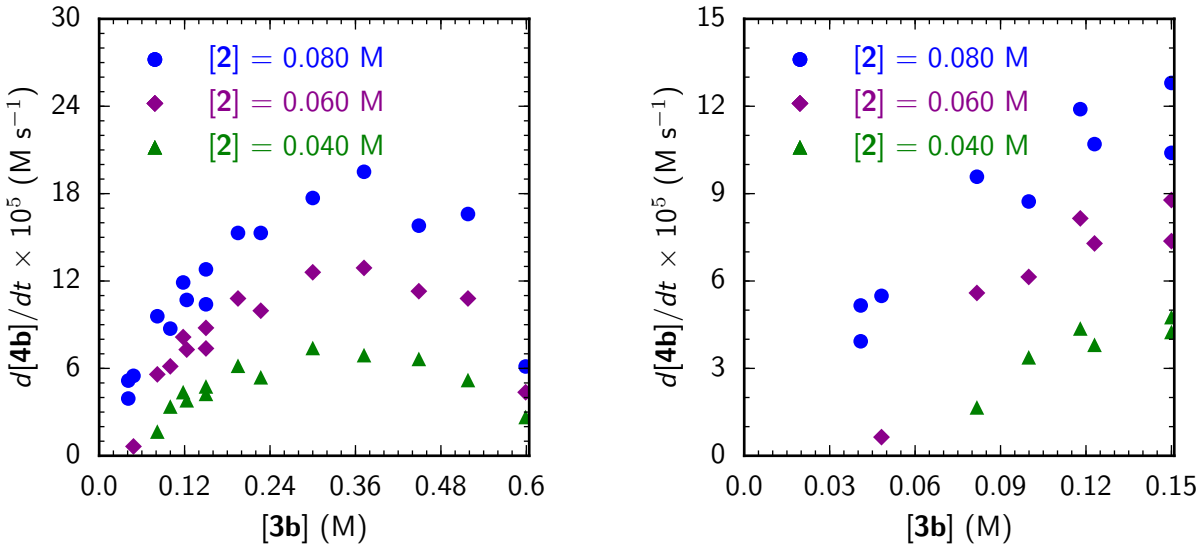

Figure S18. Rate as a function of [**3b**]. The dependence seems first order at low [**3b**], but deleterious effects on rate are observed at high [**3b**].

Table S4. Rate as a function of initial concentration of **3b** over the full course of the reaction.[a]

$[\mathbf{3b}]_0$ (M)	$d[\mathbf{4b}]/dt$ ($\times 10^{-5}$ M•s^{-1})								
	[**4b**] = 0.01 M	[**4b**] = 0.02 M	[**4b**] = 0.03 M	[**4b**] = 0.04 M	[**4b**] = 0.05 M	[**4b**] = 0.06 M	[**4b**] = 0.07 M	[**4b**] = 0.08 M	[**4b**] = 0.09 M
0.0409	6.64	3.93	1.60	NA	NA	NA	NA	NA	NA
0.0409	8.45	5.16	1.92	NA	NA	NA	NA	NA	NA
0.0482	8.23	5.49	2.79	0.64	NA	NA	NA	NA	NA
0.0817	11.5	9.58	7.60	5.59	3.56	1.66	0.64	NA	NA
0.0999	9.98	8.73	7.45	6.14	4.79	3.38	1.93	0.628	0.326
0.118	13.7	11.9	10.0	8.15	6.26	4.37	2.58	1.30	0.691
0.123	12.3	10.7	8.99	7.29	5.56	3.81	2.13	0.095	0.383
0.150	11.8	10.4	8.88	7.37	5.82	4.25	2.65	1.19	0.551
0.150	14.8	12.8	10.8	8.78	6.75	4.76	2.91	1.53	0.671
0.195	17.4	15.3	13.0	10.8	8.48	6.18	3.91	1.91	0.830
0.227	18.1	15.3	12.6	9.96	7.51	5.39	3.67	2.24	0.812
0.300	20.1	17.7	15.2	12.6	10.0	7.40	4.72	2.23	0.854
0.372	22.8	19.5	16.2	12.9	9.82	6.91	4.46	2.59	0.658
0.449	18.0	15.8	13.6	11.3	8.98	6.65	4.33	2.20	0.869
0.518	19.5	16.6	13.7	10.8	7.91	5.20	2.99	1.71	0.269
0.599	7.0	6.13	5.2	4.36	3.49	2.66	1.88	1.24	0.777

[a] All reactions run with $[\mathbf{2}]_0 = 0.100$ M and $[\mathbf{1a}]_T = 0.010$ M, in TBME at –78 °C.

In order to circumvent the medium effects to which the anomalous behavior at high silyl ketene acetal concentrations was attributed, the "different-excess" experiments were repeated with greasy silyl ketene acetal **3g** and catalyst **1a** (Scheme S9) at half the typical global concentration. The data are presented in Table S5 and visualized in Figure S19. Over a much greater range of silyl ketene acetal concentrations, the dependence of the rate on [**3g**] at 30% ([**2**] = 0.035 M) conversion of the α-chloroisochroman is roughly linear, indicative of a 1st-order rate dependence on [**3b**].[11] However, at very high concentrations [**3g**], a deleterious effect on rate is still observed upon increasing [**3g**].

Scheme S9. "Different-excess" experiments to determine the kinetic order in silyl ketene acetal **3g**.

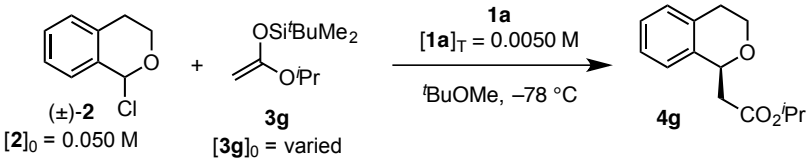

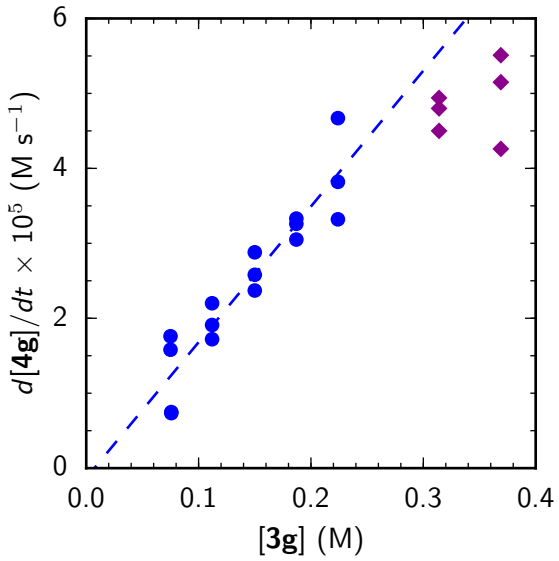

Figure S19. Rate as a function of [**3g**] at [**4g**] = 0.015 M (30% conversion of **2**).

Table S5. Rate of product formation as a function of initial concentration of silyl ketene acetal **3g**.[a]

	$-d$[**4g**]/dt ($\times 10^{-5}$ M•s^{-1})								
[**3g**]$_0$ (M)	[**4g**] = 0.005 M	[**4g**] = 0.010 M	[**4g**] = 0.015 M	[**4g**] = 0.020 M	[**4g**] = 0.025 M	[**4g**] = 0.030 M	[**4g**] = 0.035 M	[**4g**] = 0.040 M	[**4g**] = 0.045 M
0.0750	2.25	1.91	1.58	1.26	0.955	0.681	0.466	0.308	0.170
0.0750	2.34	2.06	1.76	1.47	1.18	0.892	0.617	0.391	0.248
0.0757	1.16	0.953	0.748	0.540	0.342	0.176	0.103	0.028	ND
0.0757	1.09	0.916	0.734	0.549	0.371	0.211	0.118	0.059	0.015
0.112	2.94	2.40	1.91	1.48	1.12	0.828	0.544	0.311	0.297
0.112	2.60	2.15	1.72	1.33	0.993	0.732	0.507	0.268	0.105
0.112	3.46	2.75	2.20	1.76	1.39	1.02	0.732	0.457	ND
0.150	3.80	3.18	2.58	2.03	1.53	1.11	0.757	0.440	0.165
0.150	3.55	2.95	2.37	1.84	1.38	1.01	0.701	0.381	0.100
0.150	4.29	3.56	2.88	2.28	1.75	1.29	0.872	0.502	0.331
0.187	4.75	4.03	3.33	2.69	2.09	1.58	1.13	0.717	0.350
0.187	4.53	3.89	3.26	2.64	2.05	1.57	1.11	0.730	0.381
0.187	5.39	3.90	3.05	2.58	2.09	1.50	1.05	0.726	0.500
0.224	5.62	4.69	3.82	3.01	2.28	1.69	1.20	0.715	0.276
0.224	6.61	5.63	4.67	3.75	2.92	2.17	1.56	1.02	0.486
0.224	4.76	4.03	3.32	2.63	1.98	1.41	0.943	0.556	0.171
0.314	6.28	5.37	4.50	3.60	2.76	1.96	1.28	0.788	0.321
0.314	6.80	5.87	4.94	3.99	3.06	2.13	1.27	0.633	0.055
0.314	6.72	5.75	4.80	3.87	2.97	2.11	1.39	0.833	0.294
0.369	6.07	5.16	4.26	3.36	2.51	1.73	1.11	0.676	0.198
0.369	7.31	6.42	5.51	4.61	3.68	2.77	1.87	1.09	0.602
0.369	7.49	6.30	5.15	4.03	3.00	2.13	1.44	0.849	0.311

[a] All reactions run with [**2**]$_0$ = 0.050 M (±)-**2** (0.10 mmol scale), [**1a**]$_T$ = 0.005 M in TBME at –78 °C.

3.5 Evaluation of Order in Catalyst

3.4.1 Order in Thiourea Catalyst 1a

The experiments to determine the kinetic order in thiourea catalyst **1a**, were performed with silyl ketene acetal **3b** (Scheme S10). The reactions were initiated by adding catalyst as a stock solution in THF to a solution of **2** and **3b** in TBME at –78 °C. Rate was determined from the disappearance of silyl ketene acetal **3b** and corroborated with the appearance of ester product **4b**. The concentration [**2**] was inferred from the known initial concentration, $[\mathbf{2}]_0$, and the measured amount of **4b** formed, assuming quantitative conversion to product. The data are presented in Table S7 and visualized in Figure S20. The curvature of the plots is consistent with a change from 1st-order dependence on $[\mathbf{1a}]_T$ at high catalyst concentration to 2nd-order dependence on $[\mathbf{1a}]_T$ at low catalyst concentration. The rate dependence on $[\mathbf{1a}]_T$ was fit to the rate law derived in Section 3.1 (Equation S16) at 20%, 40%, 60%, and 80% conversion of α-chloroisochroman **2**. The results of these fits are compiled in Table S6.

Scheme S10. Experiments to determine the kinetic order in thiourea catalyst **1a**.

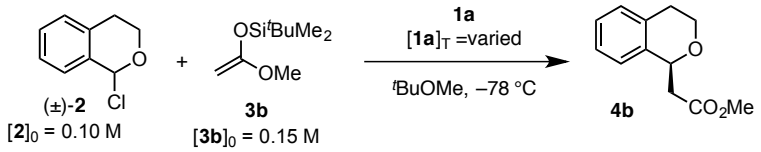

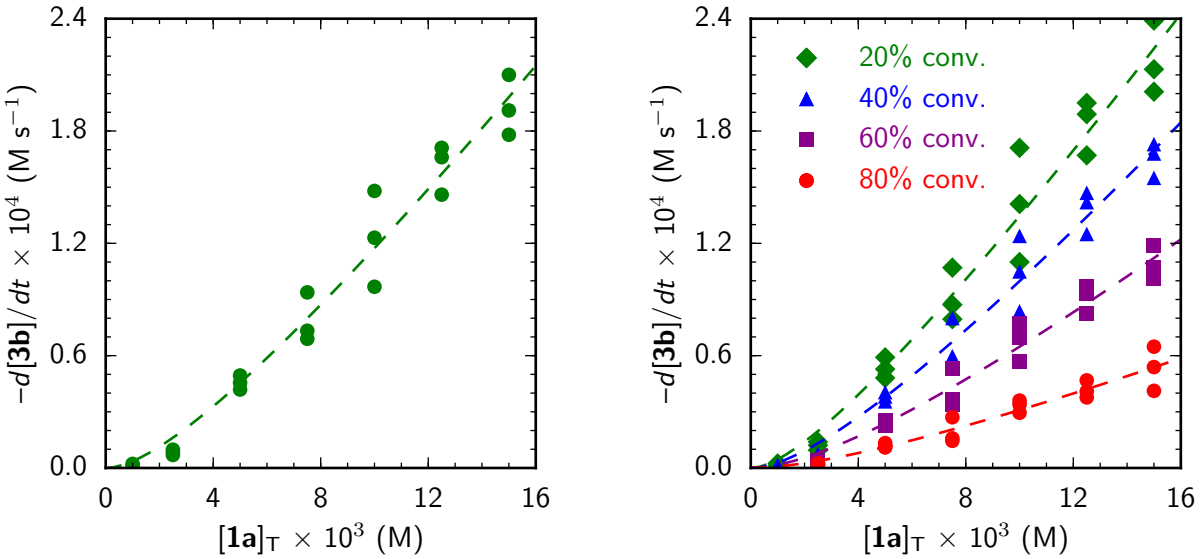

Figure S20. Rate as a function of total concentration of catalyst **1a**, at 30% conversion (left) and at multiple conversion values (right), fit to eq S16.

Table S6. Fitted parameters from Figure S20.[a]

Conversion of **2** (%)	[**2**] (M)	[**3b**] (M)	$k_{cat,obs}$ [a] (M^{-1} s^{-1})	k_{cat} (× 10^2 M^{-3} s^{-1})	K_{dim} (× 10^2 M^{-1})	R^2
20	0.08	0.13	7 ± 4	7 ± 4	1.5 ± 1.0	0.97
40	0.06	0.11	4 ± 2	6 ± 2	0.9 ± 0.6	0.97
60	0.04	0.09	2 ± 1	6 ± 2	0.7 ± 0.4	0.97
80	0.02	0.07	1.0 ± 0.6	7 ± 4	0.7 ± 0.6	0.92

[a] $k_{cat,obs} = k_{cat}$ [**2**] [**3b**]

Table S7. Rate as a function of total concentration of catalyst **1a**.[a]

	$-d[\mathbf{3b}]/dt$ ($\times 10^{-5}$ M•s^{-1})						
$[\mathbf{1a}]_T$ /mM	[**3b**] = 0.13 M (20% conv.)	[**3b**] = 0.12 M (30% conv.)	[**3b**] = 0.11 M (40% conv.)	[**3b**] = 0.10 M (50% conv.)	[**3b**] = 0.090 M (60% conv.)	[**3b**] = 0.080 M (70% conv.)	[**3b**] = 0.070 M (80% conv.)
15.0	21.3	19.1	16.8	14.4	11.9	9.27	6.48
15.0	20.1	17.8	15.5	13.1	10.7	8.09	5.39
15.0	23.9	21.0	17.3	13.7	10.1	6.81	4.12
12.5	19.5	17.1	14.7	12.2	9.69	7.17	4.68
12.5	18.9	16.6	14.2	11.8	9.33	6.76	4.09
12.5	16.7	14.6	12.5	10.4	8.25	6.03	3.77
10.0	11.0	9.68	8.37	7.03	5.68	4.32	2.95
10.0	17.1	14.8	12.4	10.1	7.71	5.44	3.39
10.0	14.1	12.3	10.5	8.76	6.99	5.25	3.60
7.50	8.72	7.33	5.97	4.64	3.40	2.31	1.45
7.50	7.95	6.90	5.83	4.76	3.68	2.60	1.58
7.50	10.7	9.38	8.01	6.65	5.29	3.96	2.71
5.00	5.91	4.94	4.05	3.24	2.53	1.90	1.33
5.00	5.28	4.55	3.82	3.09	2.38	1.70	1.12
5.00	4.81	4.19	3.56	2.92	2.29	1.68	1.10
2.50	1.21	0.976	0.758	0.564	0.408	0.301	0.232
2.50	1.39	0.849	0.566	0.470	0.346	0.292	0.257
2.50	0.951	0.695	0.483	0.350	0.285	0.224	0.154
1.00	0.125	0.113	0.156	ND	ND	ND	ND
1.00	0.243	0.218	0.157	ND	ND	ND	ND

[a] All reactions run with $[\mathbf{2}]_0 = 0.100$ M and $[\mathbf{3b}]_0 = 0.150$ M, in TBME at –78 °C.

The experiments to determine the kinetic order in thiourea catalyst **1a**, were repeated with silyl ketene acetal **3g** (Scheme S11). The reactions were initiated by adding catalyst as a stock solution in THF to a solution of **2** and **3g** in TBME at –78 °C. Rate was determined from the disappearance of silyl ketene acetal **3g** and corroborated with the appearance of ester product **4g**. The concentration [**2**] was inferred from the known initial concentration, $[\mathbf{2}]_0$, and the measured amount of **4b** formed, assuming quantitative conversion to product. The data are presented in Table S9 and visualized in Figure S21. The curvature of the plots is, again, consistent with a change from 1st-order dependence on $[\mathbf{1a}]_T$ at high catalyst concentration to 2nd-order dependence on $[\mathbf{1a}]_T$ at low catalyst concentration. The rate dependence on $[\mathbf{1a}]_T$ was fit to the rate law derived in Section 3.1 (Equation S16) at 10%, 20%, 30%, and 40% conversion of α-chloroisochroman **2**. The results of these fits are compiled in Table S8.

Scheme S11. Experiments to determine the kinetic order in thiourea catalyst **1a**.

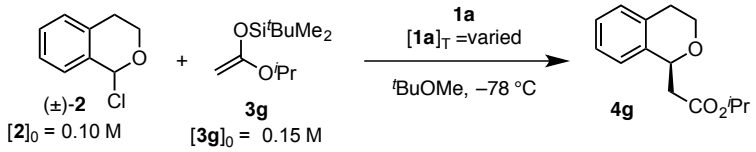

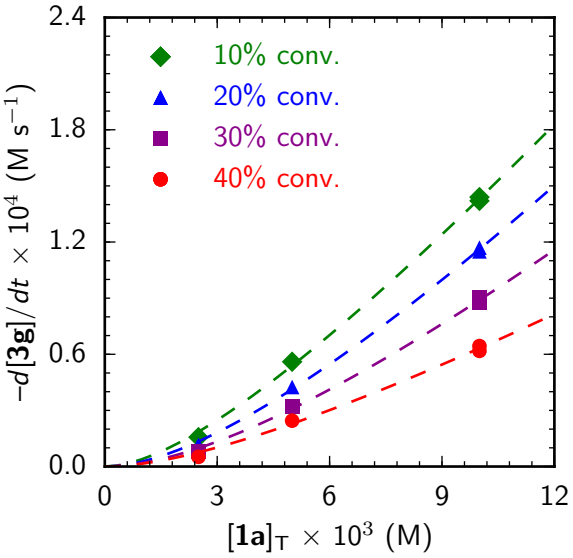

Figure S21. Rate as a function of total concentration of catalyst **1a**, fit to eq S16.

Table S8. Fitted parameters from Figure S21.[a]

Conversion of **2** (%)	[**2**] (M)	[**3g**] (M)	$k_{cat,obs}$[a] (M^{-1} s^{-1})	k_{cat} (× 10^2 M^{-3} s^{-1})	K_{dim} (× 10^1 M^{-1})	R^2
10	0.09	0.14	5 ± 1	4 ± 1	9 ± 3	0.9988
20	0.08	0.13	3.2 ± 0.5	3.1 ± 0.5	6 ± 2	0.9992
30	0.07	0.12	2.2 ± 0.5	2.7 ± 0.7	5 ± 2	0.998
40	0.06	0.11	1.9 ± 0.8	3 ± 1	6 ± 5	0.995

[a] $k_{cat,obs} = k_{cat}$ [**2**] [**3g**]

Table S9. Rate of consumption of silyl ketene acetal as a function of catalyst loading **1a**.[a]

	$-d$[**3g**]/dt ($\times 10^{-5}$ M•s^{-1})						
[**1a**]$_T$ (mM)	at [**3g**] = 0.14 M (10% conversion)	at [**3g**] = 0.13 M (20% conversion)	at [**3g**] = 0.12 M (30% conversion)	at [**3g**] = 0.11 M (40% conversion)	at [**3g**] = 0.10 M (50% conversion)	at [**3g**] = 0.090 M (60% conversion)	at [**3g**] = 0.080 M (70% conversion)
10	14.2	11.5	8.75	6.18	3.92	2.31	1.09
10	14.4	11.7	9.03	6.44	4.12	2.40	1.26
5	5.60	4.25	3.20	2.45	ND	ND	ND
2.5	1.57	1.16	0.801	0.516	0.335	0.215	0.0863

[a] All reactions run with [**2**]$_0$ = 0.100 M (0.20 mmol scale) and [**3g**]$_0$ = 0.150 M, in TBME at –78 °C.

3.4.2 Order in Urea Catalyst 1b

The experiments to determine the kinetic order in urea catalyst **1b**, were performed with silyl ketene acetal **3b** (Scheme S12). The reactions were initiated by adding catalyst as a stock solution in THF to a solution of **2** and **3b** in TBME at –78 °C. Rate was determined from the disappearance of silyl ketene acetal **3b** and corroborated with the appearance of ester product **4b**. The concentration [**2**] was inferred from the known initial concentration, $[\mathbf{2}]_0$, and the measured amount of **4b** formed, assuming quantitative conversion to product. The data are presented in Table S11 and visualized in Figure S22. The curvature of the plots is consistent with a 2nd-order dependence on $[\mathbf{1b}]_T$ over the entire concentration range examined. The rate dependence on $[\mathbf{1b}]_T$ was fit to the rate law derived in Section 3.1 (Equation S18) at 20%, 40%, and 60% conversion of α-chloroisochroman **2**. The results of these fits are compiled in Table S10.

Scheme S12. Experiments to determine the kinetic order in urea catalyst **1b**.

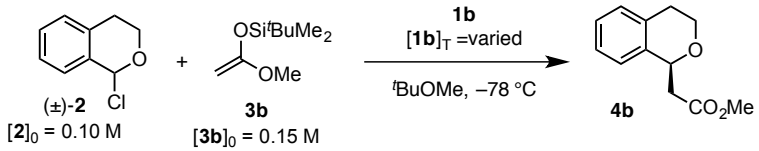

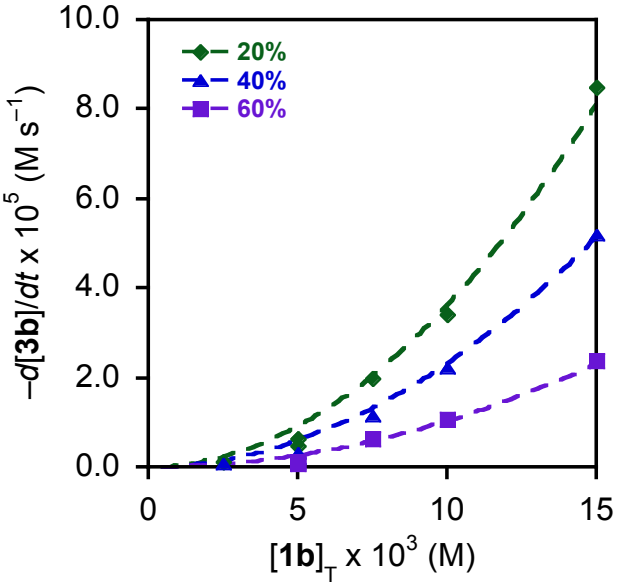

Figure S22. Rate as a function of total concentration of catalyst **1b**, fit to eq S18.

Table S10. Fitted parameters from Figure S22.[a]

Conversion of **2** (%)	[**2**] (M)	[**3b**] (M)	$k_{cat,obs}$ [a] ($\times 10^{-1}$ M^{-1} s^{-1})	k_{cat} ($\times 10^{1}$ M^{-3} s^{-1})	K_{dim} (M^{-1})	R^2
20	0.08	0.13	3.6 ± 0.7	3.5 ± 0.6	0.2 ± 3	0.99
40	0.06	0.11	2.4 ± 0.6	3.6 ± 0.8	0.8 ± 5	0.99
60	0.04	0.09	1.0 ± 0.3	2.9 ± 0.9	0.3 ± 5	0.92

[a] $k_{cat,obs} = k_{cat}$ [**2**] [**3b**]

Table S11. Rate as a function of total concentration of catalyst **1b**.

	$-d[\mathbf{3b}]/dt$ ($\times 10^{-5}$ M/s)					
$[\mathbf{1b}]_T$ /mM	[**3b**] = 0.13 M (20% conv.)	[**3b**] = 0.12 M (30% conv.)	[**3b**] = 0.11 M (40% conv.)	[**3b**] = 0.10 M (50% conv.)	[**3b**] = 0.09 M (60% conv.)	[**3b**] = 0.08 M (70% conv.)
15.0	8.49	6.84	5.22	3.70	2.39	1.44
10.0	3.42	2.83	2.23	1.64	1.06	0.572
7.50	1.99	1.53	1.17	0.885	0.648	0.381
5.00	0.632	0.452	0.320	0.222	0.124	0.080
5.00	0.461	0.327	0.211	0.136	0.0931	NA
2.50	0.124	0.0908	0.0853	NA	NA	NA
2.50	0.123	0.0742	NA	NA	NA	NA

3.5 Kinetic Isotope Effect (KIE) Experiments

Scheme S13. Competition kinetic isotope effect experiment.

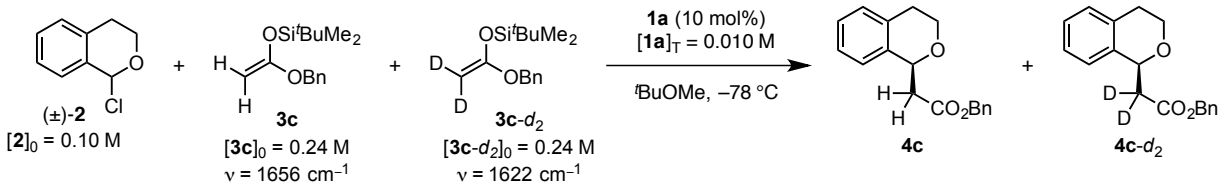

An oven-dried flask (see Figure S15) equipped with a stir bar was attached to a ReactIR probe that had been warmed with a heat gun and the system was purged with N_2. After the purge outlet was closed, the system was kept under a positive pressure of N_2 for the remainder of the experiment. The flask was allowed to cool to rt, charged with TBME (1.485 mL), then cooled to –78 °C (using a dry ice/acetone cooling bath.) After the temperature had stabilized (~ 15–20 min) a background spectrum was acquired (600–3400 cm^{-1}). All spectra were measured with a two-point correction baseline. To the reaction vessel was added a solution of silyl ketene acetal **3d** (330 μL, 0.485 mmol, 1.47 M in TBME; prepared by diluting 388.5 mg to 1.00 mL total volume in TBME), followed by a solution of silyl ketene acetal **3d**-d_2 (330 μL, 0.485 mmol, 1.47 M in TBME; prepared by diluting 391.5 mg to 1.00 mL total volume in TBME), followed by 1-chloroisochroman **2** (135 μL, 0.100 mmol, 0.741 M in TBME; prepared by dissolving 125 mg to 1.00 mL total volume in TBME). The reaction was initiated by adding catalyst as a stock solution in THF (50 μL, 0.020 mmol, 0.40 M in THF, prepared by dissolving 220 mg of **1a** to 1.00 mL total volume in THF). The reaction was quenched by the addition of NaOMe (0.15 mL, 0.5 M NaOMe in MeOH). The reaction mixture was diluted with 1 mL of 50% Et_2O in hexanes, filtered through a pipette filled with ¾ inch of silica gel using ca. 15 mL of 50% Et_2O in hexanes. The solvent was removed by rotary evaporation under reduced pressure to give the crude residue, which was purified by silica gel chromatography (6% Et_2O in hexanes).

The kinetic isotope effect (KIE) is defined as:

$$KIE = \frac{d[\mathbf{3c}]/dt}{d[\mathbf{3c}\text{–}d_2]/dt} \tag{S22}$$

Compounds 3c and 3c-d2 exhibit distinct C=O stretching frequencies, displaying maximum absorbance at 1656 cm^{-1} and 1622 cm^{-1}, respectively. Equation S19 can be substituted into Equation S22 to afford:

$$KIE = \frac{dA_{1656}/R_{0,\mathbf{3c}}dt}{dA_{1622}/R_{0,\mathbf{3c}-d_2}dt} \tag{S23}$$

Assuming that the two isotopologues exhibit the same absorption response factor (R_o) at the frequencies of maximum absorbance, Equation S23 can be simplified to describe the KIE in terms of the change of the absorbance at 1656 cm^{-1} and 1622 cm^{-1}:

$$KIE = \frac{dA_{\mathbf{3c}}/dt}{dA_{\mathbf{3c}-d_2}/dt} \quad \text{(S23)}$$

The results from two trials of this analysis are complied in Table S12

Table S12. Details of KIE experiments described in Scheme S13 and the text above.

Run 1			*Run 2*		
[**4c**] /M	$\frac{A_{\mathbf{3c}}}{A_{\mathbf{3c}-d_2}}$	$\frac{dA_{\mathbf{3c}}/dt}{dA_{\mathbf{3c}-d_2}/dt}$	[**4c**] /M	$\frac{A_{\mathbf{3c}}}{A_{\mathbf{3c}-d_2}}$	$\frac{dA_{\mathbf{3c}}/dt}{dA_{\mathbf{3c}-d_2}/dt}$
0.00	0.961	ND	0.00	0.949	ND
0.011	0.962	0.896	0.010	0.959	0.812
0.020	0.968	0.888	0.020	0.961	0.836
0.029	0.965	0.876	0.029	0.962	0.865
0.040	0.968	0.866	0.040	0.963	0.889

By averaging the four data points described by Equation S23, KIE's of 0.882 and 0.851 were obtained from runs 1 and 2, respectively. The average KIE from both runs is therefore determined to be 0.87. The observation of an inverse secondary KIE is consistent with the observation of a positive order for the silyl ketene acetal in the kinetic experiments presented above and suggest that the rate determining step is C–C bond formation between the oxocarbenium ion and the silyl ketene acetal.

4. X-ray Crystallographic Structures of Catalysts

X-ray crystallographic images below were generated based on data from the CIF files. The images were rendered using CYLview[7] rather than an ORTEP representation to enable improved clarity. The CCDC numbers corresponding to the X-ray crystallographic data for the structures have been provided in Section 1.

A. Mirror image of (*ent*-**1a**)•(*ent*-**1a**)

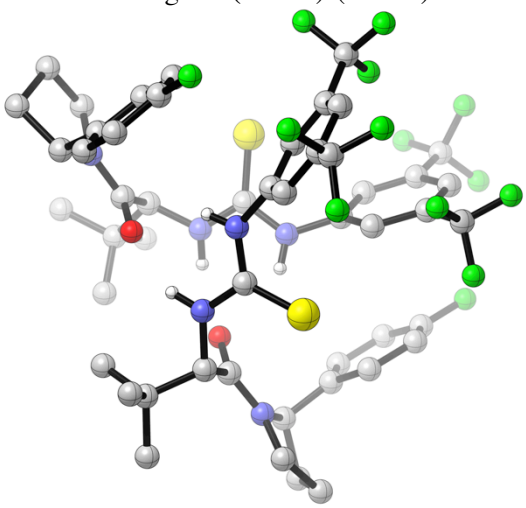

B. (**1a**)•(*ent*-**1a**), Dimer 1 of 2

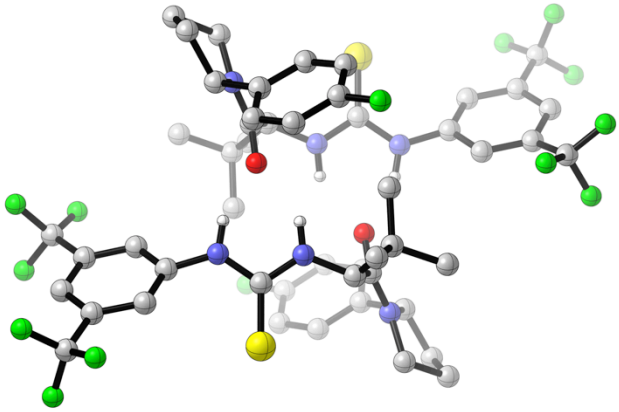

C. (**1a**)•(*ent*-**1a**), Dimer 2 of 2

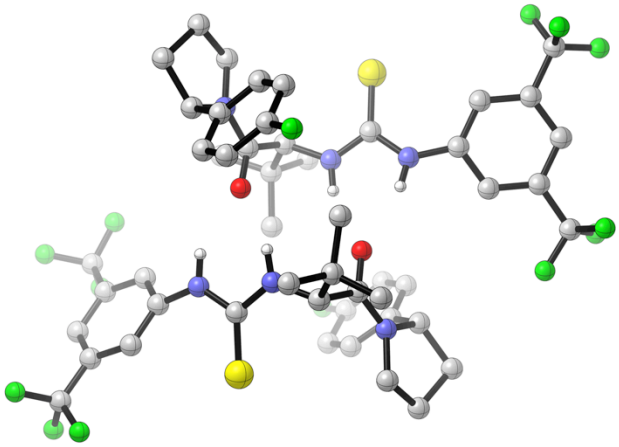

D. (**1c**)•(**1c**), (**1c** is a diastereomer of **1a**)

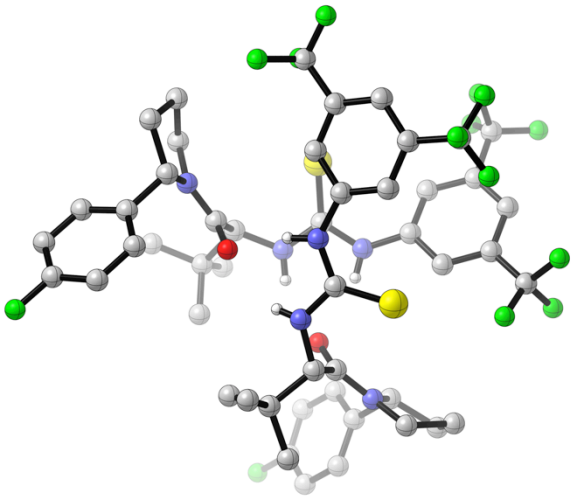

Figure S23. X-ray crystallographic structures of A. (*ent*-**1a**)•(*ent*-**1a**),[12] B. (**1a**)•(*ent*-**1a**), dimer 1 of 2,[13] C. (**1a**)•(*ent*-**1a**), dimer 2 of 2,[13] D. (**1c**)•(**1c**), **1c** is a diastereomer of **1a**. Carbon-bound hydrogen atoms have been omitted for clarity. Only one geometry is shown for structures containing partial disorder. Atom color legend: hydrogen (white), carbon (silver), nitrogen (blue), oxygen (red), fluorine (green), sulfur (yellow)

(12) The crystal structure shown in Figures S23a was obtained with *ent*-**1a** instead of **1a**. The mirror image of the structure is presented here in order to facilitate comparison with the other X-ray crystallographic structures.

(13) Two crystallographically independent dimers exist in the same crystal. Each dimer is shown independently.

A. Mirror image of [*ent*-**1a**]$_2$•Me$_4$NCl

Alternate view

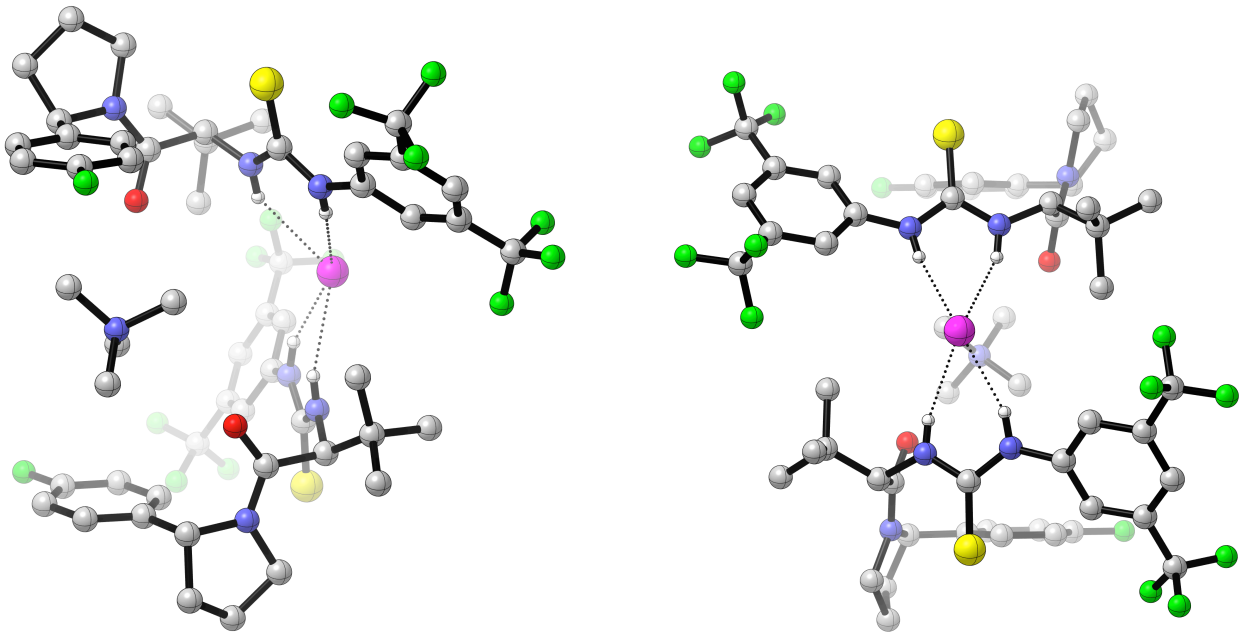

B. Mirror image of [*ent*-**1b**]$_2$•Me$_4$NCl

Alternate view

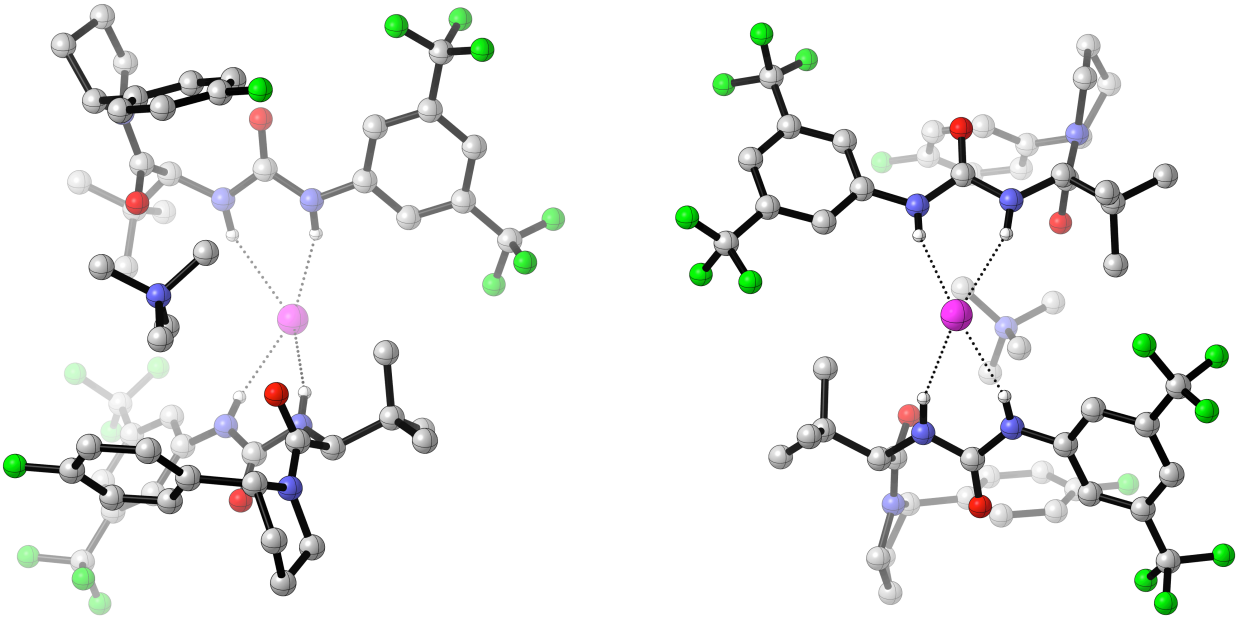

Figure S24. Mirror image of X-ray crystallographic structures of (a) **(*ent*-1a)$_2$•Me$_4$NCl** and (b) **(*ent*-1b)$_2$•Me$_4$NCl**. Carbon-bound hydrogen atoms have been omitted for clarity. Only one geometry is shown for structures containing partial disorder. Atom color legend: hydrogen (white), carbon (silver), nitrogen (blue), oxygen (red), fluorine (green), sulfur (yellow), chlorine (pink).[14]

(14) The crystal structure shown in Figures S24a and S24b were were obtained with *ent*-**1a** and *ent*-**1b** instead of **1a** and **1b**. The mirror image of the structure is presented here in order to facilitate comparison with the other X-ray crystallographic structures.

5. NMR Experiments to Determine Catalyst Solution Structure

5.1 General Information

Pulse sequences used as implemented in Varian VNMR on Varian INOVA 500 spectrometers. Our assignments were made primary with 2D NOESY and TOCSY spectra. NOESY spectra were recorded using deoxygenated solvent.

Each proton is lettered according to the diagram shown below. Because the catalyst is a mixture of amide rotamers, we use the convention (*E*)-H^a and (*Z*)-H^a to refer to the proton at position H^a in the *(E)*- and *(Z)*-amide rotamers, respectively.

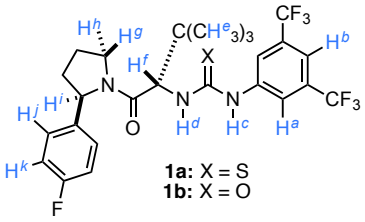

Figure S25. Labeling system used to denote hydrogen atoms in catalysts **1a** and **1b** for the discussion of the solution structure determination via NMR spectroscopy.

5.2 Assignment of Intermolecular nOe's:

When studying the 2D NOESY spectra shown below, it was straightforward to assign the nOe between protons of the *E* rotamer and protons of the *Z* rotamer as being intermolecular in origin. In contrast, the (*E*,*E*) and (*Z*,*Z*) homodimers also have characteristic nOe's, but because the dimers are symmetric, the nOe could theoretically arise from close contacts within one molecule of catalyst or from contacts between two molecules of catalyst. To determine whether a given nOe (NOESY crosspeak) is due to the monomer or the dimer, we consider the relevant H–H distance in the monomer and the dimer. We used DFT calculations at the B3LYP/6-31G(d) level of theory for this purpose. We present here the relevant distances for our analysis. A discussion of our computational methods is presented in Section 7.

(a) Type I Dimer (Solid State) **(b) Type II Dimer (Alternate Geometry)**

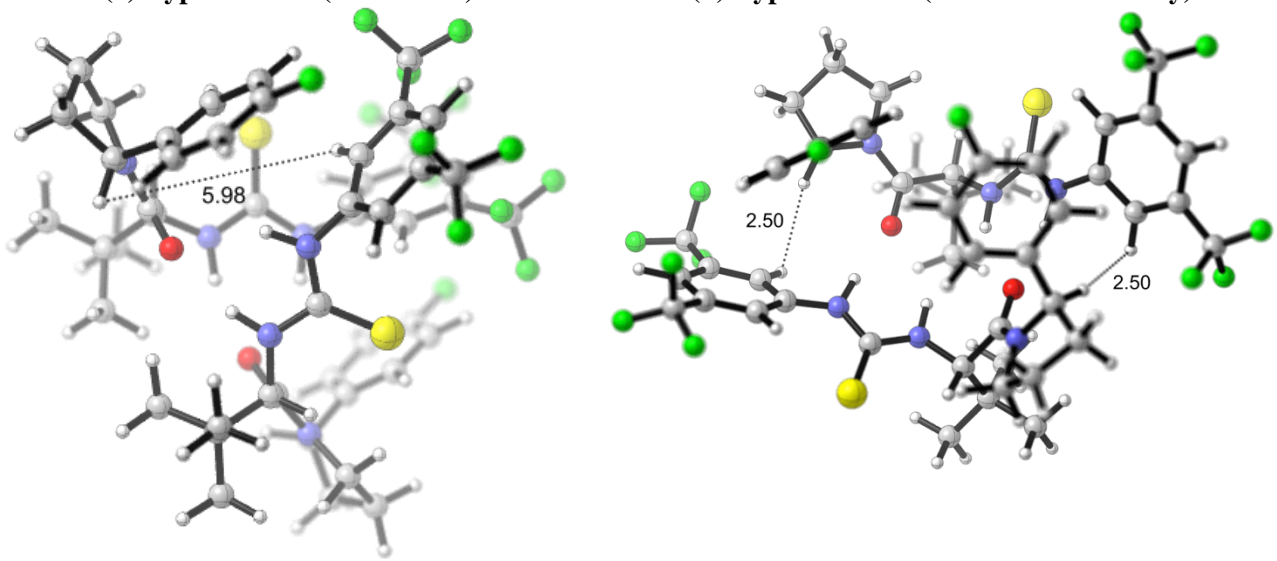

Figure S26. DFT optimized geometry of [(*Z*)-**1a**]$_2$ illustrating the (*Z*)- H^a to (*Z*)-H^i distance relevant to the very weak NOESY crosspeak observed. (a) Type I dimer (solid state form) (b) Type II dimer (alternate geometry).

(a) Type I Dimer (Solid State) **(b) Type II Dimer (Alternate Geometry)**

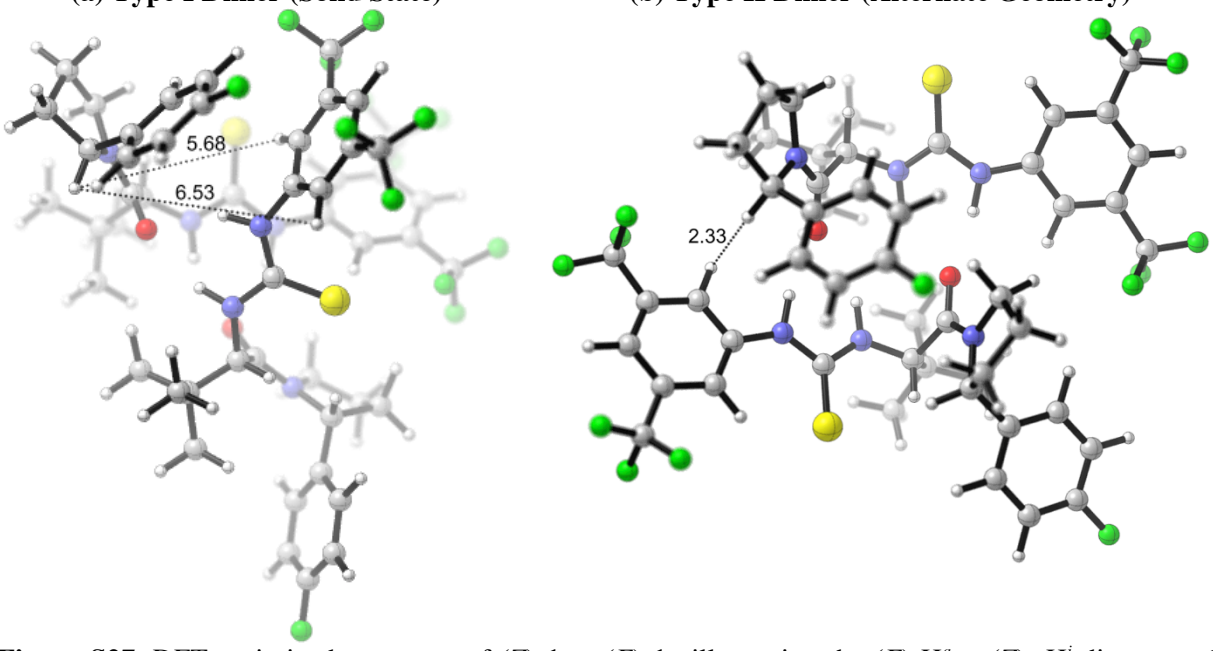

Figure S27. DFT optimized geometry of (*Z*)-**1a** • (*E*)-**1a** illustrating the (*E*)-H^a to (*Z*)- H^i distance relevant to the NOESY crosspeak observed. (a) Type I dimer (solid state form) (b) Type II dimer (alternate geometry).

(a) Type I Dimer (Solid State) **(b) Type II Dimer (Alternate Geometry)**

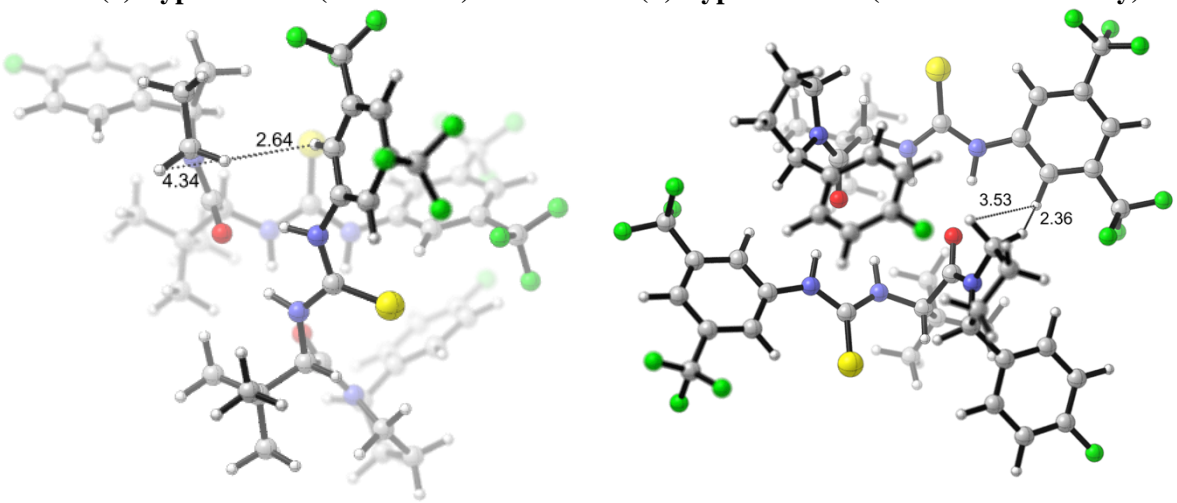

Figure S28. DFT optimized geometry of (*Z*)-**1a** • (*E*)-**1a** illustrating the (*Z*)- H^a to (*E*)- H^g/H^h distance relevant to the NOESY crosspeak observed. (a) Type I dimer (solid state form) (b) Type II dimer (alternate geometry).

(a) Type I Dimer (Solid State) **(b) Type II Dimer (Alternate Geometry)**

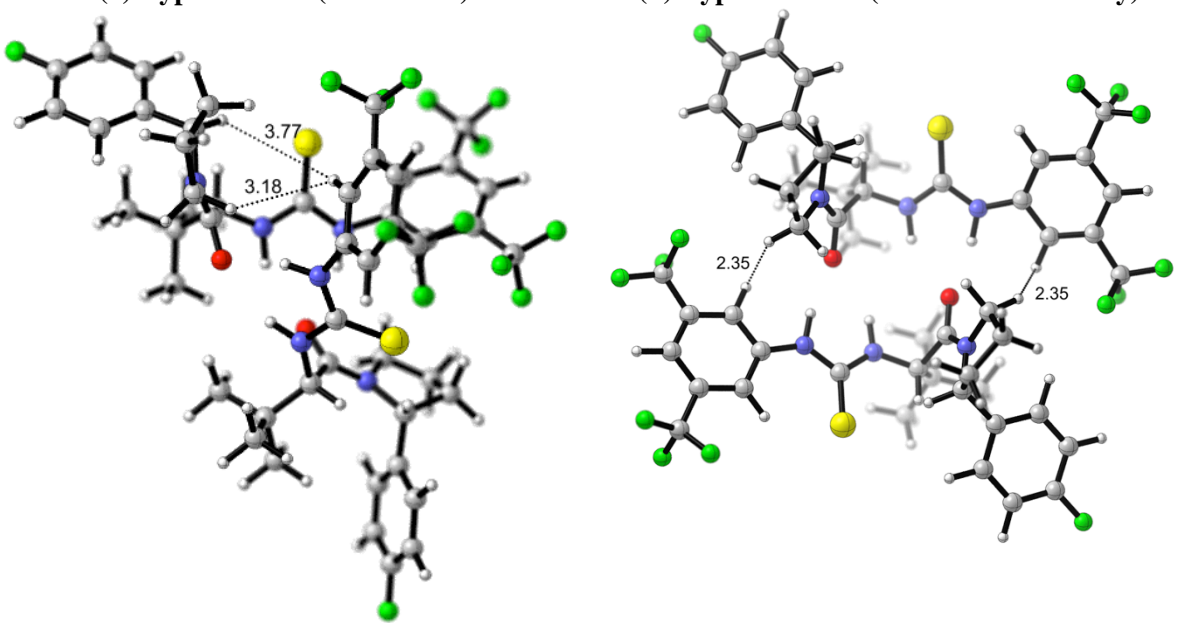

Figure S29. DFT optimized geometry of $[(E)\text{-}\mathbf{1a}]_2$ illustrating the (E)-H^a to (E)-H^g/H^h distance relevant to the NOESY crosspeak observed. (a) Type I dimer (solid state form) (b) Type II dimer (alternate geometry).

(a) (*E*)-1a (Gas phase DFT Geometry) **(b) (*Z*)-1a (Gas phase DFT Geometry)**

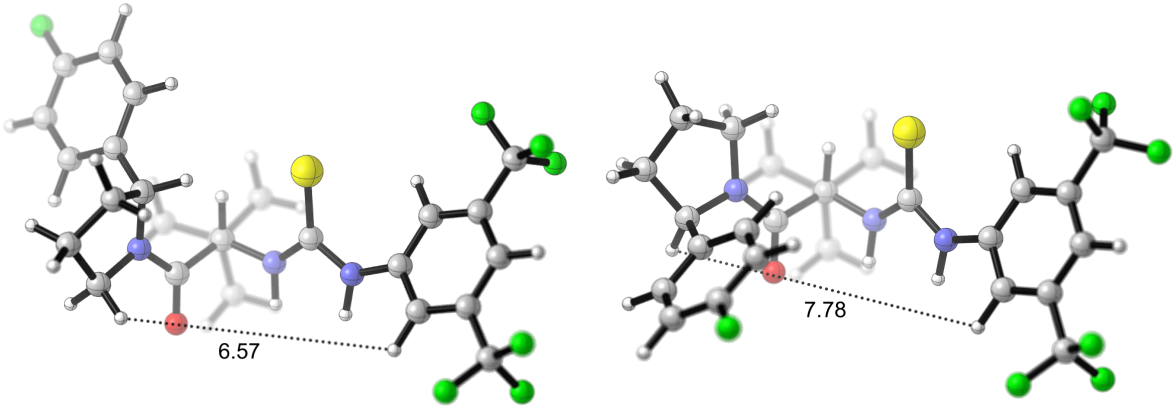

Figure S30. DFT optimized geometry of (a) (*E*)-**1a** and (b) (*Z*)-**1a** illustrating that the intramolecular distance relevant to the NOESY crosspeak observed is too large, thus supporting the interpretation that the NOESY crosspeak must be due to intermolecular interactions.

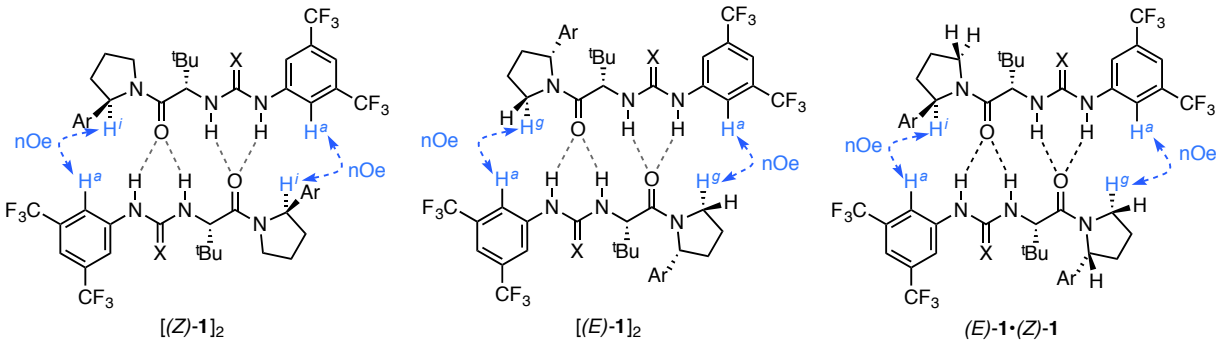

Figure S31. Summary of diagonstic nOe correlations.

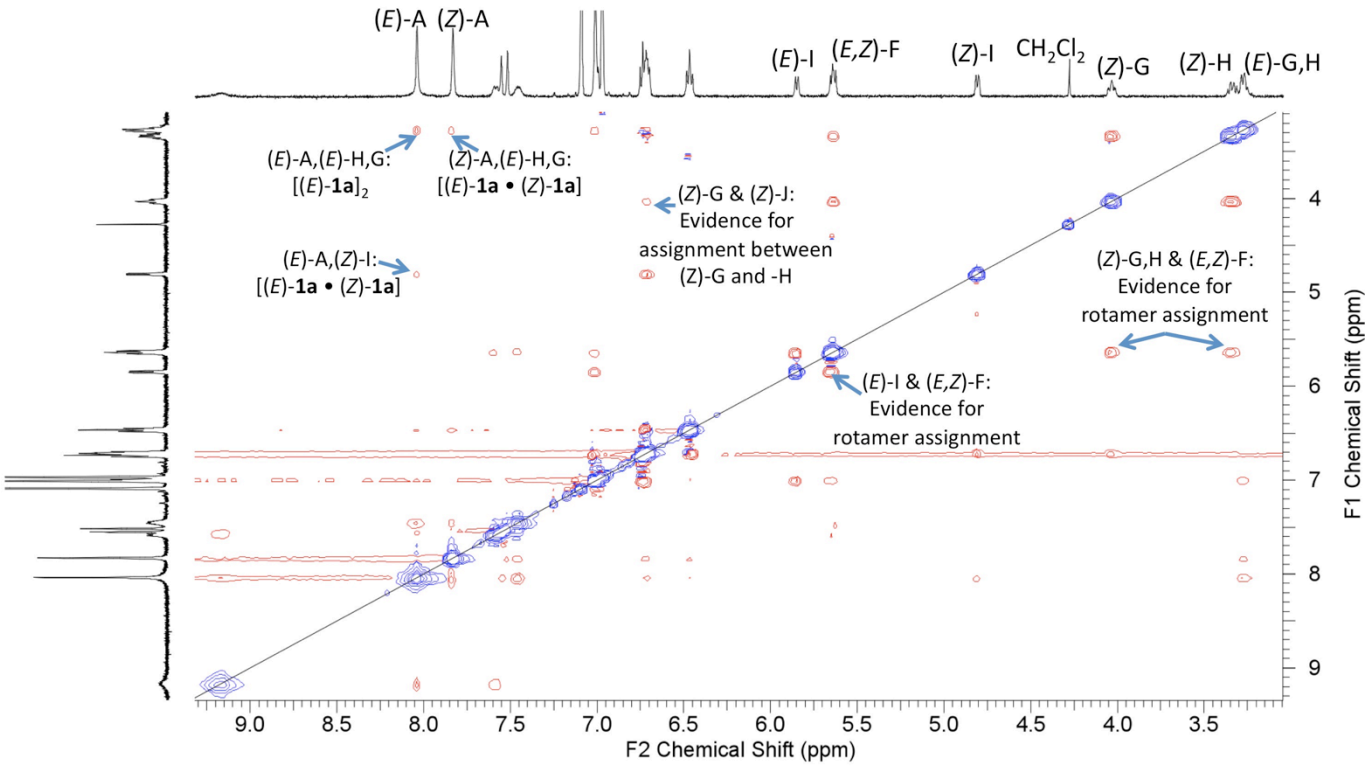

Figure S32a. NOESY spectrum of **1a** (10 mM, toluene-d_8, 25 ºC, 128 increments in the indirectly detected dimension, 16 scans per increment).

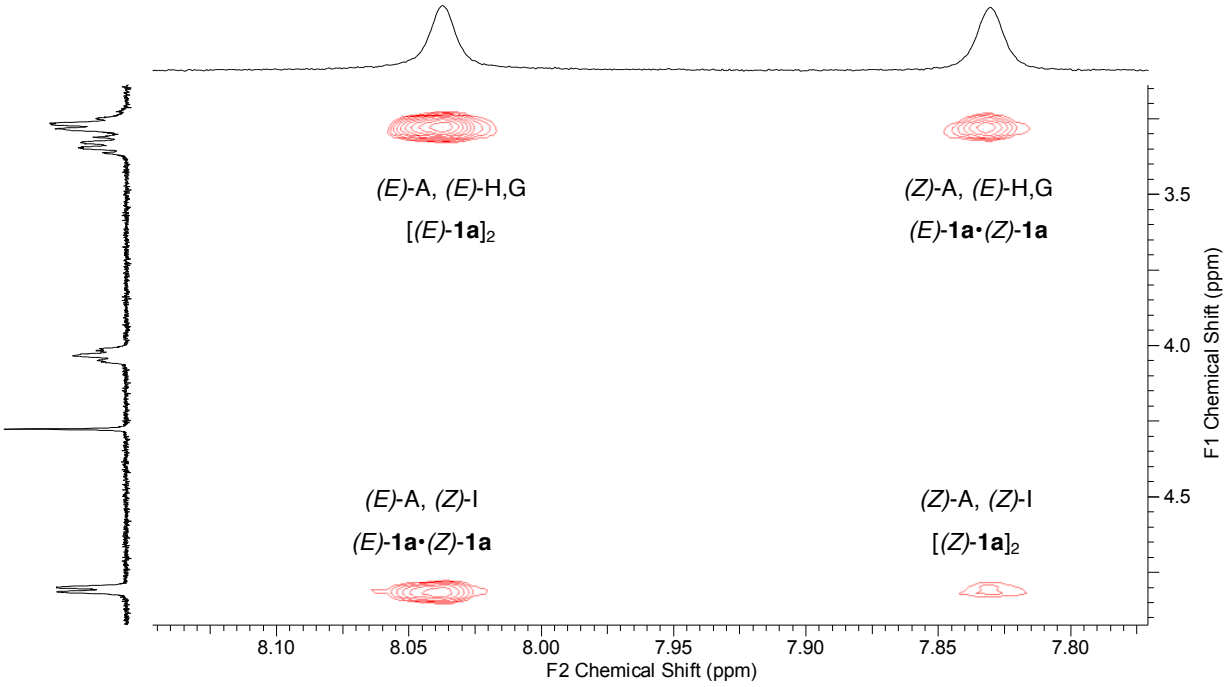

Figure S32b. Zoom in region of Figure S32a depicting NOESY spectrum of **1a** illustrating nOe cross peaks (*E*)-A ↔ (*E*)-G, (*E*)-A ↔ (*E*)-H, (*Z*)-A ↔ (*E*)-G,H, (*E*)-A ↔ (*Z*)-I, and (*Z*)-A ↔ (*Z*)-I.

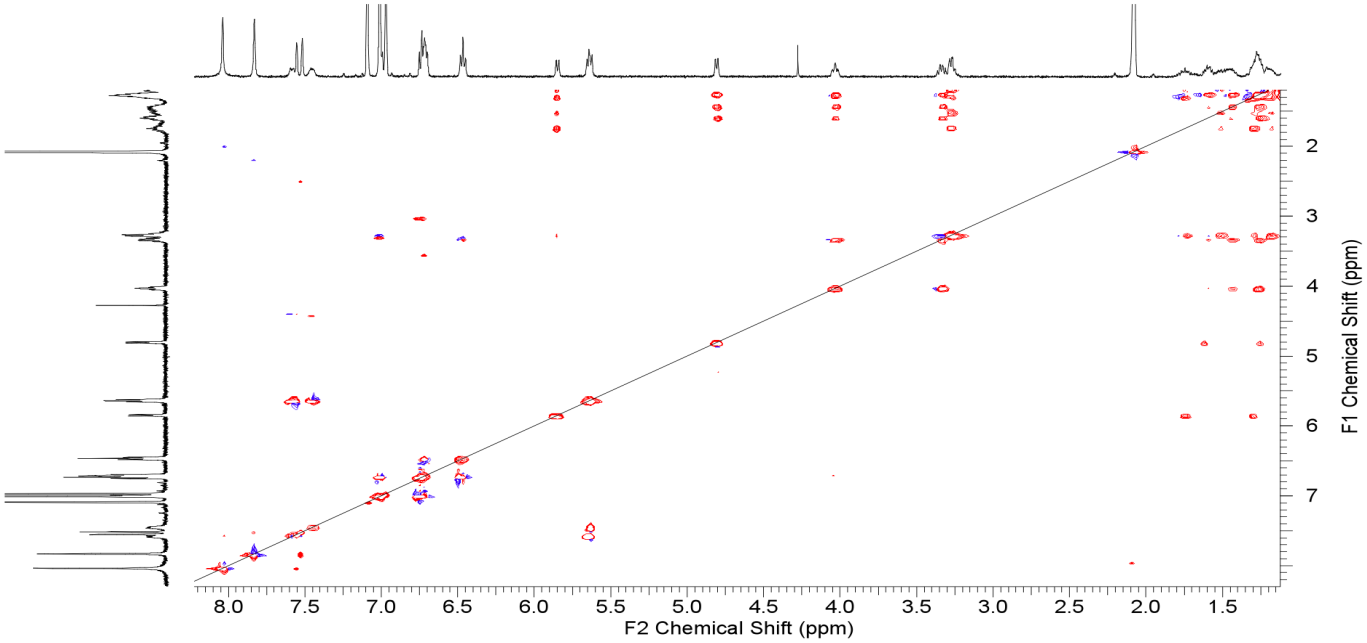

Figure S33. TOCSY spectrum of **1a** (10 mM, toluene-d_8, 25 ºC).

Assignment of the Solution Structure of Urea Catalyst **1b**

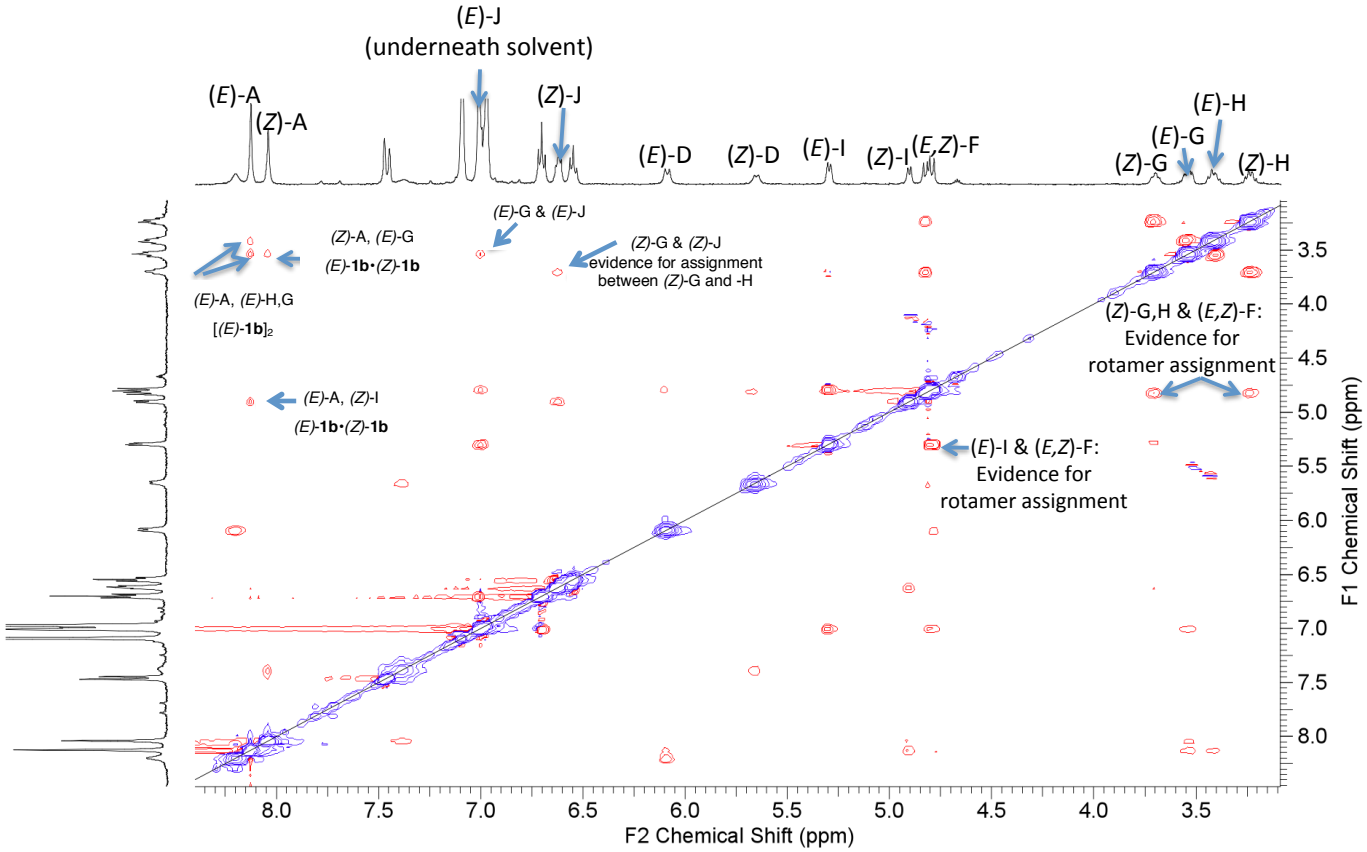

Figure S34. NOESY spectrum of **1b** (10 mM, toluene-d_8, 25 ºC).

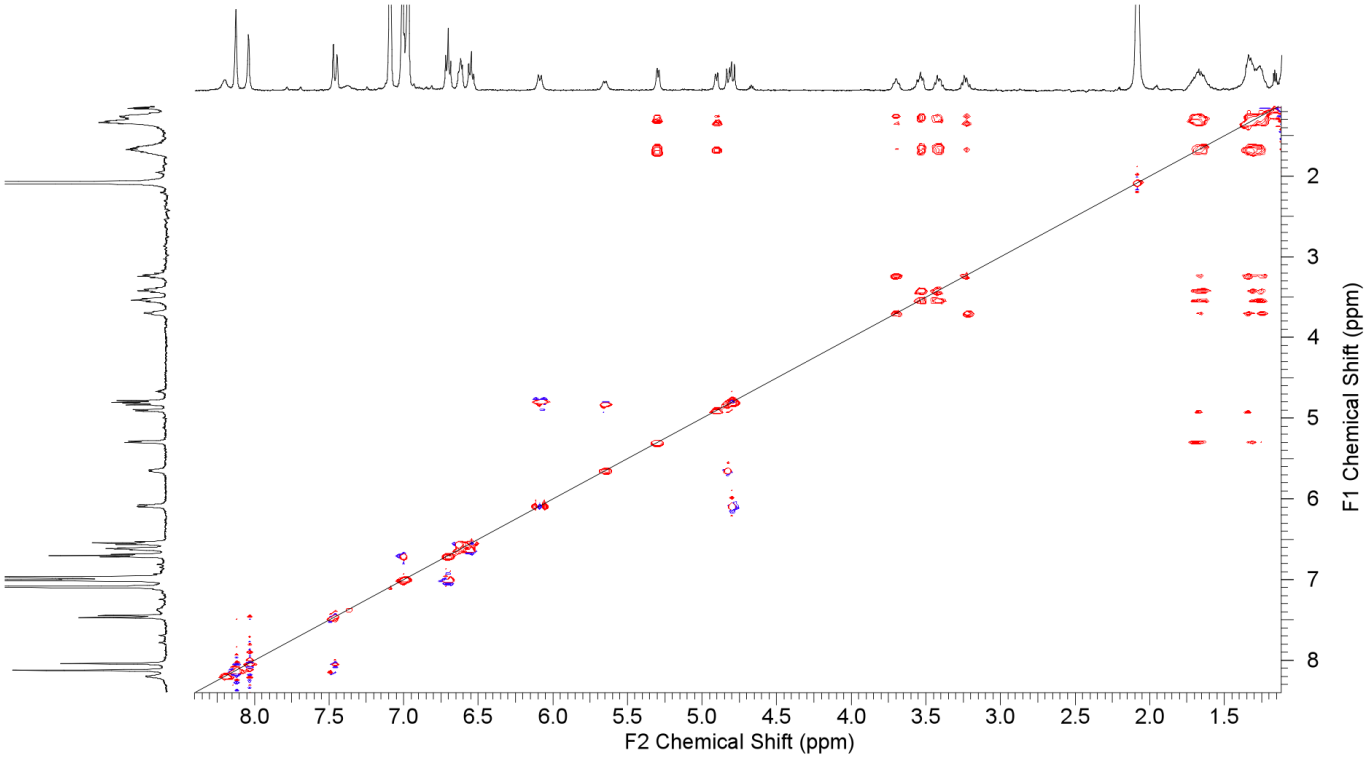

Figure S35. TOCSY spectrum of **1b** (10 mM, Toluene-d_8, 25 ºC).

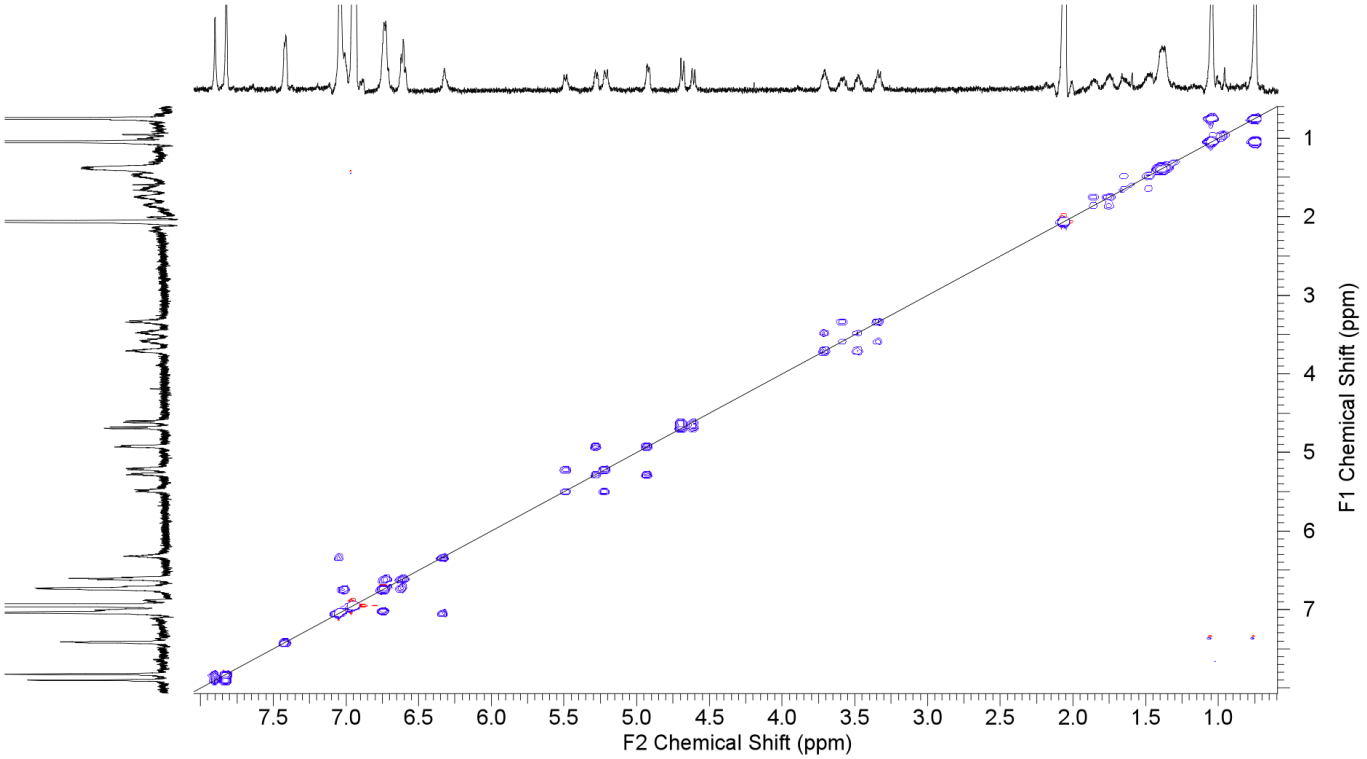

Figure S36. NOESY spectrum of **1b** (10 mM, Toluene-d_8, 80 ºC, 96 increments in the indirectly detected dimension, 16 scans per increment). Note that at this temperature, the major peaks are the same phase as the diagonal. These are due to chemical exchange between the amide rotamers of **1b**. For example, a cross-peak connects (*Z*)-A with (*E*)-A. This spectrum indicates that rotamer conversion occurs on the timescale of seconds at 80 ºC (the EXSY timescale). This is evidence for our assignment of the two sets of peaks present in the spectrum as amide rotamers.

5.3 Determination of Catalyst Dimerization Constants

Amide rotation in catalysts such as **1a** and **1b** is generally quite slow. No EXSY cross peaks are observed between amide rotamers at room temperature, but strong EXSY is observed at 70 ºC (toluene-d_8, t_{mix} = 400 ms). As such, the dimerization constants for the *(Z)-* and *(E)-* rotameric forms of the catalysts **1a** and **1b** may be determined independently by measuring changes in the chemical shifts of diagnostic ^{1}H NMR signals observed upon serial dilution.[15] The 2D NMR spectra used to assign these 1D spectra are presented in the preceding Section 5.2. The analysis was performed in toluene-d_8 at 25 °C to obtain high quality spectra and reproduced at –40 °C to more closely reproduce the low temperatures used for the kinetic experiments. At –40 °C the ^{1}H NMR spectrum of **1a** changes very little upon dilution from 15 mM to 0.1 mM. Significant peak broadening precluded a definitive assignment of the spectrum at this temperature. One resonance that changed in a well-behaved manner across the concentration range examined (labeled P3 in Figure S37) was identified. The spectrum of **1b** changes significantly on dilution, but only the peaks corresponding to the *Z* rotamer change as a function of concentration, while the peaks corresponding to the *E* rotamer remain fairly constant. Because our room temperature data show that the *(E)*-amide rotamer forms a more stable dimer than the *(Z)*-amide rotamer, this result is suggestive that *(E)*-**1b** is fully dimerized over the full concentration range, while *(Z)*-**1b** undergoes a transition to monomer at lower concentrations. While these data do not allow for a clear comparison between **1a** and **1b**, it does appear that **1a** is aggregated to at least the same extent as **1b** at –40 ºC, perhaps slightly more so. The data from analyses at both temperatures are compiled in Table S13 and visualized in Figure S37.

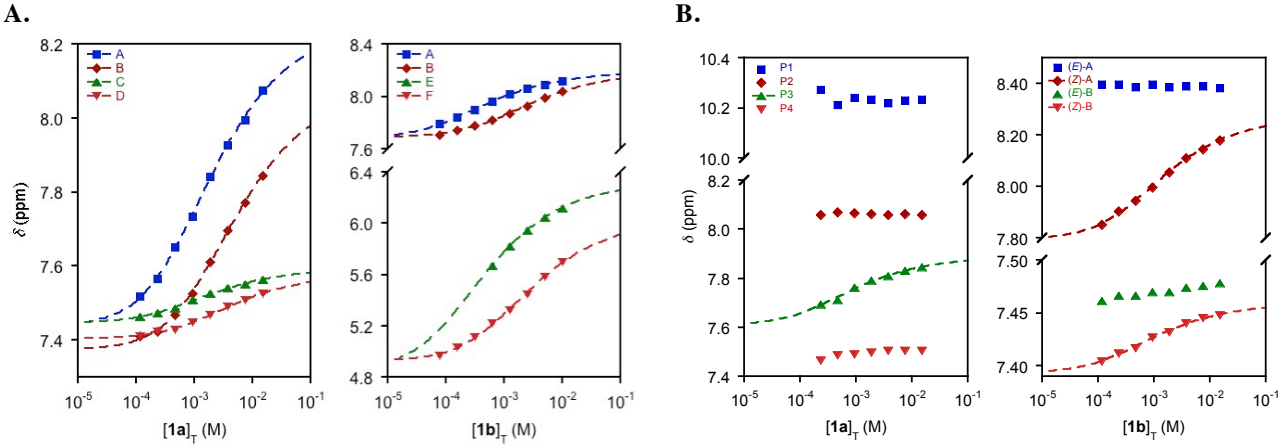

Figure S37. Dependence of key ^{1}H NMR chemical shifts of **1a** and **1b** on total catalyst concentration. Spectra were acquired in toluene-d_8 at A. 25 ºC or B. –40 °C. The dashed lines represents the fit to a simple monomer-dimer model with the parameters in Table S13.

(15) (a) Tan, H. K. S. *J. Chem. Soc., Faraday Trans* **1994**, *90*, 3521–3525; (b) Nogales, D. F.; Ma, J.-S.; Lightner, D. A. *Tetrahedron* **1993**, *49*, 2361–2372.

Table S13. Fitted parameters for the ^{1}H NMR dilution experiments with **1a** and **1b** in toluene-d_8.

A. at 25 °C						**B**. at –40 °C					
Catalyst	Peak	Proton	δ_{dimer} (ppm)	$\delta_{monomer}$ (ppm)	$K_{dim,obs} \times 10^2$ (M^{-1})	Catalyst	Peak	Proton	δ_{dimer} (ppm)	$\delta_{monomer}$ (ppm)	$K_{dim,obs} \times 10^2$ (M^{-1})
1a	A	*(E)*-H^a	8.25 ± 0.01	7.44 ± 0.01	4.9 ± 0.5	**1a**	P3	ND	7.89 ± 0.01	7.61 ± 0.04	13 ± 8
	B	*(Z)*-H^a	8.09 ± 0.02	7.374 ± 0.006	1.9 ± 0.2						
	C	*(E)*-H^b	7.595 ± 0.004	7.446 ± 0.004	6 ± 1						
	D	*(Z)*-H^a	7.580 ± 0.005	7.403 ± 0.002	2.4 ± 0.3						
1b	A	*(E)*-H^a	8.193 ± 0.003	7.68 ± 0.01	21 ± 2	**1b**	*(Z)*-H^a	*(Z)*-H^a	8.272 ± 0.009	7.80 ± 0.01	7 ± 1
	B	*(Z)*-H^a	8.19 ± 0.01	7.69 ± 0.01	3.7 ± 0.5		*(Z)*-H^b	*(Z)*-H^b	7.459 ± 0.001	7.393 ± 0.003	10 ± 2
	E	*(E)*-H^d	6.33 ± 0.01	4.9 ± 0.1	22 ± 6						
	F	*(Z)*-H^d	6.03 ± 0.04	4.93 ± 0.02	3.6 ± 0.5						

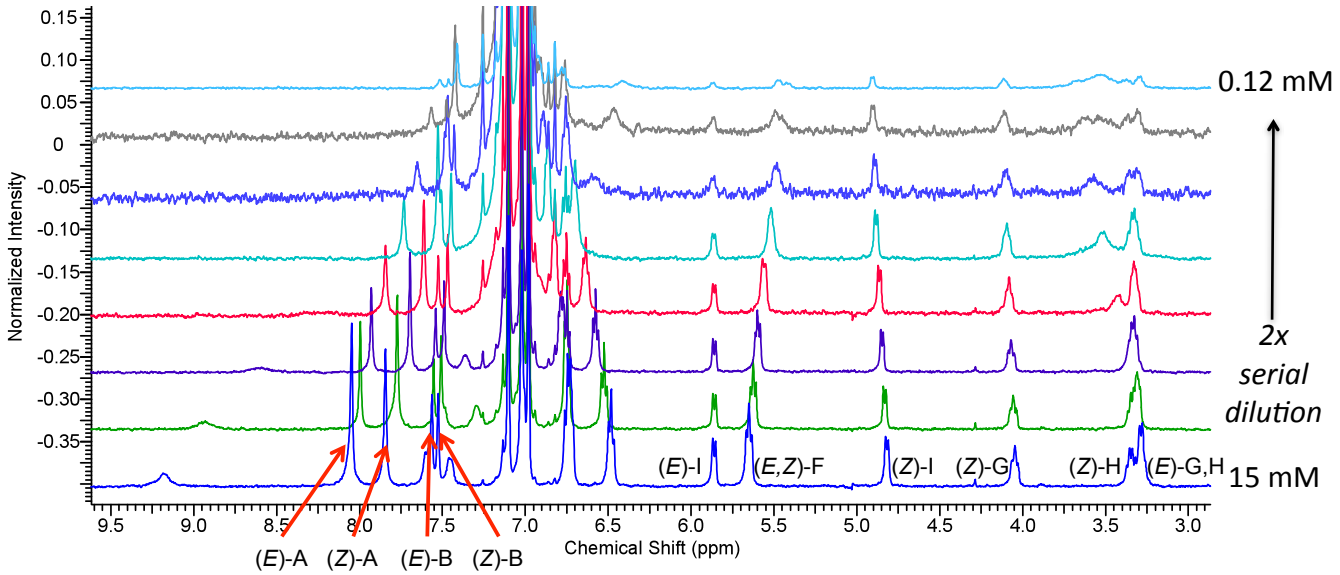

Figure S38. The effect of dilution on the ^{1}H NMR spectrum (500 MHz) of catalyst **1a** in toluene-d_8 at 25 ºC.

Table S14. Data extracted from Figure S38.

	Chemical Shift (ppm)			
$[\mathbf{1a}]_T$ (mM)	*(E)*-H^a	*(Z)*-H^a	*(E)*-H^b	*(Z)*-H^b
15	8.0740	7.8430	7.5630	7.5250
7.5	7.9940	7.7720	7.5520	7.5080
3.75	7.9280	7.6950	7.5410	7.4900
1.88	7.8420	7.6120	7.5250	7.4680
0.94	7.7330	7.5260	7.5070	7.4470
0.47	7.6510	7.4670	7.4850	7.4290
0.23	7.5650	7.4230	7.4740	7.4230
0.12	7.5170	7.4110	7.4640	7.4110

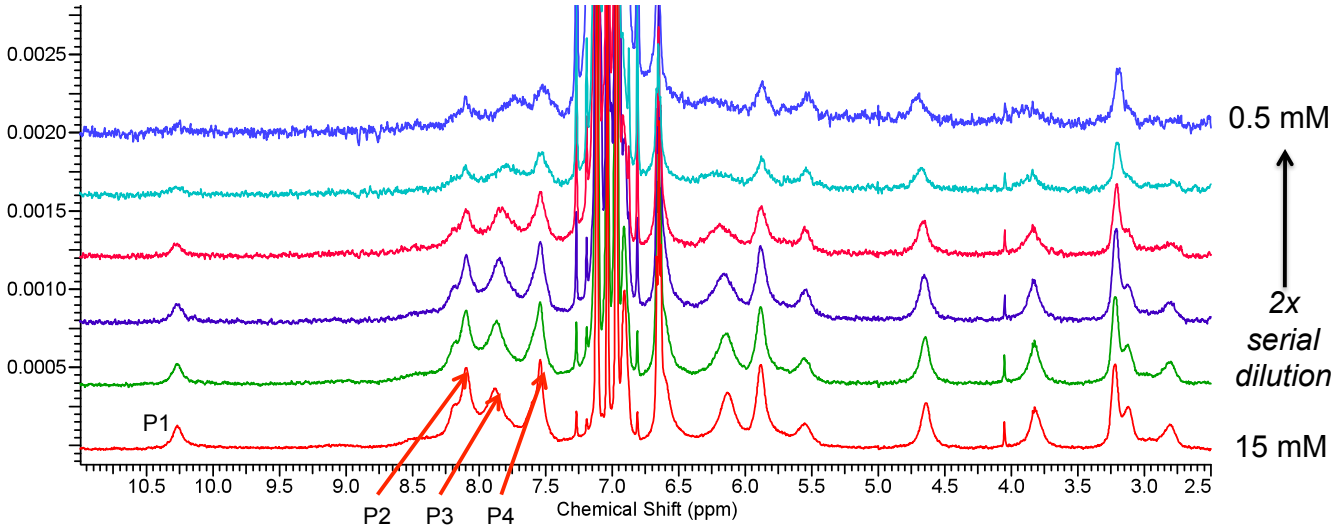

Figure S39. The effect of dilution on the ^{1}H NMR spectrum (500 MHz) of catalyst **1a** in toluene-d_8 at –40 ºC.

Table S15. Data extracted from Figure S39.

	Chemical Shift (ppm)			
$[\mathbf{1a}]_T$ (mM)	P1	P2	P3	P4
15	10.234	8.0610	7.8450	7.5070
7.5	10.231	8.0630	7.8320	7.5060
3.75	10.221	8.0590	7.8080	7.5060
1.88	10.235	8.0640	7.7910	7.4980
0.94	10.241	8.0660	7.7610	7.4920
0.47	10.214	8.0710	7.7120	7.4870
0.23	10.274	8.0610	ND	7.4660

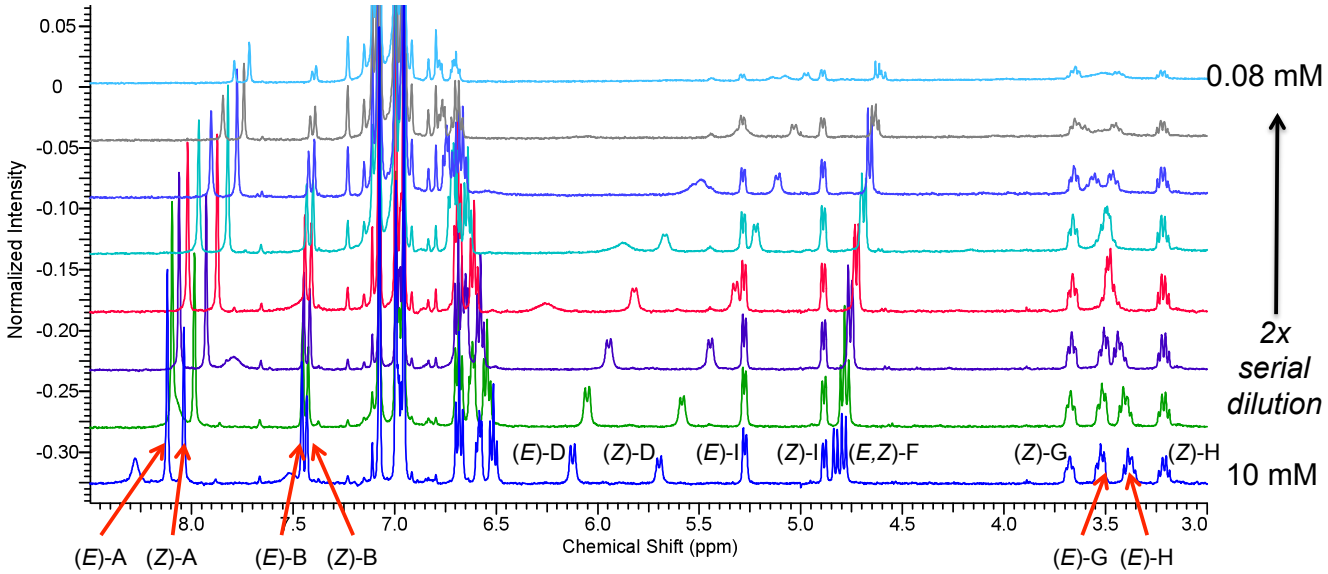

Figure S40. The effect of dilution on the ^{1}H NMR spectrum (500 MHz) of catalyst **1b** in toluene-d_8 at 25 ºC.

Table S16. Data extracted from Figure S40.

$[\mathbf{1b}]_T$ (mM)	Chemical Shift (ppm)			
	(E)-H^a	*(Z)*-H^a	*(E)*-H^d	*(Z)*-H^d
10	8.1200	8.0400	6.1200	5.7000
5.0	8.0900	7.9900	6.0500	5.5850
2.5	8.0600	7.9300	5.9450	5.4450
1.25	8.0200	7.8700	5.8200	5.3200
0.63	7.9600	7.8200	5.6700	5.2200
0.31	7.9000	7.7800	ND	5.1150
0.16	7.8400	7.7400	ND	5.0300
0.08	7.7900	7.7100	ND	4.9700

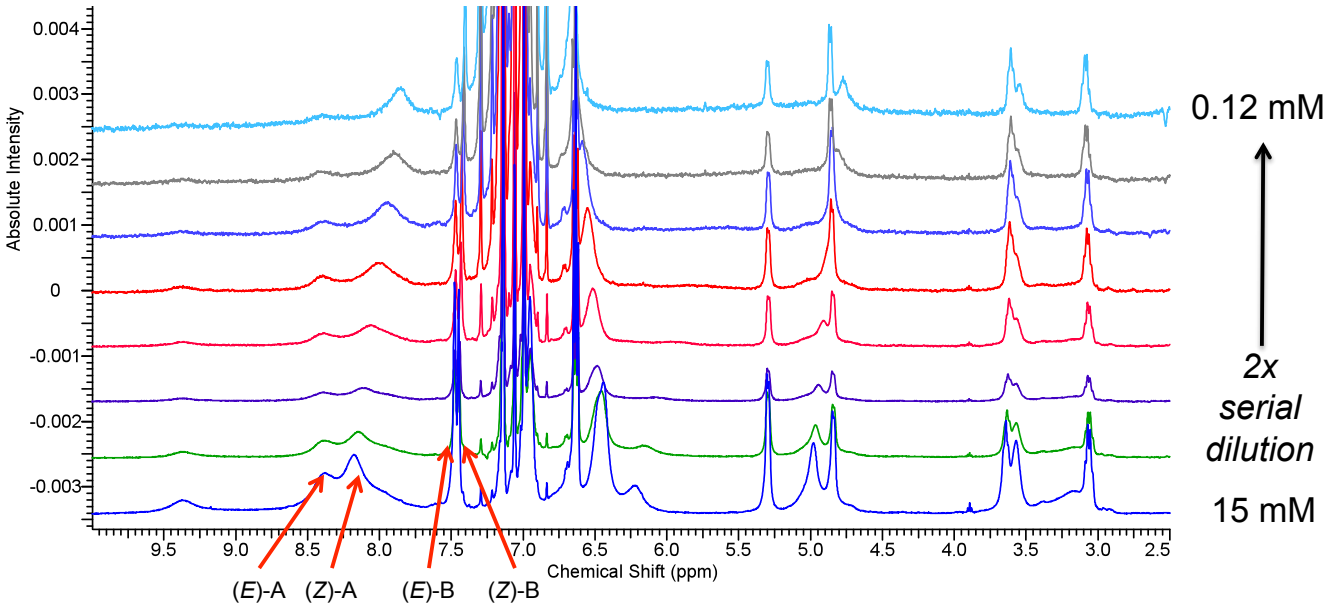

Figure S41. The effect of dilution on the ^{1}H NMR spectrum (500 MHz) of catalyst **1b** in toluene-d_8 at –40 ºC.

Table S17. Data extracted from Figure S41.

	Chemical Shift (ppm)			
$[\mathbf{1b}]_T$ (mM)	*(E)*-H^a	*(Z)*-H^a	*(E)*-H^b	*(Z)*-H^b
15	8.3840	8.1790	7.4780	7.4480
7.5	8.3890	8.1460	7.4760	7.4450
3.75	8.3910	8.1100	7.4740	7.4400
1.88	8.3860	8.0540	7.4700	7.4320
0.94	8.3970	7.9960	7.4700	7.4270
0.47	8.3850	7.9450	7.4660	7.4170
0.23	8.3970	7.9030	7.4660	7.4120
0.12	8.3980	7.8510	7.4610	7.4040

6. Nonlinear Effect Experiment

An oven-dried 1-dram vial fitted with a magnetic stirbar and a cap with a PTFE-lined septum was cooled to –78 ºC under N_2 atmosphere in a dry ice/acetone bath. The vial was charged with catalysts **1a** and *ent*-**1a** as stock solutions in TBME according to Table S18 (750 μL, 0.01 mmol; stock solution prepared by dissolving 36.6 mg **1a** or *ent*-**1a** to 5.00 mL total volume in TBME). After 5 minutes, the vial was charged with **3b** as a stock solution in TBME (125 μL, 0.15 mmol; solution prepared by diluting 452 mg **3b** to 2.00 mL total volume in TBME). After 5 minutes, the vial was charged with **2** as a stock solution in TBME (125 μL, 0.1 mmol; solution prepared by diluting 270 mg **2** to 2.00 mL total volume in TBME). This mixture was maintained for 2 h at –78 ºC before the addition of sodium methoxide (0.5 M in MeOH; 0.2 mL, 0.1 mmol). This mixture was stirred for 5 min before warming to room temperature. The product was purified by silica gel chromatography as described in Section 3.1. The data describing the dependence of the ee of product **4b** on the ee of catalyst **1a** is described in Table S18 and represented graphically in Figure S42. The deviation of the experimental data points from the hypothetical linear relationship (dotted line) is described as a nonlinear effect, which is indicative of catalyst–catalyst interaction on and/or off the productive catalytic cycle.[16]

Scheme S14. Nonlinear effect experiments.

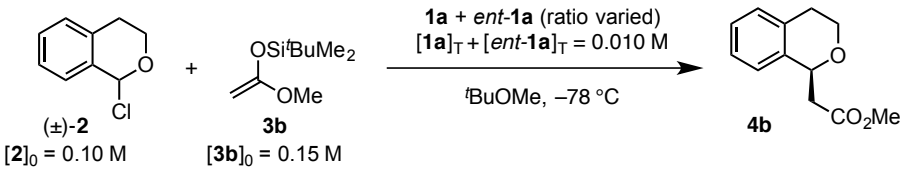

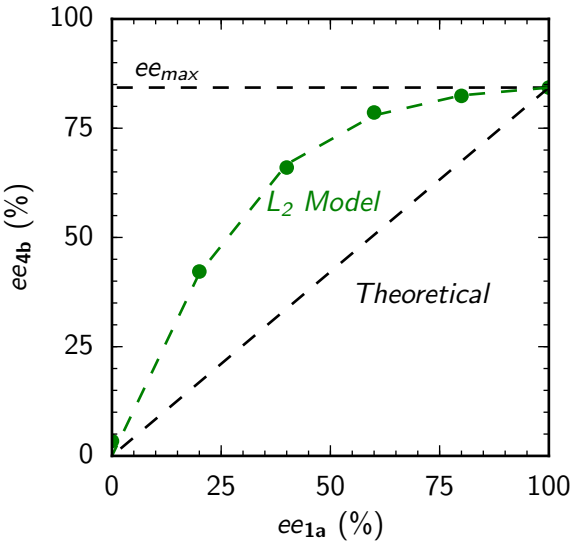

Figure S42. Illustration of the nonlinear relationship between the *ee* of product **4b** and the *ee* of catalyst **1a**. The dashed black line represents the linear relationship that would be expected if catalyst molecules did not interact under the reaction conditions. The dashed green line represents a fit to the L_2 model described below.

(16) (a) Puchot, C.; Samuel, O.; Duñach, E.; Zhao, S.; Agami, C.; Kagan, H. B. *J. Am. Chem. Soc.* **1986**, *108*, 2353–2357; (b) Guillaneux, D.; Zhao, S.; Samuel, O.; Rainford, D.; Kagan, H. B. *J. Am. Chem. Soc.* **1994**, *116*, 9430–9439; (c) Satyanarayana, T.; Abraham, S.; Kagan, H. B. *Angew. Chem. Int. Ed.* **2009**, *48*, 456–494.

Table S18. Data used to generate Figure S42.

entry	*ee* **1a** (%)[a]	**1a** stock solution (μL)	*ent*-**1a** stock solution (μL)	*ee* **4b** (%)[b]
1	100	750	0	84.3
2	80	675	75	82.4
3	60	600	150	78.6
4	40	525	225	66.0
5	20	450	300	42.2
6	0	375	375	3.4

[a] The preparations of **1a** and *ent*-**1a** are assumed to be enantiomerically pure. [b] Determined by HPLC analysis.

As described in Section 3.5, under the conditions utilized for this experiment the catalyst resting state is almost exclusively the nonproductive dimeric aggregate, where the catalyst self-dimerization constant (K_{dim} = 94 M^{-1}) describes the dimerization equilibrium for two molecules of the same enantiomer of catalyst **1a**. However, in the presence of scalemic mixtures of catalyst **1a**, catalyst dimerization results in the formation of both homodimeric (as described above) and heterodimeric/meso complexes (i.e. one molecule of $\mathbf{1a}_S$ dimerizes with one molecule of $\mathbf{1a}_R$ to form $\mathbf{1a}_S$ •$\mathbf{1a}_R$, where $\mathbf{1a}_S$ is the enantiomer of catalyst that forms (*S*)-**4** as the major product, and $\mathbf{1a}_R$ is the enantiomer of catalyst that forms (*R*)-**4** as the major product). While the heterodimeric complex has been observed in the solid state (see Section 4), the solution-state dimerization constant, K_{SR}, for formation of the heterodimeric complex is not know.

Scheme S15. Formation of homochiral and heterochiral dimeric catalyst complexes.

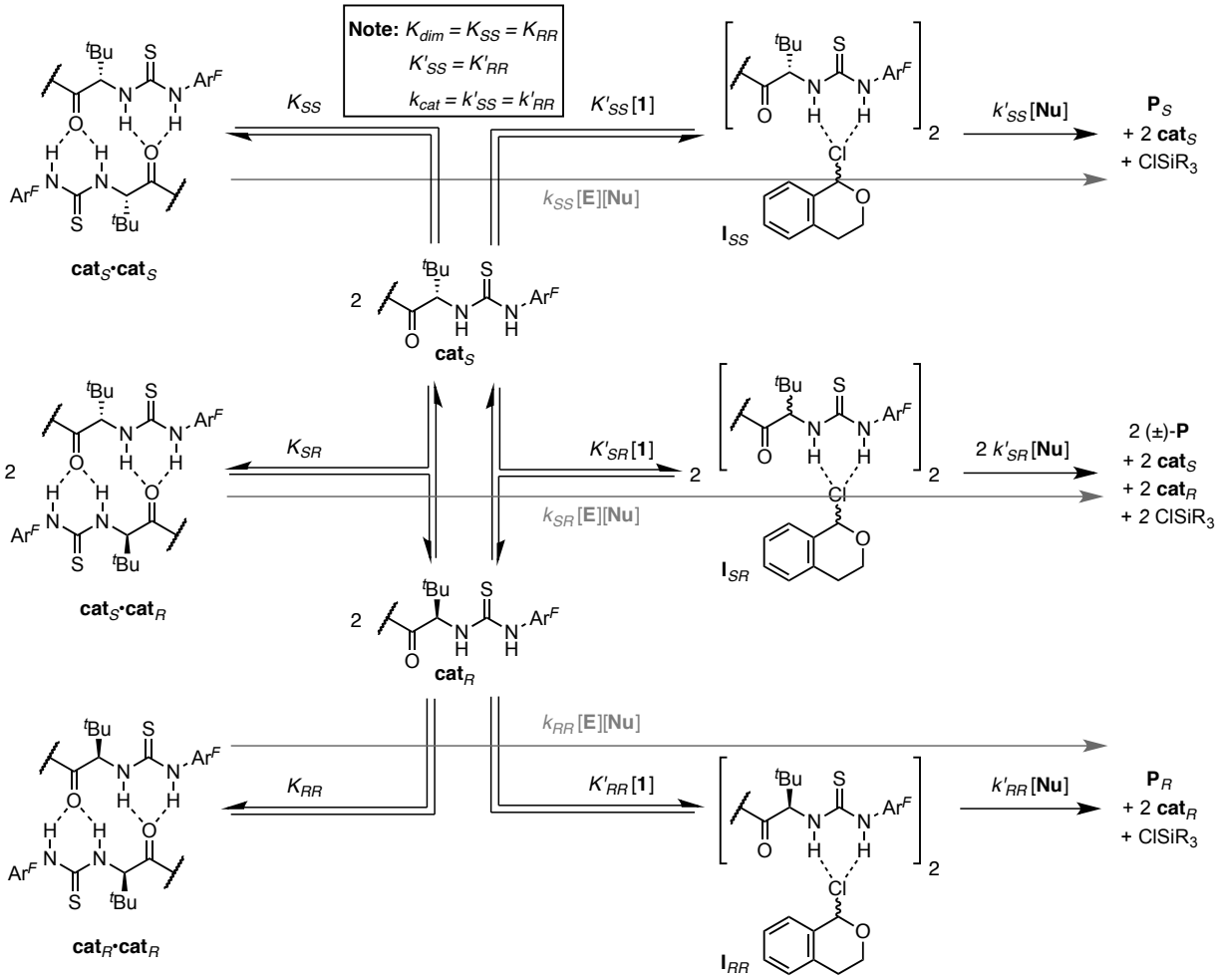

Given the proposed mechanism, in which these non-productive aggregates form off-cycle but the cooperative association of two molecules of catalyst is required for productive reaction, the net nonlinear effect observed experimentally should reflect both a reservoir effect and the impact of matched and mismatched catalyst combinations in the productive reaction pathway. These two contributions cannot be deconvoluted without additional data about the relative stabilities of the homochiral and heterochiral dimeric aggregates. Regardless, the experimental data can be fit to an L_2 model, identical in form to Kagan's ML_2 model. In this model:

$$K = \frac{[cat_S \bullet cat_R]^2}{[cat_S \bullet cat_S][cat_R \bullet cat_R]} \tag{S25}$$

$$\beta = \frac{[cat_S \bullet cat_R]}{[cat_S \bullet cat_S]+[cat_R \bullet cat_R]} \tag{S26}$$

and the relative activity of the heterodimeric and homodimeric catalyst–substrate complexes is described by:

$$g = \frac{k_{SR}}{k_{SS}} \tag{S27}$$

or

$$K' = \frac{[\mathbf{I}_{SR}]^2}{[\mathbf{I}_{SS}][\mathbf{I}_{RR}]} \tag{S28}$$

$$\beta' = \frac{[\mathbf{I}_{SR}]}{[\mathbf{I}_{SS}]+[\mathbf{I}_{RR}]} \tag{S29}$$

$$g' = \frac{k'_{SR}}{k'_{SS}} \tag{S30}$$

In order for a positive nonlinear effect, as described here, to be observed $g < 1$

With these definitions, the enantiomeric excess of product (ee_P) formed can be described as a function of the enantiomeric excess of the catalyst (ee_{cat}), where ee_{max} is the intrinsic enantioselectivity observed with enantiopure catalyst. Note that in all cases, *ee* is defined in fractional form where 1.0 indicates enantiopure material.

$$ee_P = ee_{max} ee_{cat} \frac{1+\beta}{1+g\beta} \tag{S31}$$

The experimentally determined values for ee_P and ee_{cat} were fit to equations S25–S31 using a Levenberg–Marquardt algorithm, and the fit curve is shown in Figure S42.

$$g = 0.06 \pm 0.06$$
$$K = 17 \pm 9\ M^{-1}$$

According to either interpretation, this result indicates that there is a modest energetic preference for formation the heterochiral catalyst complexes over the homochiral complexes (e.g. K = 4 M^{-1} indicates a statistical mixture of homochiral and heterochiral complexes), but the homochiral combinations are much more reactive than the heterochiral combinations. The specific contributions of each of the steps shown in Scheme S15 cannot be deconvoluted.

8. Computational Investigations on Catalyst Structure

Methods:

Calculations were performed using the Gaussian 09 program[6] on the Odyssey cluster supported by Harvard University's Faculty of Arts and Sciences Research Computing group. Default geometric and SCF convergence criteria were used. In cases where SCF convergence was difficult to achieve, a quadratic convergence algorithm was employed using the keyword `SCF=(XQC,maxconventionalcycles=25)` where QC only begins after 25 cycles of the default algorithm have failed to converge on an SCF. Minima were characterized by the presence of all positive eigenvalues of the Hessian. The B3LYP[17] functional were used as its default implementation in Gaussian 09. All molecular structures were rendered in CYLview.[7]

(17) (a) Becke, A. D. *Phys. Rev. A* **1988**, *38*, 3098–3100. (b) Lee, C.; Yang, W.; Parr, R. G. *Phys. Rev. B*. **1988**, *37*, 785–789. (c) Becke, A. D. *J. Chem. Phys*. **1993**, *98*, 1372–1377. (d) Stephens, P. J.; Devlin, F. J.; Chabalowski, C. F.; Frisch, M. J. *J. Phys. Chem*. **1994**, *98*, 11623–11627.

Monomeric Catalysts (gas phase)

(Z)-**1a**

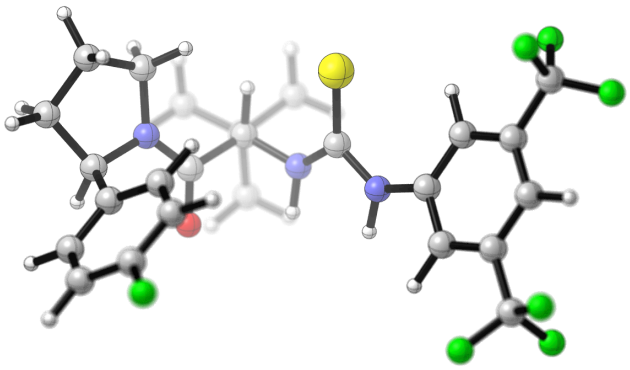

Charge: 0
Spin Multiplicity: 1
Number of Imaginary Frequencies: 0
Solvation: gas phase
Electronic Energy (AU): -2304.96413243
Gibbs Free Energy at 298.150 K (AU): -2304.551718

S	0.053824	-1.972797	-1.333915
F	-1.748105	5.658045	-0.699932
F	5.808747	2.709880	0.954869
F	3.988994	2.927447	2.136890
F	5.543204	1.549119	2.772421
O	-3.179783	-0.115320	1.778570
N	-3.946087	-0.382425	-0.338809
N	-1.055020	-1.706658	1.105211
H	-1.106298	-1.143469	1.949747
N	1.067310	-0.918839	0.954778
H	0.856661	-0.608447	1.895071
C	-4.404373	3.334231	0.123272
H	-5.380970	3.340594	0.601053
C	-3.696848	4.529385	0.011919
H	-4.094799	5.465520	0.388050
C	-2.443701	4.505974	-0.589780
C	-1.885549	3.329695	-1.072030
H	-0.901052	3.349016	-1.526656
C	-2.611203	2.143222	-0.952867
H	-2.169184	1.218741	-1.310994
C	-3.878716	2.128479	-0.360113
C	-4.730804	0.866494	-0.268622
H	-5.265472	0.887057	0.685236
C	-5.702376	0.706147	-1.461979
H	-6.063587	1.668559	-1.830499
H	-6.569464	0.112510	-1.149738
C	-4.871317	-0.069459	-2.494465
H	-4.179651	0.607312	-3.005796
H	-5.479586	-0.564647	-3.255365
C	-4.090166	-1.076164	-1.636815
H	-3.113846	-1.324518	-2.062751
H	-4.659318	-2.004632	-1.512118
C	-3.226249	-0.783025	0.740159
C	-2.393401	-2.077745	0.643669
H	-2.282831	-2.403262	-0.390016
C	0.020818	-1.516318	0.285757
C	2.356937	-0.541481	0.528541
C	3.077902	-1.207092	-0.471633
H	2.635163	-2.041579	-0.994488
C	4.367078	-0.778104	-0.786578
C	4.967237	0.285962	-0.114642
H	5.971187	0.603354	-0.366630
C	4.250643	0.930366	0.892273
C	2.955435	0.528327	1.208609
H	2.404553	1.059232	1.978895
C	-2.978265	-3.272955	1.474304
C	-2.114488	-4.516867	1.189774
H	-1.072085	-4.349401	1.474653
H	-2.487210	-5.374361	1.760131
H	-2.132799	-4.783261	0.127733
C	-2.975153	-2.983514	2.988097
H	-3.544845	-2.084297	3.231744
H	-3.412907	-3.831484	3.525409
H	-1.955735	-2.854226	3.367070
C	-4.422856	-3.547410	1.014065
H	-4.465508	-3.789031	-0.053576
H	-4.831447	-4.404770	1.558401
H	-5.083023	-2.694409	1.203008
C	5.111748	-1.453535	-1.911218
F	4.875266	-0.845613	-3.094942
F	6.448208	-1.420087	-1.711236
F	4.751830	-2.746425	-2.049034
C	4.898404	2.034617	1.686459

(E)-**1a**

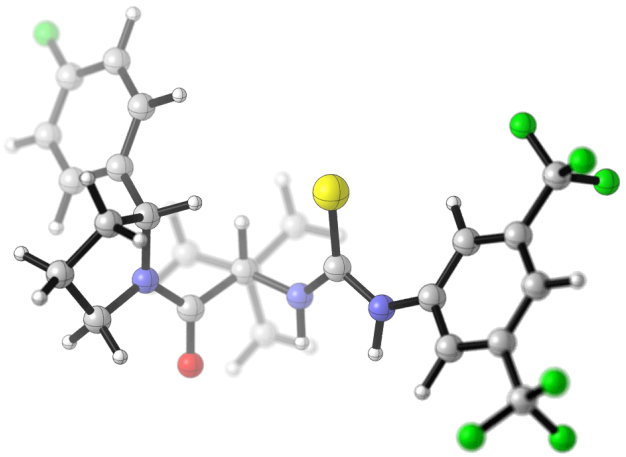

Charge: 0
Spin Multiplicity: 1
Number of Imaginary Frequencies: 0
Solvation: gas phase
Electronic Energy (AU): -2304.96329425
Gibbs Free Energy at 298.150 K (AU): -2304.550712

S	-0.093848	1.276040	-0.085486
F	7.621207	2.935018	-0.563307
F	-7.085070	-1.489950	-1.564513
F	-5.568221	-3.019609	-1.226307
F	-6.815605	-2.340930	0.416884
O	2.277053	-3.058624	0.934492
N	3.157114	-1.729960	-0.671619
N	0.527689	-0.893193	1.380226
H	0.279194	-1.819567	1.710372
N	-1.676989	-0.706699	0.873065
H	-1.705168	-1.645797	1.249747
C	4.278420	1.792460	-1.374245
H	3.322132	2.204574	-1.685327
C	5.357491	2.652144	-1.173579
H	5.268238	3.722795	-1.321200
C	6.570667	2.112098	-0.763436
C	6.729301	0.749375	-0.542441
H	7.688872	0.368331	-0.210367
C	5.637710	-0.094901	-0.747838
H	5.746693	-1.156499	-0.551410
C	4.401898	0.410436	-1.172268
C	3.208175	-0.485078	-1.476770
H	2.293364	0.092515	-1.319235
C	3.226868	-1.041643	-2.924131
H	3.672917	-0.334817	-3.627135
H	2.196871	-1.235832	-3.243796
C	4.001383	-2.360488	-2.801416
H	5.078524	-2.167002	-2.774224
H	3.809476	-3.046753	-3.630064
C	3.519177	-2.927615	-1.460861
H	4.274514	-3.518570	-0.935001
H	2.634188	-3.564617	-1.570987
C	2.500366	-1.921879	0.505296
C	1.977286	-0.702807	1.292599
H	2.134660	0.226548	0.748356
C	-0.419450	-0.150637	0.747906
C	-2.931726	-0.253057	0.415245
C	-3.295022	1.099660	0.373262
H	-2.583375	1.861617	0.654680
C	-4.573254	1.452505	-0.055415
C	-5.509944	0.486739	-0.425560
H	-6.495735	0.775874	-0.767661
C	-5.148304	-0.856745	-0.359967
C	-3.868522	-1.227361	0.049734
H	-3.594849	-2.277782	0.064417
C	2.622686	-0.538922	2.714720
C	2.169629	0.820473	3.282612
H	1.079675	0.879034	3.357070
H	2.582925	0.965458	4.286470
H	2.508012	1.651036	2.654708
C	2.199922	-1.659619	3.685527
H	2.452018	-2.647203	3.294835
H	2.708284	-1.521296	4.645564
H	1.123391	-1.630260	3.887679
C	4.156344	-0.542926	2.575617
H	4.503140	0.228008	1.881369
H	4.616275	-0.345737	3.549476
H	4.527966	-1.511510	2.225968
C	-4.980518	2.905000	-0.048298
F	-5.855682	3.179310	-1.040701
F	-5.588246	3.237488	1.114412
F	-3.923679	3.728176	-0.193642
C	-6.156265	-1.926672	-0.689560

DFT-Optimized (B3LYP/6-31G(d,p) Geometries from XRD Data for [(*Z*)-1a]$_2$:

[(*Z*)-**1a**]$_2$:

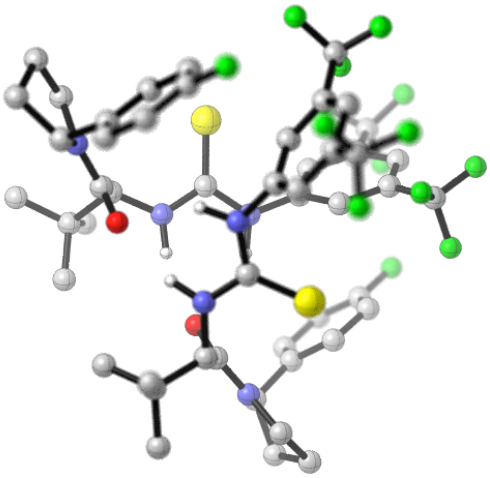

Charge: 0
Spin Multiplicity: 1
Number of Imaginary Frequencies: 0
Solvation: gas phase
Electronic Energy (AU): -4609.96093843
Gibbs Free Energy at 298.150 K (AU): -4609.100790

S	0.223687	-0.116476	-3.221624
F	6.226227	-1.844134	0.772650
F	-2.325277	-5.332026	0.887271
F	-0.925173	-3.878322	1.707253
F	-3.054885	-3.671188	2.088306
O	1.891551	2.939948	-0.603310
N	3.069478	2.745854	-2.520321
N	-0.415920	2.154480	-1.910009
H	-0.800768	2.582195	-1.067986
N	-1.492106	0.283900	-1.183419
H	-1.881134	0.901507	-0.474015
C	5.637678	1.650549	0.017405
H	5.925580	2.630300	0.390549
C	6.132598	0.511407	0.649772
H	6.790510	0.576209	1.509486
C	5.758815	-0.736366	0.162219
C	4.904683	-0.871612	-0.924436
H	4.615847	-1.857256	-1.268683
C	4.409695	0.280986	-1.536943
H	3.710461	0.174347	-2.360371
C	4.777156	1.555093	-1.085243
C	4.361670	2.832887	-1.803925
H	4.287335	3.635296	-1.065562
C	5.329114	3.197419	-2.953964
H	6.365152	2.950029	-2.713567
H	5.270315	4.274135	-3.151686
C	4.773980	2.403725	-4.145541
H	5.093371	1.359529	-4.085443
H	5.101458	2.796114	-5.111351
C	3.248830	2.512493	-3.974022
H	2.715278	1.608114	-4.281658
H	2.858847	3.356573	-4.545285
C	1.902816	2.871840	-1.848038
C	0.578872	2.915082	-2.648655
H	0.722115	2.384904	-3.591368
C	-0.593428	0.816739	-2.064329
C	-1.967135	-1.058364	-1.205501
C	-2.673552	-1.538681	-2.313237
H	-2.818340	-0.901586	-3.176194
C	-3.181213	-2.834294	-2.300065
C	-2.991004	-3.662258	-1.191047
H	-3.379712	-4.672883	-1.189238
C	-2.291254	-3.174041	-0.092247
C	-1.777391	-1.872818	-0.090683
H	-1.235021	-1.499071	0.772632
C	0.036952	4.353841	-2.991314
C	-1.270209	4.186420	-3.793743
H	-2.047029	3.697239	-3.201514
H	-1.645780	5.168213	-4.101467
H	-1.110017	3.588360	-4.697295
C	-0.241292	5.187349	-1.729732
H	0.669866	5.354094	-1.150707
H	-0.641585	6.165487	-2.018362
H	-0.977515	4.714037	-1.075094
C	1.046829	5.119203	-3.867566
H	1.195107	4.629501	-4.835295
H	0.665540	6.125077	-4.070459
H	2.018959	5.232182	-3.376987
C	-4.019193	-3.324371	-3.451500
F	-3.870005	-4.652926	-3.647749
F	-5.336113	-3.105925	-3.227951
F	-3.706424	-2.701782	-4.607468
C	-2.139566	-4.020080	1.142969
S	-0.223700	-0.117047	3.221421
F	-6.226651	-1.843605	-0.772123
F	0.924687	-3.878338	-1.708023
F	3.054408	-3.671447	-2.089015
F	2.324552	-5.332392	-0.888295
O	-1.891014	2.939702	0.603647
N	-3.068911	2.745825	2.520707
N	0.416416	2.154014	1.910229
H	0.801359	2.581801	1.068286
N	1.492205	0.283332	1.183329
H	1.881458	0.900986	0.474097
C	-5.637395	1.650966	-0.016921
H	-5.925086	2.630770	-0.390089
C	-6.132544	0.511914	-0.649272
H	-6.790431	0.576836	-1.508995
C	-5.759017	-0.735926	-0.161698
C	-4.904906	-0.871332	0.924954
H	-4.616235	-1.857030	1.269190
C	-4.409679	0.281177	1.537438
H	-3.710436	0.174408	2.360843
C	-4.776886	1.555354	1.085723
C	-4.361128	2.833072	1.804376
H	-4.286693	3.635466	1.066007
C	-5.328449	3.197796	2.954461
H	-6.364540	2.950567	2.714125
H	-5.269465	4.274508	3.152143
C	-4.773381	2.404055	4.146041
H	-5.100725	2.796557	5.111850
H	-5.092974	1.359916	4.086024
C	-3.248222	2.512544	3.974427
H	-2.714802	1.608085	4.282052
H	-2.858054	3.356578	4.545631
C	-1.902258	2.871614	1.848380

C	-0.578287	2.914668	2.648950
H	-0.721568	2.384451	3.591637
C	0.593638	0.816210	2.064322
C	1.967009	-1.059019	1.205224
C	2.673208	-1.539668	2.312958
H	2.817991	-0.902767	3.176058
C	3.180609	-2.835379	2.299612
C	2.990364	-3.663110	1.190420
H	3.378849	-4.673786	1.188483
C	2.290837	-3.174564	0.091631
C	1.777234	-1.873231	0.090241
H	1.235027	-1.499213	-0.773061
C	-0.036225	4.353355	2.991682
C	1.271114	4.185773	3.793793
H	2.047769	3.696616	3.201328
H	1.646810	5.167511	4.101540
H	1.111102	3.587621	4.697316
C	-1.045878	5.118619	3.868278
H	-1.193846	4.628854	4.836023
H	-0.664574	6.124498	4.071114
H	-2.018157	5.231576	3.377990
C	0.241742	5.187026	1.730146
H	-0.669570	5.353946	1.151415
H	0.642205	6.165084	2.018813
H	0.977726	4.713745	1.075214
C	4.018335	-3.325890	3.451050
F	3.868401	-4.654355	3.647353
F	5.335373	-3.108211	3.227466
F	3.705963	-2.703094	4.607011
C	2.139052	-4.020368	-1.143741

(*Z*)-**1a** • (*E*)-**1a**:

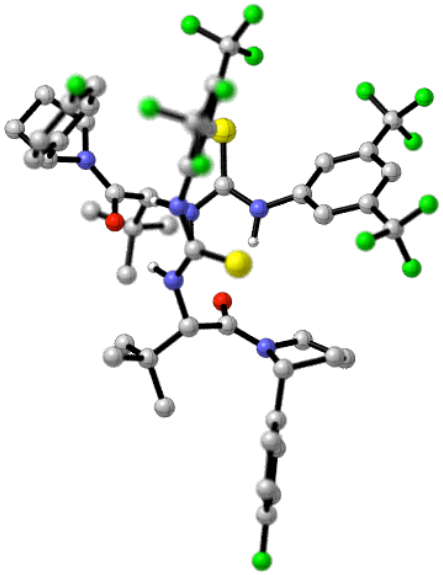

Charge: 0
Spin Multiplicity: 1
Number of Imaginary Frequencies: 0
Solvation: gas phase
Electronic Energy (AU): -4609.96147851
Gibbs Free Energy at 298.150 K (AU): -4609.104329

S	-2.260738	1.435177	-2.768165
F	-5.251539	-2.346836	3.674519
F	2.170758	5.589231	1.874592
F	2.349650	3.432956	2.142059
F	3.720878	4.482970	0.824907
O	-1.159130	-2.779512	-1.542161
N	-3.215247	-2.739126	-2.480324
N	-0.424795	-0.526218	-2.952529
H	0.454750	-0.917845	-2.621581
N	0.330760	1.357463	-1.954550
H	1.148273	0.767216	-1.794958
C	-3.889575	-4.234926	0.898837
H	-3.438944	-5.205905	0.709754
C	-4.286002	-3.912201	2.195353
H	-4.149997	-4.601296	3.021617
C	-4.864606	-2.668615	2.424464
C	-5.041598	-1.745401	1.402377
H	-5.475880	-0.776184	1.613407
C	-4.627342	-2.082374	0.113408
H	-4.738120	-1.343440	-0.673632
C	-4.059534	-3.333726	-0.161632
C	-3.722548	-3.795616	-1.572997
H	-2.954947	-4.570296	-1.501570
C	-4.967049	-4.293334	-2.345265
H	-5.682267	-4.795701	-1.690811
H	-4.654196	-5.003875	-3.119219
C	-5.524850	-3.015330	-2.988462
H	-6.107784	-2.447362	-2.258407
H	-6.173250	-3.216219	-3.844700
C	-4.263759	-2.236256	-3.401452
H	-4.373036	-1.152439	-3.298383
H	-4.001248	-2.458387	-4.436930
C	-1.913083	-2.375387	-2.448881
C	-1.368353	-1.448519	-3.559383
H	-2.183209	-0.834348	-3.945480
C	-0.733074	0.738310	-2.557956
C	0.462042	2.688136	-1.506247
C	-0.079570	3.783464	-2.192322
H	-0.690591	3.625194	-3.069465
C	0.160695	5.074401	-1.725604
C	0.954728	5.302629	-0.600948
H	1.133814	6.310428	-0.247844
C	1.498471	4.208957	0.068788
C	1.241889	2.907322	-0.363605
H	1.616554	2.061976	0.205542
C	-0.699711	-2.190109	-4.782178
C	-0.265221	-1.115190	-5.800126
H	0.488790	-0.445072	-5.380401
H	0.163298	-1.593414	-6.687248
H	-1.115070	-0.504689	-6.123567
C	0.527627	-3.013088	-4.355086
H	0.258981	-3.804315	-3.651320
H	0.977821	-3.482581	-5.236243
H	1.299220	-2.393024	-3.890684
C	-1.703731	-3.132064	-5.472738
H	-2.538695	-2.578941	-5.914241
H	-1.203360	-3.662918	-6.288877
H	-2.104188	-3.888273	-4.790041
C	-0.375804	6.251034	-2.500481
F	-0.625110	7.306882	-1.695083
F	0.512228	6.671100	-3.433681
F	-1.517815	5.951522	-3.150267
C	2.423081	4.430242	1.235211
S	1.371109	-0.225430	2.391574
F	9.556100	-3.206939	1.617296
F	-3.915213	2.951397	0.154438
F	-5.513691	1.590583	0.717059
F	-5.001748	3.259401	2.017154
O	2.387039	-0.844541	-1.743501
N	4.117044	-0.328551	-0.391660
N	1.087329	-2.018746	0.395903
H	0.515833	-2.360021	-0.375014
N	-0.839335	-1.003668	1.057534
H	-1.252499	-1.526393	0.287670
C	6.432030	-1.514625	2.333851
H	5.790184	-1.301626	3.184879
C	7.608516	-2.235896	2.534023
H	7.898372	-2.592184	3.516421
C	8.418126	-2.504957	1.437060
C	8.083335	-2.077961	0.157814
H	8.737438	-2.314486	-0.674309
C	6.903141	-1.356482	-0.021489
H	6.627752	-1.040474	-1.022444
C	6.061455	-1.063385	1.059321
C	4.803216	-0.218454	0.924501
H	4.095420	-0.481660	1.713134
C	5.110373	1.296541	0.998155
H	5.933830	1.510154	1.683058
H	4.223800	1.823840	1.359668
C	5.414953	1.683174	-0.455257
H	5.263772	2.749239	-0.637661
H	6.451155	1.441067	-0.710319
C	4.435972	0.825811	-1.269731
H	4.839552	0.479400	-2.225747
H	3.512243	1.368738	-1.489597
C	3.028792	-1.076741	-0.695862

C	2.530002	-2.182695	0.265917
H	2.947803	-2.013650	1.257453
C	0.510627	-1.121895	1.239404
C	-1.723693	-0.206463	1.832218
C	-1.816019	-0.376875	3.217653
H	-1.167608	-1.084268	3.717408
C	-2.739038	0.369720	3.945301
C	-3.585225	1.277949	3.306021
H	-4.302165	1.854221	3.877309
C	-3.492510	1.433969	1.925666
C	-2.557702	0.705336	1.184081
H	-2.480909	0.851294	0.110351
C	2.887482	-3.658086	-0.135998
C	2.347450	-4.588409	0.970451
H	1.259170	-4.529732	1.053066
H	2.615908	-5.626187	0.746476
H	2.773398	-4.335280	1.947281
C	4.414674	-3.821782	-0.213343
H	4.899638	-3.577707	0.735451
H	4.659135	-4.861196	-0.455499
H	4.857331	-3.190689	-0.989272
C	2.280900	-4.069352	-1.488101
H	2.653311	-3.442009	-2.300706
H	2.556135	-5.106605	-1.708131
H	1.188821	-4.017004	-1.489515
C	-2.892668	0.123436	5.423571
F	-3.340683	1.222362	6.070031
F	-3.782133	-0.867112	5.666640
F	-1.727774	-0.243504	5.997601
C	-4.470344	2.321962	1.204805

[(*E*)-**1a**]$_2$:

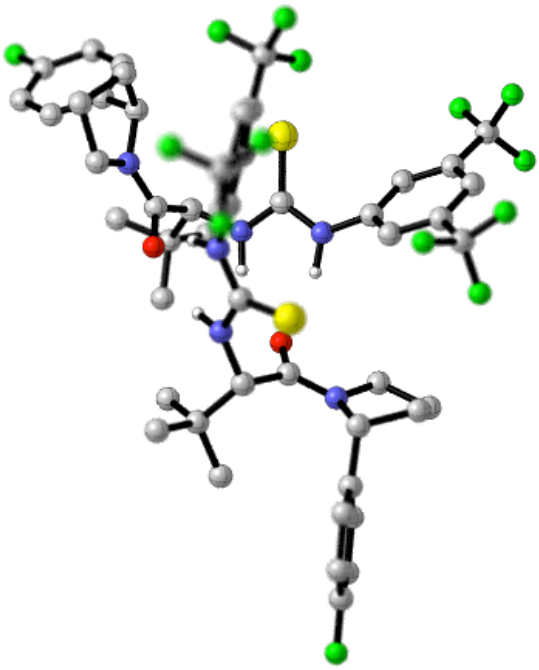

Charge: 0
Spin Multiplicity: 1
Number of Imaginary Frequencies: 0
Solvation: gas phase
Electronic Energy (AU): -4609.96180125
Gibbs Free Energy at 298.150 K (AU): -4609.106837

S	-2.575706	0.737241	-2.058246
F	-9.324499	-4.347738	-1.185374
F	3.185356	5.244257	-1.614162
F	2.827532	3.832880	0.006670
F	4.266863	3.359064	-1.550055
O	-1.698721	-2.250054	1.133360
N	-3.856664	-1.614712	0.964300
N	-1.342015	-1.606918	-1.542363
H	-0.476858	-2.079311	-1.290802
N	0.052159	0.105392	-2.065308
H	0.775384	-0.570927	-1.813497
C	-6.869897	-1.681116	-1.278496
H	-6.595593	-0.839014	-1.908960
C	-7.949811	-2.483453	-1.647817
H	-8.521341	-2.289826	-2.549148
C	-8.286811	-3.559976	-0.836096
C	-7.576914	-3.854430	0.322448
H	-7.864356	-4.709859	0.924318
C	-6.502002	-3.039595	0.675344
H	-5.929859	-3.283988	1.564564
C	-6.132250	-1.942869	-0.115284
C	-5.015927	-0.983923	0.270076
H	-4.652166	-0.473202	-0.624935
C	-5.479787	0.064184	1.312745
H	-6.528449	0.334869	1.172143
H	-4.878511	0.971484	1.208591
C	-5.198818	-0.608968	2.662516
H	-5.991514	-1.320769	2.912383
H	-5.126293	0.106758	3.484955
C	-3.868915	-1.331557	2.421017
H	-3.751821	-2.258010	2.989963
H	-3.017988	-0.688671	2.669805
C	-2.697978	-2.047424	0.410701
C	-2.579081	-2.252146	-1.117420
H	-3.388995	-1.725792	-1.621209
C	-1.244135	-0.294566	-1.886365
C	0.498584	1.387368	-2.471692
C	0.024387	1.982517	-3.648741
H	-0.731707	1.483068	-4.239022
C	0.522097	3.220179	-4.042829
C	1.501550	3.873398	-3.288576
H	1.878057	4.841137	-3.596394
C	1.974494	3.271736	-2.127605
C	1.472725	2.034155	-1.708471
H	1.814431	1.595712	-0.774845
C	-2.614889	-3.745859	-1.610476
C	-2.599106	-3.724967	-3.153113
H	-1.693198	-3.250982	-3.539849
H	-2.639244	-4.748514	-3.540075
H	-3.461897	-3.181166	-3.552675
C	-1.415655	-4.562162	-1.098933
H	-1.390434	-4.596997	-0.007969
H	-1.490833	-5.589663	-1.470698
H	-0.459501	-4.164395	-1.451439
C	-3.909697	-4.428483	-1.139202
H	-4.799577	-3.911503	-1.505644
H	-3.939997	-5.454910	-1.519524
H	-3.973237	-4.481073	-0.048016
C	0.060964	3.850799	-5.331345
F	-0.138934	5.179355	-5.187748
F	0.987394	3.700525	-6.308840
F	-1.086728	3.309193	-5.784833
C	3.055608	3.935109	-1.315286
S	2.565281	0.710976	2.071993
F	9.352262	-4.359014	1.088564
F	-2.813555	3.822647	0.024728
F	-4.269828	3.320159	1.556504
F	-3.193602	5.206252	1.664477
O	1.713583	-2.197377	-1.156887
N	3.872130	-1.570370	-0.963603
N	1.346285	-1.635819	1.533623
H	0.483945	-2.109350	1.274524
N	-0.058215	0.063530	2.072532
H	-0.777214	-0.614953	1.815156
C	6.893636	-1.701227	1.268595
H	6.622257	-0.876301	1.922433
C	7.977092	-2.510904	1.609571
H	8.554404	-2.340241	2.511726
C	8.310540	-3.564678	0.767294
C	7.593444	-3.829511	-0.393762
H	7.878630	-4.667916	-1.019989
C	6.514886	-3.007448	-0.718178
H	5.937436	-3.227954	-1.610047
C	6.148887	-1.932943	0.103617
C	5.030473	-0.963364	-0.248056
H	4.666283	-0.483690	0.663797
C	5.493744	0.120762	-1.253408
H	6.541584	0.388753	-1.102390
H	4.890066	1.022669	-1.119850
C	5.215826	-0.506977	-2.625510
H	5.142948	0.236482	-3.423114
H	6.010199	-1.208390	-2.898109
C	3.887118	-1.240006	-2.410453

H	3.773439	-2.147673	-3.009694
H	3.035052	-0.591554	-2.639352
C	2.711226	-2.016878	-0.426006
C	2.586496	-2.265839	1.095414
H	3.393881	-1.753570	1.617672
C	1.240325	-0.327310	1.889579
C	-0.510223	1.340128	2.490786
C	-0.046034	1.920631	3.679026
H	0.705575	1.413558	4.268724
C	-0.547761	3.152634	4.085586
C	-1.521301	3.815083	3.331684
H	-1.901209	4.778252	3.649263
C	-1.983976	3.228280	2.158872
C	-1.478423	1.996389	1.728029
H	-1.813396	1.569675	0.786583
C	2.623264	-3.772638	1.545660
C	2.592774	-3.796849	3.088068
H	1.681208	-3.337990	3.479725
H	2.633579	-4.831205	3.445029
H	3.449359	-3.261496	3.511642
C	3.925733	-4.435767	1.067820
H	4.809887	-3.923060	1.453907
H	3.958820	-5.471094	1.422545
H	3.998173	-4.460505	-0.023764
C	1.432697	-4.579025	0.999616
H	1.418248	-4.583660	-0.092096
H	1.508461	-5.616182	1.343322
H	0.471324	-4.195336	1.353230
C	-0.099914	3.764594	5.387763
F	0.086800	5.097469	5.270717
F	-1.029578	3.585693	6.357447
F	1.050889	3.226249	5.837110
C	-3.057374	3.902509	1.345340

Alternative Geometry Located by Calculations (B3LYP/6-31G(d,p)) in the Gas Phase: Type II Dimers

[(*Z*)-**1a**]$_2$:

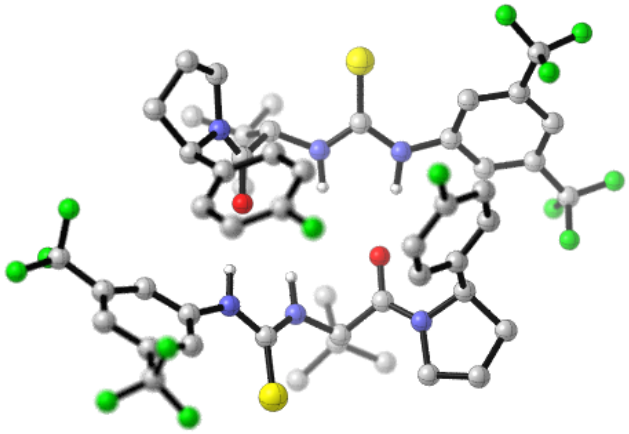

Charge: 0
Spin Multiplicity: 1
Number of Imaginary Frequencies: 0
Solvation: gas phase
Electronic Energy (AU): -4609.97070747
Gibbs Free Energy at 298.150 K (AU): -4609.111634

O	1.601867	1.271634	1.529048
C	1.219006	2.450587	1.393268
C	0.001929	2.943916	2.195699
H	-0.343959	3.903220	1.812749
N	-1.084212	2.008787	1.925848
C	-2.248453	2.334746	1.289361
N	-3.012652	1.226659	1.034310
H	-2.608927	0.322718	1.287180
C	0.289890	3.137235	3.728588
H	-0.850969	1.023474	1.998094
C	1.470906	4.112561	3.901503
H	1.669659	4.271402	4.966079
H	2.393634	3.730933	3.451141
H	1.251139	5.092290	3.463868
C	-0.966097	3.753131	4.375593
H	-1.832594	3.095163	4.268042
H	-0.793785	3.912867	5.445345
H	-1.222324	4.715335	3.922513
C	0.619300	1.811850	4.436234
H	1.503272	1.330133	4.012044
H	0.805683	1.997418	5.499416
H	-0.219362	1.113029	4.372087
S	-2.692297	3.919897	0.912926
N	1.813545	3.310985	0.539147
C	1.450757	4.736729	0.326768
C	2.993007	2.916067	-0.263492
C	2.416486	5.201618	-0.773622
H	0.400805	4.835655	0.038950
C	3.632004	4.282748	-0.596619
H	3.657881	2.319018	0.363270
H	1.968357	5.049072	-1.760189
H	4.270239	4.229492	-1.480491
H	4.247587	4.612325	0.247798
H	2.658764	6.262596	-0.677060
H	1.610118	5.302788	1.249682
C	2.639217	2.106876	-1.506610
C	3.649189	1.354553	-2.122653
C	1.362852	2.113325	-2.079867
C	3.394299	0.596599	-3.263775
H	4.647851	1.351236	-1.696963
C	1.090720	1.378129	-3.234592
H	0.559566	2.676350	-1.615503
C	2.110627	0.621375	-3.795478
H	4.161862	-0.021284	-3.716181
H	0.107806	1.369555	-3.691077
C	-4.294085	1.118192	0.465953
C	-4.764498	1.921115	-0.583566
C	-5.094304	0.068737	0.932961
C	-6.011623	1.655063	-1.144796
H	-4.157753	2.734581	-0.953479
C	-6.329818	-0.197804	0.343275
H	-4.741787	-0.544100	1.755881
C	-6.805539	0.596093	-0.696779
H	-7.768961	0.396392	-1.148828
O	-1.601471	-1.270910	1.528925
C	-1.218898	-2.450031	1.393805
C	-0.001856	-2.943151	2.196414
H	0.344039	-3.902565	1.813740
N	1.084281	-2.008086	1.926326
C	2.248520	-2.334221	1.289926
N	3.012688	-1.226195	1.034522
H	2.608978	-0.322194	1.287208
C	-0.289841	-3.136043	3.729354
H	0.850950	-1.022762	1.998151
C	-1.470581	-4.111656	3.902529
H	-1.669449	-4.270076	4.967147
H	-2.393363	-3.730532	3.451848
H	-1.250429	-5.091511	3.465372
C	0.966280	-3.751372	4.376637
H	1.832566	-3.093137	4.269043
H	0.793893	-3.910927	5.446404
H	1.222876	-4.713590	3.923798
C	-0.619660	-1.810513	4.436541
H	-1.503811	-1.329223	4.012235
H	-0.805933	-1.995765	5.499797
H	0.218764	-1.111436	4.372104
S	2.692380	-3.919481	0.913972
N	-1.813724	-3.310790	0.540250
C	-1.451223	-4.736708	0.328585
C	-2.993163	-2.916055	-0.262519
C	-2.417076	-5.201958	-0.771542
H	-0.401299	-4.835988	0.040786
C	-3.632425	-4.282790	-0.594916
H	-3.657896	-2.318573	0.363982
H	-1.968963	-5.049952	-1.758200
H	-4.270707	-4.229862	-1.478772
H	-4.248010	-4.611840	0.249706
H	-2.659532	-6.262847	-0.674466
H	-1.610676	-5.302268	1.251789
C	-2.639318	-2.107559	-1.506072
C	-3.649188	-1.355319	-2.122380
C	-1.363026	-2.114607	-2.079485
C	-3.394264	-0.598020	-3.263930
H	-4.647798	-1.351548	-1.696571
C	-1.090864	-1.380074	-3.234624
H	-0.559817	-2.677592	-1.614938

C	-2.110666	-0.623378	-3.795779
H	-4.161744	0.019797	-3.716567
H	-0.108003	-1.371965	-3.691234
C	4.294132	-1.117875	0.466171
C	4.764586	-1.921102	-0.583101
C	5.094329	-0.068282	0.932902
C	6.011724	-1.655201	-1.144369
H	4.157856	-2.734676	-0.952800
C	6.329869	0.198088	0.343186
H	4.741779	0.544795	1.755628
C	6.805626	-0.596101	-0.696624
H	7.769061	-0.396530	-1.148702
C	-6.464636	2.446086	-2.344728
C	-7.081802	-1.423415	0.780788
C	6.464776	-2.446549	-2.344071
C	7.081841	1.423811	0.780401
F	-5.913643	3.672677	-2.389265
F	-6.120878	1.813845	-3.498994
F	-7.806527	2.593154	-2.371274
F	-7.062302	-1.581254	2.121489
F	-8.367993	-1.411399	0.384539
F	-6.512800	-2.545279	0.253666
F	1.833276	-0.143809	-4.877400
F	5.913748	-3.673136	-2.388321
F	6.121097	-1.814594	-3.498517
F	7.806664	-2.593665	-2.370509
F	8.368022	1.411732	0.384118
F	6.512803	2.545548	0.253043
F	7.062376	1.581953	2.121066
F	-1.833277	0.141166	-4.878147

(*Z*)-**1a** • (*E*)-**1a**:

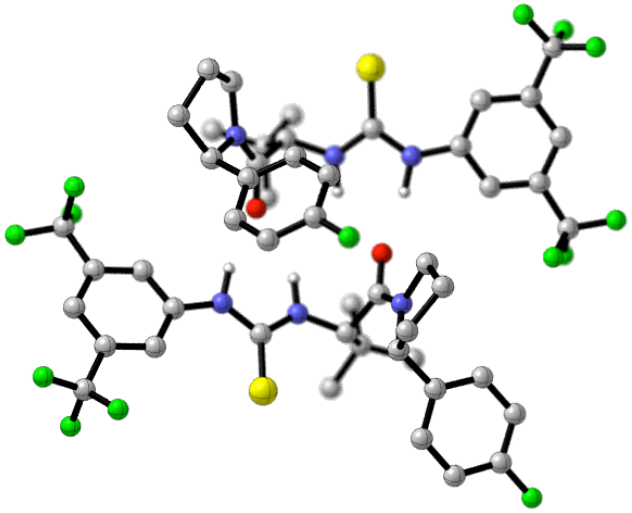

Charge: 0
Spin Multiplicity: 1
Number of Imaginary Frequencies: 0
Solvation: gas phase
Electronic Energy (AU): -4609.96985776
Gibbs Free Energy at 298.150 K (AU): -4609.115538

O	1.477870	0.500006	0.969593
C	1.045313	1.636163	0.677317
C	0.000339	2.293703	1.596210
H	-0.288540	3.271423	1.216061
N	-1.188566	1.448345	1.487905
C	-2.390644	1.831700	0.963659
N	-3.219293	0.749309	0.793853
H	-2.763189	-0.156033	0.915744
C	0.475938	2.512675	3.075325
H	-1.020139	0.450101	1.581030
C	1.807929	3.286245	3.057569
H	2.116469	3.518433	4.081919
H	2.612704	2.703394	2.597463
H	1.719925	4.231764	2.514051
C	-0.593134	3.366819	3.786149
H	-1.566601	2.868489	3.787908
H	-0.299921	3.540547	4.826934
H	-0.718798	4.339513	3.301106
C	0.656873	1.196863	3.853346
H	1.422072	0.561491	3.403775
H	0.957491	1.420300	4.882457
H	-0.279334	0.632169	3.905907
S	-2.775715	3.435017	0.602299
N	1.412708	2.250619	-0.463362
C	2.241576	1.525058	-1.455194
C	0.902488	3.542100	-0.994762
C	2.288510	2.454809	-2.677573
H	3.235215	1.318608	-1.053217
C	1.044785	3.340085	-2.522059
H	-0.154003	3.648964	-0.739604
H	3.199730	3.059924	-2.659957
H	1.123447	4.293445	-3.048770
H	0.163223	2.815169	-2.901725
H	2.276586	1.892860	-3.613846
H	1.760858	0.565813	-1.672913
C	1.655986	4.755164	-0.466765
C	0.954497	5.956082	-0.290189
C	3.030401	4.734078	-0.188489
C	1.600160	7.114611	0.140372
H	-0.114582	5.984993	-0.483410
C	3.691561	5.883530	0.243904
H	3.600704	3.816157	-0.289360
C	2.964377	7.057883	0.398076
H	1.063215	8.045578	0.285083
H	4.753171	5.877134	0.465153
C	-4.569074	0.623907	0.438367
C	-5.376882	1.625860	-0.122103
C	-5.123729	-0.652201	0.642334
C	-6.694807	1.328393	-0.473907
H	-4.971294	2.614378	-0.282502
C	-6.429725	-0.935294	0.256469
H	-4.523484	-1.424262	1.112291
C	-7.235524	0.054009	-0.304925
H	-8.253195	-0.161217	-0.603102
O	-1.579829	-1.627013	0.964751
C	-1.238182	-2.802808	0.721956
C	-0.170175	-3.473903	1.601701
H	0.122082	-4.435154	1.181335
N	1.014591	-2.626645	1.501053
C	2.180494	-2.988769	0.877620
N	2.996385	-1.903184	0.695029
H	2.546034	-1.000116	0.856865
C	-0.628091	-3.742037	3.076892
H	0.846641	-1.631841	1.624963
C	-1.928905	-4.568414	3.043085
H	-2.240675	-4.818635	4.061915
H	-2.754128	-4.019798	2.575709
H	-1.792557	-5.512155	2.503105
C	0.475549	-4.564594	3.770325
H	1.424785	-4.022171	3.784628
H	0.190175	-4.775463	4.806380
H	0.646245	-5.518723	3.262382
C	-0.864988	-2.447235	3.874231
H	-1.653146	-1.834388	3.431951
H	-1.159233	-2.695867	4.899370
H	0.046668	-1.845326	3.936189
S	2.525738	-4.576917	0.420632
N	-1.724907	-3.477650	-0.339573
C	-1.475436	-4.900463	-0.683657
C	-2.640912	-2.818709	-1.300086
C	-2.143247	-5.066131	-2.056648
H	-0.404816	-5.118095	-0.708128
C	-3.265988	-4.020502	-2.044494
H	-3.408846	-2.276363	-0.746470
H	-1.426477	-4.844494	-2.853421
H	-3.611982	-3.744869	-3.042782
H	-4.129032	-4.381539	-1.475229
H	-2.506288	-6.084995	-2.210574
H	-1.944877	-5.549035	0.064269
C	-1.919124	-1.829463	-2.208055
C	-2.620559	-0.722202	-2.703625
C	-0.582792	-2.001636	-2.591161
C	-2.010986	0.199835	-3.553458
H	-3.655342	-0.565643	-2.411879
C	0.044066	-1.092356	-3.444137
H	-0.007104	-2.837319	-2.206673
C	-0.682739	-0.002934	-3.905800
H	-2.543750	1.066819	-3.928071

H	1.077828	-1.219841	-3.746610
C	4.327200	-1.757368	0.278285
C	5.151067	-2.759631	-0.256468
C	4.842402	-0.456143	0.403351
C	6.445514	-2.434782	-0.666924
H	4.774890	-3.767350	-0.359294
C	6.123551	-0.148004	-0.039758
H	4.223082	0.317701	0.844234
C	6.945770	-1.135326	-0.579583
H	7.943133	-0.899740	-0.926550
C	7.338435	-3.537008	-1.180481
C	6.571736	1.284711	0.055293
C	-6.925656	-2.348594	0.398237
C	-7.565851	2.435200	-1.015379
F	-0.067299	0.906397	-4.699582
F	7.963269	-4.177573	-0.166816
F	6.644634	-4.467548	-1.868518
F	8.302290	-3.059636	-1.999728
F	6.474170	1.759553	1.316290
F	7.841068	1.460093	-0.353442
F	5.786998	2.094336	-0.714445
F	3.599145	8.170797	0.819634
F	-8.134066	3.148338	-0.018120
F	-6.862233	3.302995	-1.772379
F	-8.571208	1.951420	-1.779127
F	-8.265420	-2.435626	0.306257
F	-6.406704	-3.148233	-0.573904
F	-6.554907	-2.895500	1.577385

[(*E*)-**1a**]$_2$:

Charge: 0
Spin Multiplicity: 1
Number of Imaginary Frequencies: 0
Solvation: gas phase
Electronic Energy (AU): -4609.96814830
Gibbs Free Energy at 298.150 K (AU): -4609.113292

O	-1.782486	-0.628043	0.820659
C	-1.651607	-1.824860	0.484287
C	-0.796949	-2.761242	1.357522
H	-0.779596	-3.765861	0.939854
N	0.569278	-2.252804	1.249014
C	1.623158	-2.908595	0.673887
N	2.700316	-2.071337	0.532640
H	2.495277	-1.086280	0.709101
C	-1.291603	-2.902745	2.839707
H	0.675683	-1.254910	1.410082
C	-2.779659	-3.301396	2.828421
H	-3.122059	-3.490665	3.850859
H	-3.410393	-2.507495	2.414759
H	-2.951008	-4.211551	2.245608
C	-0.471119	-4.031677	3.495454
H	0.599447	-3.808939	3.479352
H	-0.775125	-4.155527	4.540175
H	-0.619692	-4.986843	2.982642
C	-1.112201	-1.614474	3.663178
H	-1.697420	-0.787938	3.256039
H	-1.440144	-1.792042	4.692883
H	-0.061968	-1.309612	3.707156
S	1.568583	-4.534702	0.222887
N	-2.178567	-2.284917	-0.667840
C	-2.826398	-1.341845	-1.609117
C	-1.994883	-3.635048	-1.264239
C	-3.120583	-2.185474	-2.858280
H	-3.732035	-0.917178	-1.172655
C	-2.101584	-3.329539	-2.777689
H	-0.990736	-3.999666	-1.036934
H	-4.140771	-2.578134	-2.818054
H	-2.392630	-4.213210	-3.349218
H	-1.123315	-2.996437	-3.141863
H	-3.030132	-1.598914	-3.775652
H	-2.135989	-0.515260	-1.810409
C	-3.008109	-4.660537	-0.775069
C	-2.605029	-5.998705	-0.662613
C	-4.338367	-4.332916	-0.473765
C	-3.501006	-6.993747	-0.273547
H	-1.573056	-6.266382	-0.873076
C	-5.247314	-5.315933	-0.082825
H	-4.680484	-3.304063	-0.524402
C	-4.813273	-6.633276	0.007315
H	-3.195148	-8.029756	-0.178558
H	-6.277007	-5.073005	0.155290
C	4.025676	-2.264434	0.119303
C	4.564765	-3.432485	-0.442447
C	4.858098	-1.143102	0.270662
C	5.897429	-3.440520	-0.856745
H	3.942951	-4.307609	-0.563089
C	6.173837	-1.162177	-0.179300
H	4.460903	-0.246220	0.734268
C	6.713751	-2.313660	-0.748124
H	7.736278	-2.332403	-1.101744
O	1.782502	0.628046	0.820679
C	1.651614	1.824859	0.484298
C	0.796952	2.761243	1.357527
H	0.779600	3.765861	0.939857
N	-0.569274	2.252805	1.249014
C	-1.623154	2.908596	0.673885
N	-2.700308	2.071336	0.532630
H	-2.495267	1.086276	0.709081
C	1.291601	2.902750	2.839714
H	-0.675681	1.254911	1.410086
C	2.779655	3.301407	2.828431
H	3.122051	3.490678	3.850870
H	3.410393	2.507509	2.414771
H	2.951001	4.211563	2.245618
C	0.471110	4.031678	3.495457
H	-0.599456	3.808935	3.479352
H	0.775112	4.155530	4.540179
H	0.619680	4.986844	2.982646
C	1.112202	1.614478	3.663184
H	1.697424	0.787944	3.256046
H	1.440143	1.792047	4.692890
H	0.061970	1.309612	3.707160
S	-1.568580	4.534704	0.222890
N	2.178568	2.284912	-0.667834
C	2.826403	1.341838	-1.609106
C	1.994878	3.635038	-1.264241
C	3.120583	2.185462	-2.858273
H	3.732043	0.917178	-1.172642
C	2.101579	3.329521	-2.777688
H	0.990729	3.999654	-1.036936
H	4.140769	2.578127	-2.818050
H	2.392620	4.213192	-3.349223
H	1.123311	2.996412	-3.141860
H	3.030135	1.598896	-3.775643
H	2.135999	0.515248	-1.810394
C	3.008099	4.660535	-0.775076
C	2.605014	5.998701	-0.662626
C	4.338358	4.332920	-0.473771
C	3.500987	6.993749	-0.273566
H	1.573039	6.266372	-0.873090
C	5.247302	5.315943	-0.082837
H	4.680481	3.304068	-0.524404

C	4.813255	6.633285	0.007297
H	3.195125	8.029757	-0.178582
H	6.276997	5.073021	0.155279
C	-4.025670	2.264433	0.119296
C	-4.564762	3.432486	-0.442447
C	-4.858090	1.143098	0.270650
C	-5.897426	3.440521	-0.856742
H	-3.942949	4.307611	-0.563085
C	-6.173830	1.162174	-0.179309
H	-4.460893	0.246215	0.734252
C	-6.713746	2.313660	-0.748126
H	-7.736274	2.332403	-1.101744
C	-6.967654	-0.110985	-0.073844
C	-6.483327	4.719886	-1.401091
C	6.483328	-4.719883	-1.401101
C	6.967663	0.110980	-0.073830
F	-5.688098	-7.586129	0.387898
F	5.553693	-5.481658	-2.013092
F	7.028036	-5.470094	-0.416939
F	7.465214	-4.475359	-2.298480
F	8.245592	-0.039029	-0.464829
F	6.974312	0.598326	1.185850
F	6.421975	1.089771	-0.854483
F	-6.421966	-1.089771	-0.854500
F	-6.974301	-0.598336	1.185835
F	-8.245584	0.039024	-0.464842
F	-7.465217	4.475365	-2.298468
F	-7.028033	5.470093	-0.416924
F	-5.553695	5.481665	-2.013081
F	5.688076	7.586143	0.387875